

LES RAPPORTS DE CAMPAGNES A LA MER

MD I99/SISMO-SMOOTH à bord du R/V Marion Dufresne



La Réunion 25 septembre – La Réunion 30 octobre 2014

Réf : OCE 2015/01

Dépôt légal 2^{ème} trimestre 2015

ISSN : 1636-8525

ISBN : 978-2-910180-72-7



Sylvie Leroy & Mathilde Cannat (*chief scientist*)
Hélène Leau (*OPEA IPEV*)



Table of Contents

Participants.....	4
1. Objectives of the cruise Sismo-Smooth.....	7
2. Operational summary and maps	13
3. Multichannel Seismic.....	20
3.1. Equipment design.....	20
3.2. Data Acquisition	21
3.3. Seismic Processing.....	23
3.3.1. Processing choices	24
3.3.2. Final workflow	34
4. Wide-Angle Seismic survey.....	38
4.1. OBSs specifications and deployment	38
4.1.1. Canadian OBS.....	39
4.1.2. French OBS.....	40
4.1.3. Taiwanese OBS	42
4.1.4. Source for shooting	43
4.2. Data recorded.....	43
4.2.1. Extraction of the data from the instruments and check of raw files	43
4.2.1.1. Canadian instruments	44
4.2.1.2. French instruments	44
4.2.1.3. Taiwanese instruments	44
4.2.2. Clock drift.....	44
4.2.2.1. Canadian instruments	44
4.2.2.2. French instruments	44
4.2.2.3. Taiwanese instruments	45
4.2.3. Shot tables and conversion into segy files	45
4.2.3.1. Creation of the shot tables.....	45
4.2.3.2. Conversion into SEG-Y	48
4.2.4. Examples of data in 2D and 3D.....	49
4.2.4.1. Examples in 2D	49
4.2.4.2. Example in 3D	52
4.3. Recording of local seismicity	53
4.4. Summary and Quality Control OBS DATA	55

5. Magnetism.....	63
5.1. Magnetic field data acquisition	63
5.2. Data Processing	63
5.3. Interpretation	64
6. Sub-bottom profiles (SBP)	68
6.1. The 3.5 kHz sub-bottom profiler of the Marion Dufresne	68
6.2. 3.5 KHz data acquisition and shipboard processing.....	68
7. Multibeam Bathymetry	69
8. Conclusions.....	70
9. Annex.....	71
9.1. Source designs	71
9.1.1. SMT 20s.....	71
9.1.2. OBS 90s	71
9.1.3. OBS 150 m	72
9.1.4. OBS 300 m	72
9.2. Summary of sources used for each profiles	73
9.3. Streamer designs and geometry	74

Participants

IPEV

LEAU	Hélène	<i>OPEA - IPEV</i>
JAOUEN	Alain	<i>IPEV</i>
FOUCHARD	Sacha	<i>IPEV</i>
MORIN	Xavier	<i>IPEV</i>
RIGAUT	Frédéric	<i>IPEV</i>

Genavir

GUEDES	Jean-Charles	<i>Responsible for seismics</i>
NEDELEC	Erwan	<i>Responsible for source</i>
APPRIOUAL	David	<i>Gunner</i>
GASCON	Gilles	<i>Electronician</i>
GUIOMAR	Stéphane	<i>Electronician</i>
HENNEBELLE	Franck	<i>Electronician</i>
LE DOZE	Philippe	<i>Gunner</i>
LOUZAOUEN	Serge	<i>Electronician</i>
MORVAN	Nicolas	<i>Gunner</i>
VULTAGGIO	Gérard	<i>Mecanician</i>

Scientists

LEROY	Sylvie	<i>Chief scientist – ISTEP – UPMC - CNRS</i>
CANNAT	Mathilde	<i>Co-Chief scientist - IPGP - CNRS</i>
AUTIN	Julia	<i>Univ. Strasbourg - IPGS</i>
HUOT	Gabriel	<i>IPGP PhD student</i>
JOURDAIN	Aurélien	<i>IPGP PhD student</i>
LOUDEN	Keith	<i>Dalhousie University</i>
MOMOH	Ekeabino	<i>IPGP PhD student</i>
SAUTER	Daniel	<i>CNRS Univ. Strasbourg - IPGS</i>
SERGENT	Lionel	<i>Mines Paris Tech</i>
SINGH	Satish	<i>IPGP</i>
WANG	Shiou-Ya	<i>National Central Univ. Taiwan, PhD student</i>
WATREMEZ	Louise	<i>Univ. Bordeaux III – Southampton OC</i>
DANIEL	Romuald	<i>OBS INSU & Taiwan</i>
LI	Xuan	<i>OBS INSU & Taiwan</i>
STANDEN	Graham	<i>OBS Dalhousie U. -GeoForce</i>
IULIUCCI	Robert	<i>OBS Dalhousie U. -GeoForce</i>

Crew (CMA-CGM)

DUDOUIT	Thierry	<i>Master</i>
CHAVANEL	Grégoire	<i>Chief mate</i>
MARTIN	Sébastien	<i>Chief engineer</i>
DAMIENS	Mickael	<i>Chef radioelectronician</i>
TAPIE	Jean-Baptiste	<i>Second engineer</i>
BAREYT	Cyril	<i>Mate</i>
CHIOARU	Dragos	<i>Mate</i>
SACHET	Christian	<i>Mate</i>
VACARUS	Daniela	<i>Mate</i>

LEDUGUE	André	<i>Engineer</i>
RAZAFINDRAFAHATRA	Toavina	<i>Cadet</i>
SOLINAS	Jean	<i>Ass. Steward</i>
CLAIRFEUILLE	Pascal	<i>Boatswain</i>
VIRLAN	Doru	<i>Boatswain</i>
DUMITRIU	Nicolae	<i>Mechanic</i>
RAOELIARIMANITRA	André Tantely Marcel	<i>Mechanic</i>
SACIANU	Gheorghe	<i>Mechanic</i>
SOFRONIE-IONITA	Dumitru	<i>Mechanic</i>
BRAY	Yannick	<i>Ass elect.</i>
RITEAU	Gurvan	<i>Ass engin</i>
MOREAU	Nicolas	<i>Electr.</i>
CORNET	Claude	<i>Chief cook</i>
BRUGER	Emmanuel	<i>Boatswain</i>
RAKOTONIAINA	Olivier	<i>Cook</i>
RAKOTONINDRINA	Roger	<i>Cook</i>
GAVRILA	Ionel	<i>Helmsman</i>
MANOFU	Gheorghe	<i>Helmsman</i>
MARCU	Ionel	<i>Helmsman</i>
RAFANO HARANA	Rodolphe	<i>Seaman</i>
ABDULA	Fichiret	<i>Seaman</i>
ALBERT	Marius	<i>Seaman</i>
ANDRIAMIALY	Romuli	<i>Seaman</i>
ARTHUR	Jean de Dieu	<i>Seaman</i>
BABA CARDIA	Sulleman	<i>Seaman</i>
BERTHIN	Jose	<i>Seaman</i>
BOTOU	Richard	<i>Seaman</i>
CHOW	Emilien	<i>Seaman</i>
RAFANO HARANA	Jean-Luc	<i>Seaman</i>
RAHARIJAONA	Maminiaina Raveloarison	<i>Seaman</i>
RAKOTONANDRASANA	Andrianjafinarivo Patrick	<i>Seaman</i>
RAMANANKILANA	Soloniaina	<i>Seaman</i>
RASENDRALAHY	Jean-Claude	<i>Seaman</i>
RASOLOMANAMPITOANA	Rakotoarimanana Thierry	<i>Seaman</i>
STEPHANO	Dany Maurice	<i>Seaman</i>
ZAFISAMBATRA	Patrick	<i>Seaman</i>
RASAMOELINA	Armand Nicolas	<i>Asst cook</i>
RATSIMIHETY	Richard Denis	<i>Asst cook</i>

Marine Mammals Observers

CHAUTARD	Manon	<i>Univ. La Rochelle</i>
FALCHETTO	Hélène	<i>Univ. La Rochelle</i>
GADENNE	Hélène	<i>Univ. La Rochelle</i>

Doctor

HERRMANN	Pierre
----------	--------



1. Objectives of the cruise Sismo-Smooth

Seismic characterization of exhumed ultramafic seafloor at the Southwest Indian Ridge

Context

Exhumation of mantle derived rocks at the seafloor is common at slow spreading ridges, and is observed or inferred in the distal parts of many divergent continental margins (Ocean Continent transition-OCT). It is therefore a fundamental plate tectonic process. It involves large normal fault displacements, and has consequences in terms of magmatic and hydrothermal processes, two parameters that (with divergence rates) control the thermal evolution of the plate boundary. At rifted margins, these thermal conditions, prevailing during the final rifting stages, are particularly relevant to oil and gas exploration. In ridge and in OCT settings, mantle exhumation may also favor specific deep seafloor ecosystems (hydrogen and methane produced during serpentinization may be used as a fuel for microbial activity).

A key question for OCTs is how to predict the presence of exhumed mantle rocks underlying thick post-rift sedimentary sequences. This presence is commonly inferred from seismic characteristics such as a high VP/VS ratio (Christensen, 1966; Miller and Christensen, 1997), or a low downward velocity gradient (eg Canales et al., 2000). At mid ocean ridges, where the sediments are thin or locally absent, serpentinized mantle rocks can be sampled at the seafloor. Therefore, an important question there is: how deep does serpentinization extend, and what is the proportion between serpentinized mantle and intrusive magmatic rocks within the seismic crust?

During the Sismo-Smooth cruise, we addressed these questions by taking advantage of an exceptional region of the mid-oceanic ridge system that has a very low magma supply and where ultramafics are exhumed over distances of up to 100 kms or more along-and across the ridge axis, with a very small proportion of magmatic intrusions (Sauter et al., 2013). This region therefore provides a natural laboratory, to evaluate the seismic characteristics of serpentinized mantle rocks and to establish the « geophysical fingerprints » of an exhumed serpentinized mantle domain.

While the importance of tectonically-dominated accretion (leading to exhumation of ultramafics and gabbros) at slow spreading ridges is now recognized (Cannat et al., 1995; Smith et al., 2006; Escartin et al., 2008), the dynamics of the large offset axial faults that accommodate this accretion are not yet well constrained. Questions that are raised concern: the factors that favor long-lasting activity of axial faults, which then develop into detachments; the conditions that promote the abandonment of a fault and the initiation of a new master fault; and the conditions that cause axial master faults to flip polarity, allowing for deeply-derived ultramafic or gabbroic rocks to be exposed on both plates. A secondary objective of the Sismo-Smooth cruise was to test hypothesis concerning the modalities of mantle exhumation at melt-poor mid-ocean ridges.

The results of the cruise will also be relevant for the investigation of OCTs where mantle exhumation has also been interpreted to occur by asymmetric detachment faulting. However, the studies of these structures (Müntener and Manatschal, 2006; Tucholke and Sibuet, 2007; Péron-Pinvidic et al., 2007; Sibuet et al., 2007) suggest that these faults are rooted at very shallow levels and are far more complex than the classical lithospheric scale detachment faults proposed by Wernicke et al. (1985). An increasing interest by the hydrocarbon industry coupled with the development of improved seismic imaging methods (in particular

combination of reflection and refraction seismic investigations) now enables to demonstrate that exhumed mantle associated with hyper extended crust might form more than 50% of the world's deep margins (e.g. Iberia-Newfoundland margins, where mantle exhumation is best documented, but also the Central and South Atlantic, the S Australian margins, the northern Red Sea and the eastern Gulf of Aden (Leroy et al., 2010).

The study area

The Sismo-Smooth study area is located in the eastern part of the ultraslow spreading (14 mm.yr⁻¹ full rate; Patriat et al., 2008) Southwest Indian Ridge (SWIR) between 62°E and 65°E. The eastern Southwest Indian Ridge (SWIR) is among the deepest mid-oceanic ridges on Earth. This region of the SWIR is known as a magma-poor end-member in the oceanic ridge system (Cannat et al., 1999; 2008; Dick et al., 2003). It displays the widest expanses known to date of seafloor with no evidence for a volcanic upper crustal layer.

This nonvolcanic ocean floor has no equivalent at faster spreading ridges and has been called “smooth seafloor” (Cannat et al., 2006) because it occurs in the form of broad ridges up to 2000 m high with a smooth, rounded topography and with no resolvable volcanic cones on the shipboard bathymetric data. The discovery of this new type of seafloor was made during the SWIR 61-64 cruise of R/V Marion Dufresne in 2003. Then, during the “SMOOTHSEAFLOOR” R/V Marion Dufresne cruise in October 2010, a detailed geological-geophysical survey of the smooth seafloor areas was conducted, determining the rock types exposed, searching for hydrothermal activity and mapping the volcanic, tectonic and sedimentary structures. 35 dredges and 15 CTDs were carried out and over 1000 km of TOBI sidescan sonar and deep towed magnetometer profiles were collected in two smooth seafloor corridors, up to 10 Ma old seafloor (Sauter et al., 2013; Figure 1).

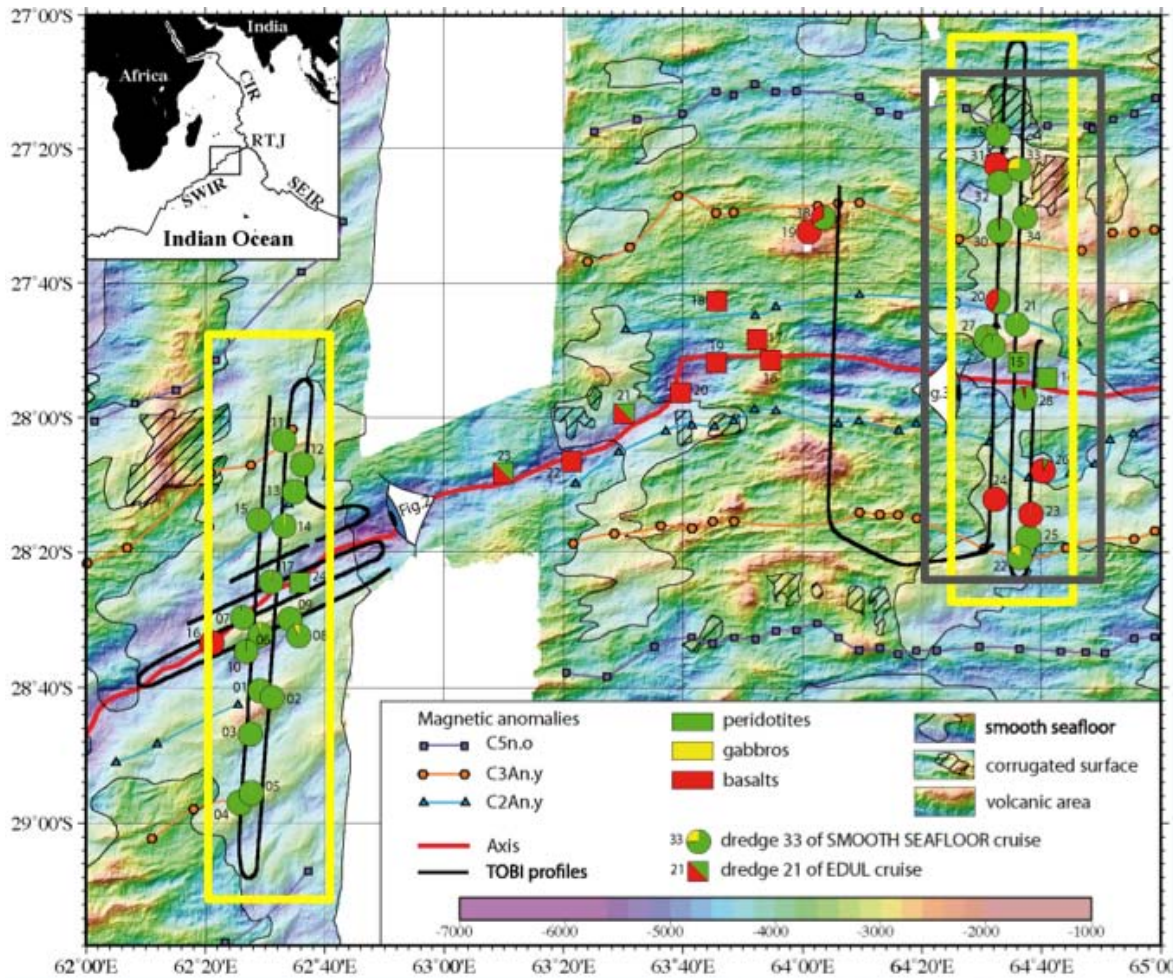


Figure 1: Bathymetric map showing (in yellow boxes) the two corridors of eastern SWIR seafloor that were explored with sidescan sonar (TOBI: black lines) and dredges (dots) during the SmoothSeafloor cruise in October 2010 (Sauter et al., 2013). Black dotted lines show the limits between volcanic and smooth seafloor domains (Cannat et al., 2006). *Magenta triangles* are picks for magnetic anomaly 5 (~10 Ma) and the orange line is the present-day ridge axis. Red (SmoothSeafloor) and orange (EDUL cruise, 2003) dots are dredges that recovered variably serpentinized peridotites, with or without basalts and minor gabbros; Blue dots are dredges with basalts only. The Sismo-Smooth area corresponds to the white rectangle over the eastern smooth seafloor corridor near 64°40'E.

The easternmost SWIR is also well documented in terms of gravity (shipboard measurements acquired over the tracks of bathymetric surveys; Cannat et al., 2006), and magnetics (also along ship tracks: Sauter et al., 2009, and deep towed along TOBI tracks: Bronner et al., 2011). A seismic experiment was conducted some 150 km to the east in the mid-1990s (Figure 2; Muller et al., 1999; Minshull et al., 2006), unfortunately restricted to volcanic areas, missing the expanses of smooth seafloor which had not yet been discovered. The seismic velocity interpretation of these data shows that the average crustal thickness is 3.4 km, with large lateral variations that appear to be taken up mostly by changes in the thickness of the lower crustal layer 3 (Figure 2). A crustal thickness model was derived for the whole region from the gravity data, using a constant crustal density of 2700 kg/m³, and using the seismic constraints as a benchmark (Cannat et al., 2006). It shows the thickest model crust (up to 8 km) beneath three volcanic centers that are widely spaced (250 and 170 km respectively), and the thinnest model crust (less than 3.5 km and down to 2 km) beneath the smooth seafloor areas.

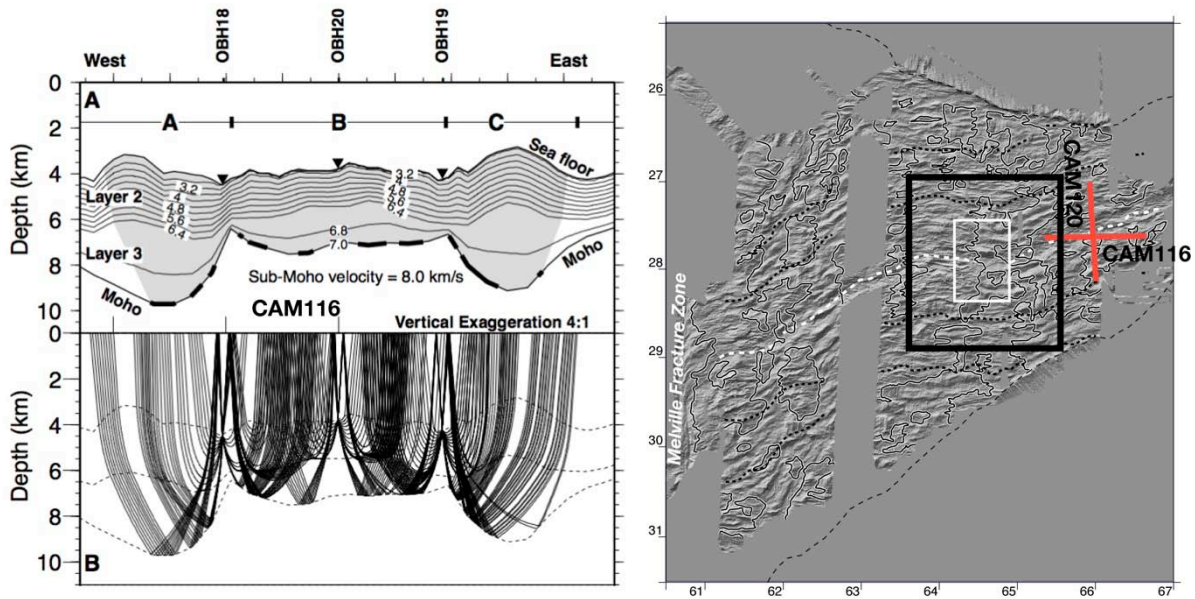


Figure 2: Isovelocity contours and total ray coverage for seismic model of Müller et al., 1999 along refraction profile CAM 116. This profile is part of a seismic experiment carried out to the east of the Sismo-Smooth area (white rectangle). According to this velocity model, crustal thickness variations are mostly accommodated by thinning of layer 3, and the average crustal thickness (over CAM 116 and 120) is 3.4 km, about half the world average for oceanic crustal thickness. This reveals the melt-poor character of this region of the SWIR. The CAM seismic experiment did not explore smooth seafloor domains. Ocean Bottom Hydrophones are shown as black triangles.

The main result of the “SMOOTHSEAFLOOR” cruise was that serpentized mantle-derived peridotites do indeed crop out widely throughout the smooth seafloor areas, while gabbros and basalts are rare. This is in contrast with domains of exhumed ultramafic rocks documented so far at the Mid-Atlantic Ridge (MAR) that also expose abundant gabbroic and basaltic rocks (Cannat et al., 1995a; Bach et al., 2004; Dick et al., 2008; Picazo et al., 2012).

Mantle-derived rocks in the Sismo-Smooth area crop out on moderate slopes facing either toward or away from the axial valley, forming ridges with variable profiles: symmetrical, steeper inward, or steeper outward. Combined TOBI sidescan sonar images and dredging show that sparse volcanic formations form a thin cover directly over exhumed ultramafics (Figure 3). These results show that mantle exhumation has been the main process which shaped the smooth seafloor areas of the eastern SWIR over the past 10 Myrs.

The critical concept here, as in other regions where mantle-derived rocks are exposed, is that ultramafic rocks near ridges are tectonically exposed in the footwall of large offset axial normal faults (Dick et al., 1981; Karson, 1991; Cannat, 1993). It follows that wherever ultramafic rocks are exposed, there has to have been an active exhumation fault surface (see Figure 4 and sketches in Tucholke et al., 2008). We have proposed conceptual models for the tectonic evolution of the eastern SWIR corridors of mantle exhumation (Figure 4; Sauter et al., 2013), which stand the test of the available geological, sidescan sonar, gravity and magnetic data and will now be tested against the Sismo-Smooth seismic data.

The area selected for the Sismo-Smooth seismic experiment is part of the Smoothseafloor survey area. It has been imaged by TOBI and sampled by several dredges (Figures 3 and 4). It includes a steep northern rift valley wall that is interpreted as the most recent and presently

active exhumed fault block, corresponding to a south-facing master fault (in red in Figure 4). The rift valley floor and the seafloor of the Antarctic plate to the south are also made mostly of ultramafic rocks, with thin and discontinuous volcanic veneers (mapped by red contours in Figure 3). This earlier ultramafic seafloor is interpreted as the exhumed surface of an earlier large offset normal fault (also called "detachment"), which was rotated to very low angle (4°; Figure 4) then covered by lavas after being exposed in the axial region.

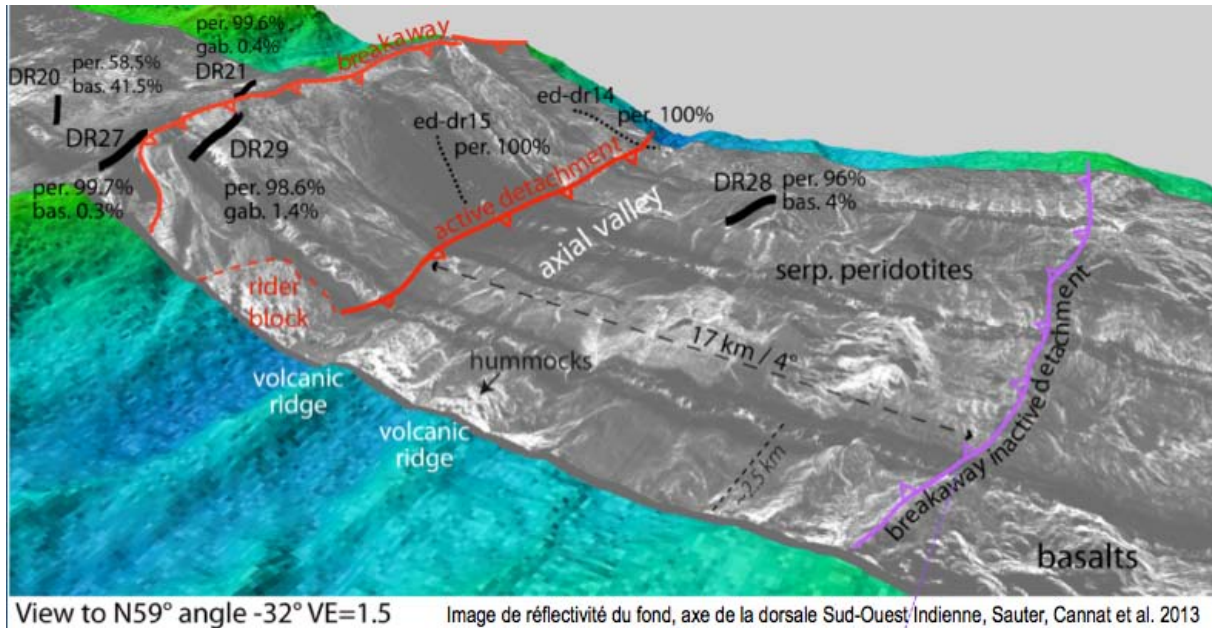


Figure 3. Sidescan sonar (TOBI) image of the axial valley in the Sismo-Smooth area. Dredges of the Edul (dashed) and Smooth-seafloor cruises are shown with proportion of the recovered lithologies (per.= serpentinized peridotites; bas.= basalts; gab.= gabbros). The hummocky portions of the imaged seafloor correspond to volcanic edifices. The most recent axial detachment is sketched in red. It dips to the south and it cuts through, and offsets, ultramafic seafloor formed along an earlier detachment fault (purple) that was facing north. See Figure 4 for a cross-section view of this inferred « flip-flop » detachment system.

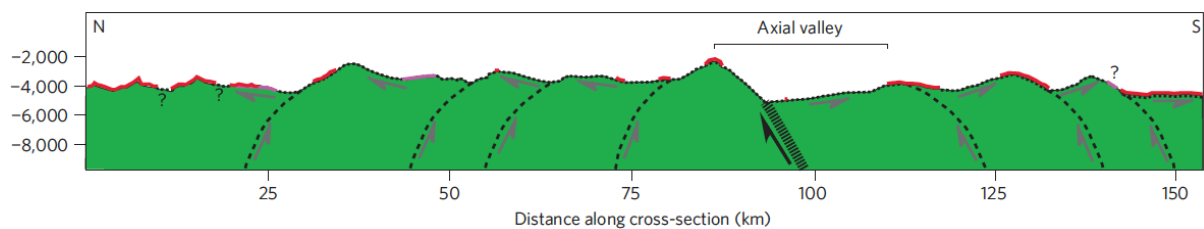


Figure 4. Conceptual across-axis section in the Sismo-Smooth area based on bathymetry, TOBI imaging and dredging data (Sauter et al., 2013). The active axial detachment is shown as a thick line and black arrow. Dotted lines are exposed detachment surfaces (red when corrugated). Dashed lines and grey arrows represent inferred inactive detachment faults. The detachment geometry at depth is speculative and based on results of numerical models of oceanic detachment faults (Lavie et al., 1999).

References

- Bach, W., Garrido, C., Paulick, H., Harvey, J., and Rosner, M., 2004, Seawater-peridotite interactions: first insights from ODP Leg 209, MAR 15 N: *Geochemistry Geophysics Geosystems*, v. 5, no. 9.
- Bronner, Munsch, Carlut, Searle, Sauter, Cannat, Deep-tow magnetic survey above large exhumed mantle domains of the eastern Southwest Indian ridge. AGU fall 2011.
- Canales et al. Crustal and upper mantle seismic structure beneath the rift mountains and across a nontransform offset at the Mid-Atlantic Ridge (35 N). *J. Geophys. Res* (2000) vol. 105 pp. 2699-2719
- Cannat et al. Formation of the axial relief at the very slow spreading Southwest Indian Ridge (49 to 69 E). *Journal of Geophysical Research* (1999) vol. 104 (B10) pp. 22825
- Cannat et al. Modes of seafloor generation at a melt-poor ultraslow-spreading ridge. *Geology* (2006) vol. 34 (7) pp. 605
- Cannat, M., Mevel, C., Maia, M., Deplus, C., Durand, C., Gente, P., Agrinier, P., Belarouchi, A., Dubuisson, G., and Humler, E., 1995, Thin crust, ultramafic exposures, and rugged faulting patterns at the Mid-Atlantic Ridge (22 {degrees}-24 {degrees} N): *GEOLOGY*, v. 23, no. 1, p. 49.
- Cannat. Emplacement of mantle rocks in the seafloor at mid-ocean ridges. *Journal of Geophysical Research-Solid Earth* (1993) vol. 98 (B3)
- Christensen. Serpentinites, peridotites, and seismology. *International Geology Review* (2004) vol. 46 (9) pp. 795-816
- Dick, H., Lin, J., and Schouten, H., 2003, An ultraslow-spreading class of ocean ridge: *Nature*, v. 426, no. 6965, p. 405–412.
- Dick, H., Tivey, M., & Tucholke, B. (2008). Plutonic foundation of a slow-spreading ridge segment: Oceanic core complex at Kane Megamullion, 23° 30' N, 45° 20' W. *Geochemistry Geophysics Geosystems*, 9(5), Q05014.
- Dick, H.J.B., Thompson, W.B., and Bryan, W.B., 1981, Low angle faulting and steady-state emplacement of plutonic rocks at ridge-transform intersections: *EOS, Transactions, American Geophysical Union*, v. 62, p. 406.
- Escartin, J., Smith, D., CANN, J., Schouten, H., Langmuir, C., and Escrig, S., 2008, Central role of detachment faults in accretion of slow-spreading oceanic lithosphere: *Nature*, v. 455, no. 7214, p. 790–794.
- Karson, J.A., 1991, Seafloor spreading on the Mid-Atlantic Ridge : implications for the structure of ophiolites and oceanic lithosphere produced in slow-spreading environments, in Malpas, J., Moores, E.M., Panayiotous, A., and Xenophontos, C., eds., *Proceedings of Symposium "Troodos 1987": Cyprus*, Geological Survey Department.
- Lavier, L., Roger Buck, W., and Poliakov, A., 1999, Self-consistent rolling-hinge model for the evolution of large-offset low-angle normal faults: *GEOLOGY*, v. 27, no. 12, p. 1127.
- Leroy, S., Lucazeau, F., d'Acremont, E., Watremez, L., Autin, J., Rouzo, S., Bellahsen, N., Tiberi, C., Ebinger, C., Beslier, M.-O., Perrot, J., Razin, P., Rolandone, F., Sloan, H., Stuart, G., Al-Lazki, A., Al-Toubi, K., Bache, F., Bonneville, A., Goutorbe, B., Huchon, P., Unternehr, P. & Khanbari, K. 2010. Contrasted styles of rifting in the eastern Gulf of Aden: a combined wide-angle MCS and Heat flow survey. *Geochemistry, Geophysics, Geosystems*. 11(Q07004), 1-14 doi:10.1029/2009GC002963.
- Miller et Christensen. Seismic velocities of lower crustal and upper mantle rocks from the slow-spreading Mid-Atlantic Ridge, south of the Kane transform zone (MARK). *Proceedings of the Ocean Drilling Program. Scientific results* (1997) vol. 153 pp. 437-454
- Minshull T.A., Muller M.R., Robinson, C.J., White, R.S., Bickle, M.J., 1998. Is the oceanic Moho a serpentinization front? In: Mills R.A. and Harrison K., eds., *Modern Ocean Floor Processes and the Geological Record*. Geological Society of London, Spec. Publ., 148, 71-80.
- Muller et al. Segmentation and melt supply at the Southwest Indian Ridge. *Geology* (1999) vol. 27 (10) pp. 867
- Müntener O. and Manatschal G., 2006. High degrees of melt extraction recorded by spinel harzburgite of the Newfoundland margin: The role of inheritance and consequences for the evolution of the southern North Atlantic. *Earth and Planetary Science Letters*, 252, 437-452.
- Patriat, P., Sloan, H. & Sauter, D. From slow to ultra-slow: A previously undetected event at the Southwest Indian Ridge at 24 Myr. *Geology* 36, 207_210 (2008).
- Péron-Pinvidic G., Manatschal G., Minshull T.A., Dean S., 2007. Tectosedimentary evolution of the deep Iberia-Newfoundland margins: Evidence for a complex breakup history. *Tectonics*, 26, doi:10.1029/2006TC001970.
- Picazo, S., Cannat, M., Delacour, A., Escartín, J., Rouméjon, S., and Silantyev, S., 2012, Deformation associated with the denudation of mantle-derived rocks at the Mid-Atlantic Ridge 13°-15°N: The role of magmatic injections and hydrothermal alteration: *Geochemistry Geophysics Geosystems*, v. 13, no. 9, p. n/a–n/a, doi: 10.1029/2012GC004121.
- Sauter, D., Cannat, M., Rouméjon, S., Andréani, M., Birot, D., Bronner, A., Brunelli, D., Carlut, J., Delacour, A., Guyader, V., MacLeod, C.J., Manatschal, G., Mendel, V., Ménez, B., et al., 2013, Continuous exhumation of mantle-derived rocks at the Southwest Indian Ridge for 11 million years: *Nature Geoscience*, v. 6, no. 4, p. 314–320, doi: 10.1038/ngeo1771.
- Sibuet J.C., Srivastava S., Manatschal G., 2007. Exhumed mantle-forming transitional crust in the Newfoundland-Iberia rift and associated magnetic anomalies. *Journal of Geophysical Research-Solid Earth*, v. 112.
- Smith et al. Widespread active detachment faulting and core complex formation near 13 N on the Mid-Atlantic Ridge. *Nature* (2006) vol. 442
- Tucholke B.E. and Sibuet J.-C. 2007. Tectonic and sedimentary evolution of the Newfoundland-Iberia rift. In Tucholke B.E., Sibuet J.-C. and Klaus A., eds, *Proceedings of the Ocean Drilling Program, Scientific Results*, Ocean Drilling Program, College Station, TX.
- Tucholke et al. Role of melt supply in oceanic detachment faulting and formation of megamullions. *Geology* (2008) vol. 36 (6) pp. 455

Wernicke B. (1985), Uniform-sense normal simple shear of the continental lithosphere. *Can. J. Earth Sci.*, 22, 108-125.

2. Operational summary and maps

The cruise took place between September 25 and October 30 2014, with several operational stages that are summarized in Table 1. Corresponding maps can be found at the end of this section, while details on each type of operation can be found in the corresponding chapters of this report. Magnetic anomalies were measured with no interruption during MCS operations (magnetometer attached to the streamer's tail buoy).

Table 1. *Sismo-Smooth* cruise: summary of principal operations

Operation	Starts	Ends	Duration	Data collected	MAP #
1- Transit from La Reunion S20°53.54/E55°18.16 to S27°50.31/E64°25.38	25/9/14-10:30	28/9/14-01:37	63h07	Mag, Multibeam*, SBP*	1
2- OBS Deployment (38) configuration #1	28/9/14-01:37	28/9/14-18:27	16h50	-	2
3- MCS-SMOO1-14	28/9/14-18:27	2/10/14-19:37	97h10	MCS, OBS, Mag	3, 4
4- Airgun maintenance	2/10/14-19:37	3/10/14-13:44	18h07	-	
5- MCS-P0310+SMOO15-32	3/10/14-13:44	8/10/14-00 :00	106h16	MCS, OBS, Mag	3, 4
6- Airgun configuration change and repairs	8/10/14-00:00	9/10/14-09:14	33h14	SBP*	5
7- WideAngle SMOOR1-32	9/10/14-09:14	13/10/14- 04:55	91h41	OBS	2
8- OBS Recovery (18) and Deployment (18) configuration #2	13/10/14- 04:55	16/10/14-00:54	68h	-	6
9- MCS-SMOO33-38	16/10/14-00:54	19/10/14-20:01	91h07	MCS, OBS, Mag	7
10- Rescue of tail buoy	19/10/14-20:01	20/10/14-04:44	8h43	-	
11- MCS repairs and OBS Partial Recovery (13)	20/10/14-04:44	21/10/14-20:49	40h05	-	8
12- MCS-SMOO39-43	21/10/14-20:49	23/10/14-06:22	33h33	MCS, OBS, Mag	8
13- OBS Final Recovery	23/10/14-06:22	27/10/14 10:45		-	
14- Transit to La Reunion					1

* Multibeam and SBP have not worked continuously during these operations. Check section 6 and 7 for details.

Operational stage 1. Transit from La Reunion was slow due to sea conditions. The multibeam and sea bottom profiler (SBP) were operated along the way but worked sporadically (chapter 6). Magnetic anomalies were recorded continuously (chapter 5).

Operational stage 2. We then deployed 38 OBSs (configuration 1; see Map 2) : 20 Canadian OBSs, 10 Taiwanese OBSs, and 8 of the 9 French OBSs (we did not deploy one of the 2 broadband instruments because one of the 9 acoustic systems was out of order). Deployment operations went uneventfully.

Operational stage 3. Followed 4 days of multichannel seismics (including time for deployment of the streamer and air guns) over profiles SMOO1 to SMOO14. This included 12 relatively wide-spaced profiles over the OBS box (Map 3), and 2 (SMOO 13 and 14) of the close-spaced

(100m) profiles of the smaller pseudo-3D MCS (Maps 4a and 4b). Table 2 in chapter 3 contains information on the MCS configuration(s).

Operational stage 4. We then performed a full maintenance of the MCS system.

Operational stage 5. During the next 4.5 days we completed the pseudo-3D MCS profiles (SMOO 15 to 30 ; Maps 4a and 4b), and shot two longer MCS lines (SMOO 31 and 32 ; Map 3). Table 2 in chapter 3 contains information on the MCS configuration(s).

Operational stage 6. was a full refit of the air gun configuration, in preparation for wide-angle shooting. It took 1.5 days during which we carried out a SBP survey of the axial valley (Map 5; Chapter 6).

Operational stage 7. Nearly 4 days of wide-angle shooting (no streamer) over OBS configuration 1. We numbered the profiles that passed over the OBSs (profiles SMOOR1 to 12 ; Map 2). We also shot along two concentric rectangular tracks around the OBS box (Map 2). These surrounding tracks are not numbered as profiles. Table 3 in chapter 4 contains information on the shooting configuration(s).

Operational stage 8. We then recovered all the Canadian OBSs but 2 that did not release (C3 and C4), for redeployment along OBS configuration 2 (Map 6).

Operational stage 9. Nearly 4 days of MCS shooting with the new, more powerful source, over OBS configuration 2: profiles SMOO33 to 38 (Map 7). Between the end of profile 35 and the start of profile 36, we performed a partial maintenance of the port air guns, during which we kept shooting with the starboard air guns and experimented with deeper guns (short profile « EXP. » in Map 7). After this maintenance and before SMOO36, we also shot a « return to 36 » profile (Map7). Table 2 in chapter 3 contains information on the MCS configuration(s).

Operational stage 10. Just after the end of profile SMOO38, we lost the streamer's tail buoy, due to a shark attack. We thus had to retrieve the whole MCS system and recover the buoy.

Operational stage 11. After recovery of the tail buoy, we had to repair the streamer. This took 40 h, during which we decided to start OBS recovery. We were able to recover 13 of the 38 deployed instruments. A Table of OBS deployment and recovery times can be found in section 4 (wide angle seismics).

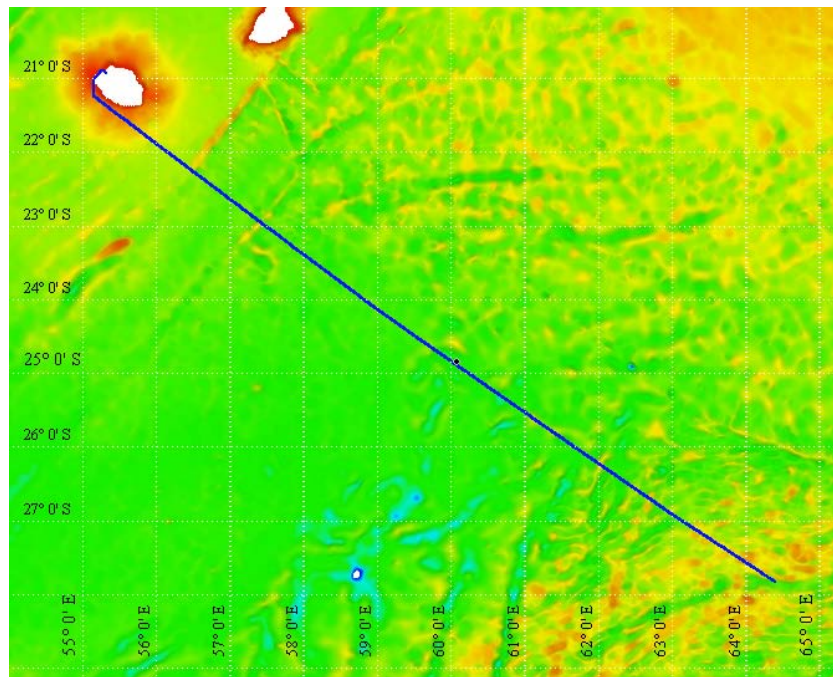
Operational stage 12. After repairs of the streamer, we resumed MCS operation, shooting profiles SMOO39 to 43 (Map 8). Table 2 in chapter 3 contains information on the MCS configuration(s).

Operational stage 13. We then spent a bit over 4 days recovering the 28 OBSs that were still on the bottom. Duration of this last operation was largely controlled by the timing of automatic release for those OBSs that had not previously responded to release orders. This was the case of three Canadian and one Taiwanese OBSs.

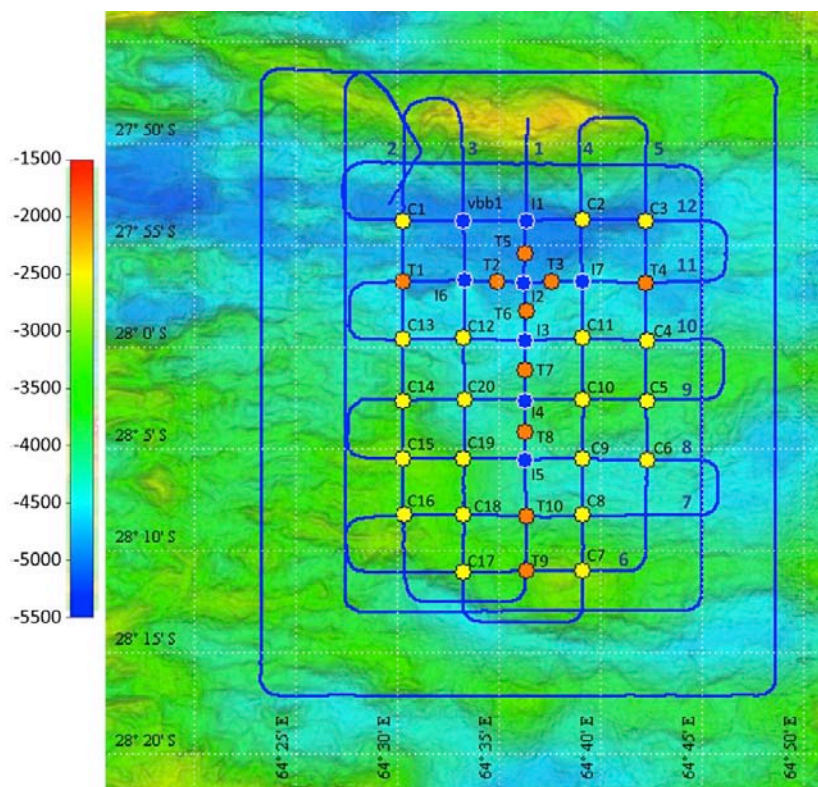
Operational stage 14. Transit back to La Reunion.

Navigation Files

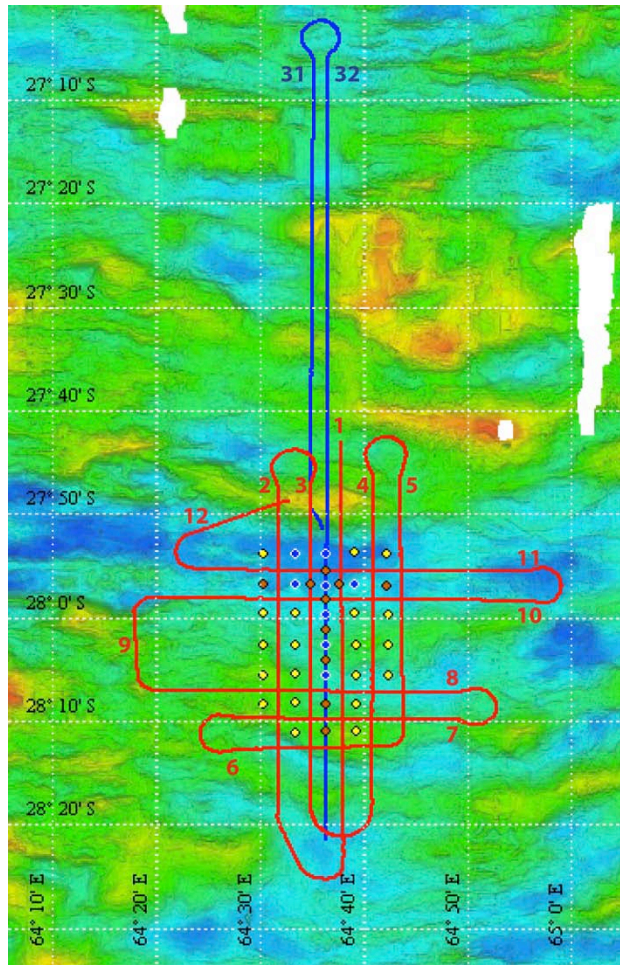
The ship's navigation files are based on data from a GPS (called GPS#3) that was located at the bow of the ship. The navigation files for the air guns and streamer are, by contrast, based on the GPS position of the ship's rear end (calculated using data from a second GPS – called GPS#1- located on the helicopter deck). The distance between these two references is 120 meters.



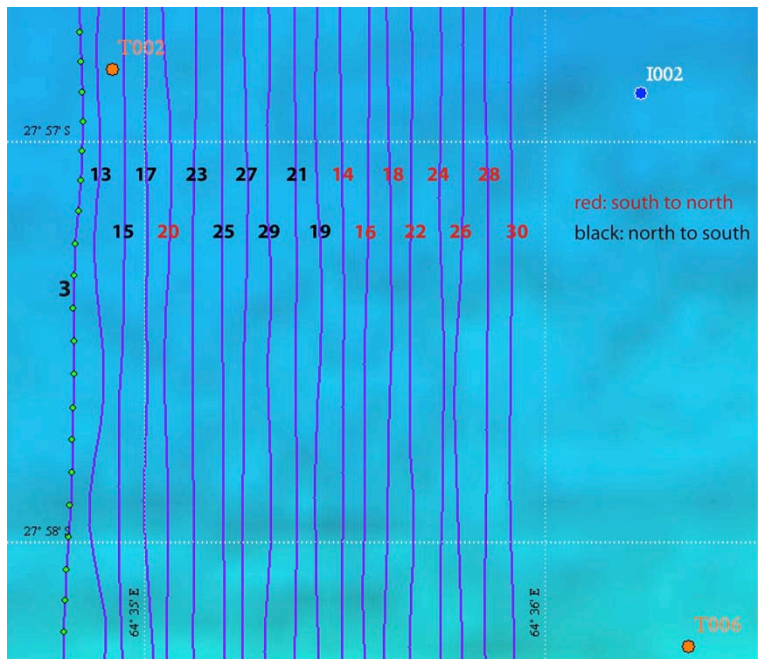
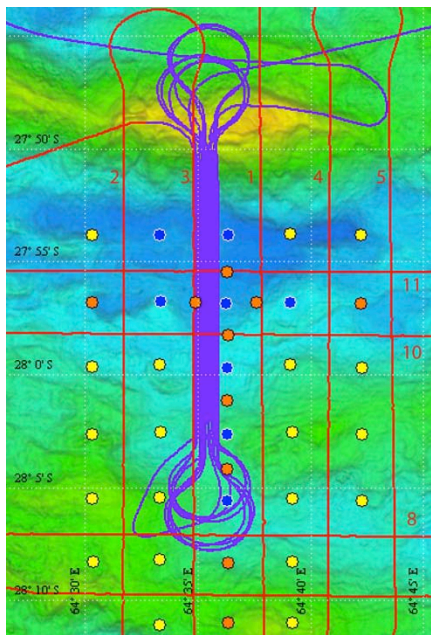
MAP 1. Transit from and to La Reunion.



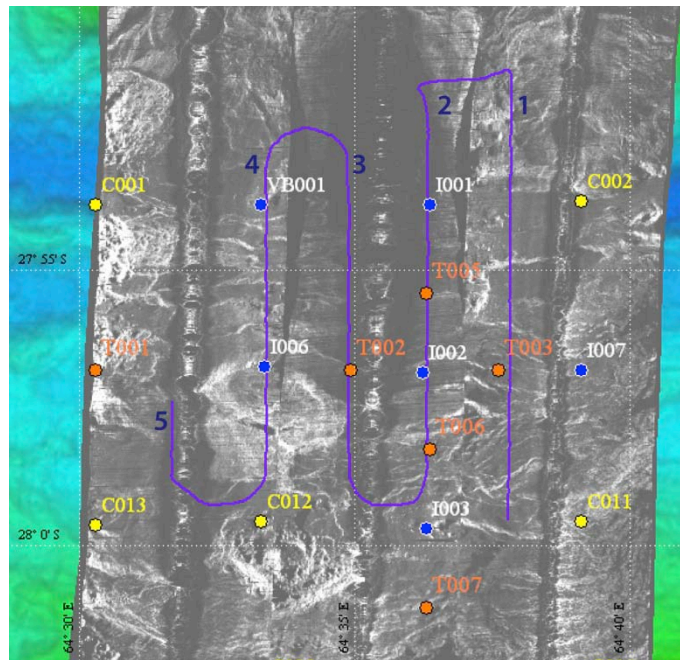
MAP2. Bathymetric map showing the location of the 38 OBSs deployed as part of OBS configuration #1: 20 Canadian OBSs (sites C1 to 20), 10 Taiwanese OBSs (sites T1 to 10), 7 French short period OBSs (I1 to 7) and one French « very broadband OBS » (site vb01). The map also shows the location of the wide-angle seismic profiles shot over this OBS network (operational stage 7; Table 1). OBSs T9, C3 and C4 were not recovered.



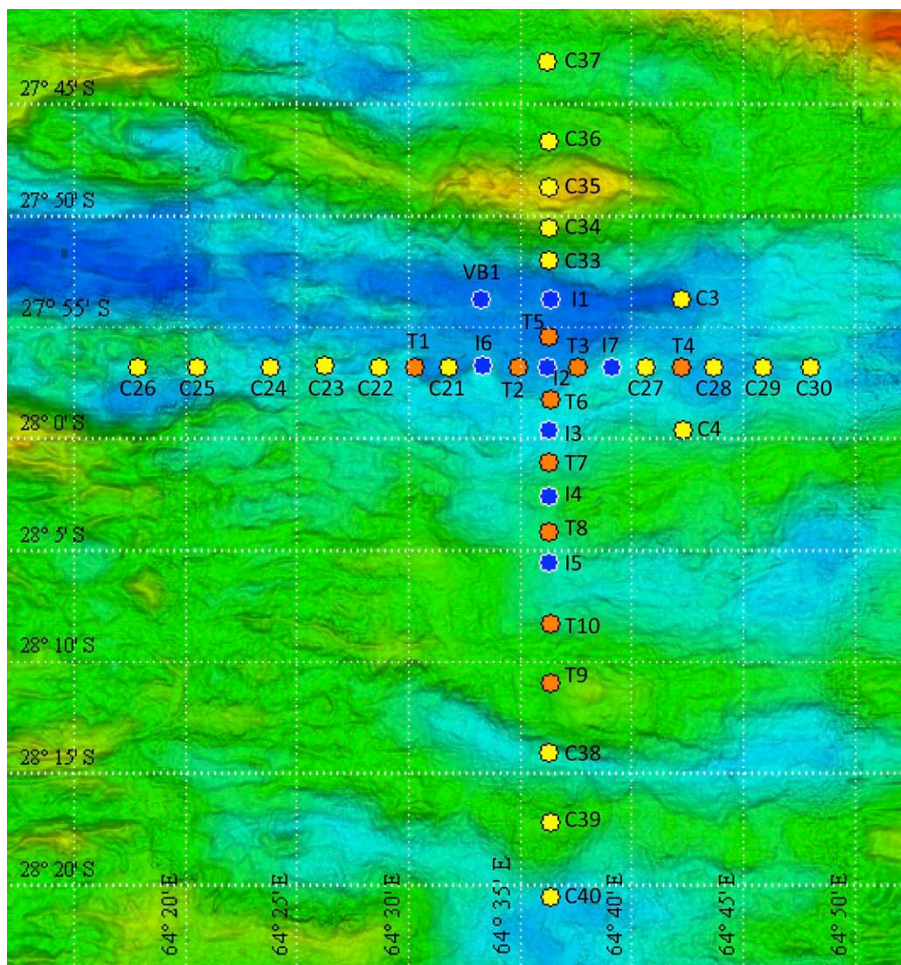
MAP3. Bathymetric map showing the location of MCS profiles SMOO1 to 12 (operational stage 3; Table 2) and SMOO31 to 32 (operational stage 5) over OBS configuration 1.



MAPs 4. Location of the pseudo-3D MCS profiles SMOO13 to 30 (operational stages 3 and 5; Table 2). a- general location of these pseudo-3D MCS profiles; b- detail showing profiles numbers and sense (north to south or south to north).

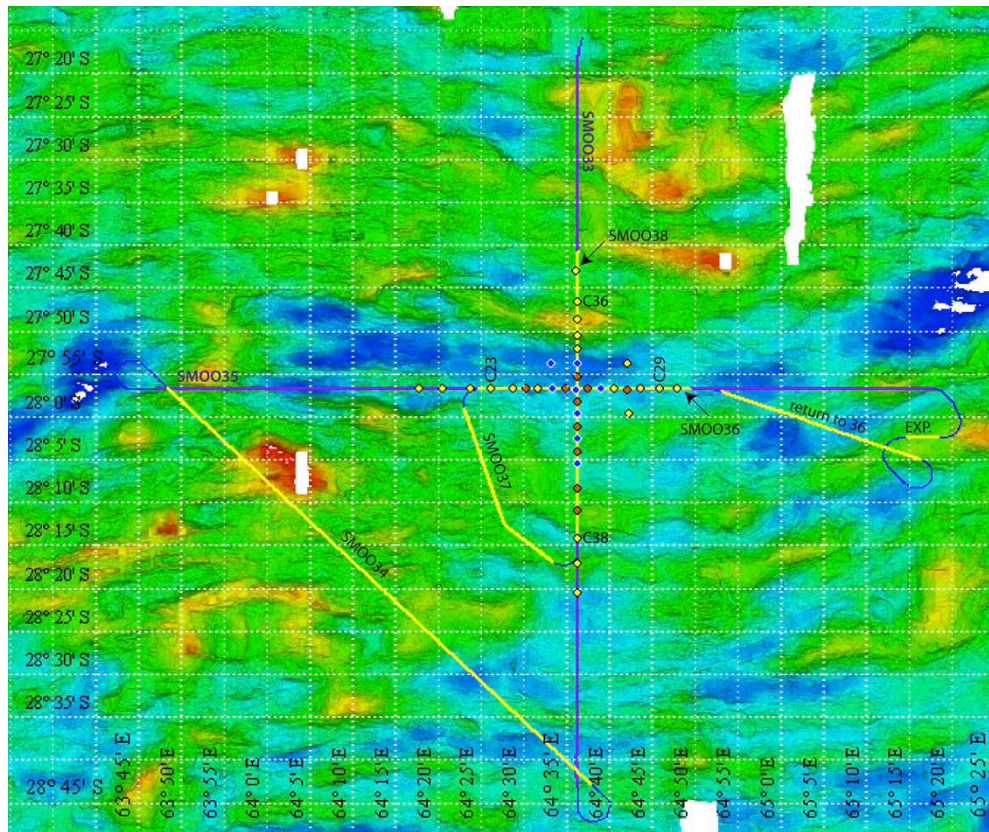


MAP 5. Image of TOBI sidescan with location of sub-bottom profiler (SBP) profiles 1 to 5 (operational stage 6; Table 1) relative to the OBSs (configuration 1).

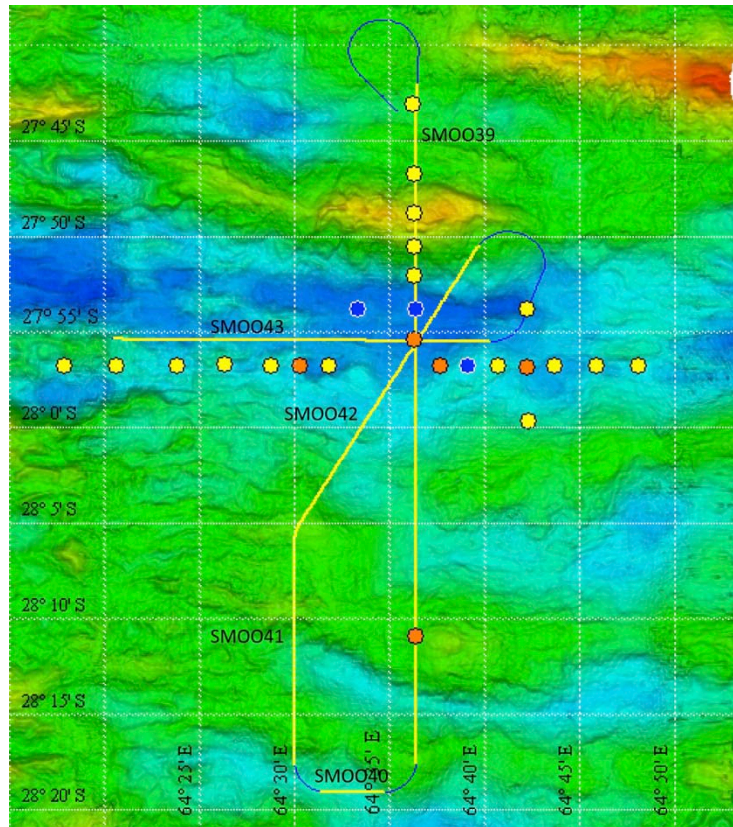


MAP 6. Bathymetric map showing the location of the 38 OBSs deployed as part of OBS configuration #2 (operational stage 8; Table 1): 20 Canadian OBSs (sites C3, C4, C21 to C30, and C33 to C40), 10 Taiwanese OBSs (sites T1 to 10), 7 French short period OBSs (I1 to 7) and one French « very broadband OBS » (site vb1).

OBSs T9, C3, C4 and C37 were not recovered.



Map 7. Bathymetric map showing the location of MCS profiles SMOO33 to 38 (operational stage 9; Table 2) over OBS configuration 2. Profiles shown in yellow have a 150 m shooting interval. Profiles SMOO33 and 35 (in purple) have a shot interval of 300 m except between OBSs C36 and C38 (SMOO33) and between OBSs C23 and C29 (SMOO35) where the shot interval is 150 m. Profiles « EXP. » and « return to 36 » were shot during and after repairs of the portboard air guns.



MAP 8. Bathymetric map showing the location of MCS profiles SMOO39 to 43 (operational stage 12; Table 1) over OBS configuration 2 minus the OBSs recovered during operational stage 11 (Table 1). All of these profiles have a 150 m shooting interval.

3. Multichannel Seismic

3.1. Equipment design

The strategy of acquisition was to collect MCS profiles with two different designs related to the goals. We tried to favor the fold and the penetration. As the terrain has no sedimentary cover, the acoustic waves are reflected from the seafloor.



Seismic source:

The source was first performed for a MCS acquisition.

Guns are deployed in two lines (see Annex X for design)

The deployment of the guns array goes well and was towed at a mean depth of 12 m (see table 2).

The guns were fired at 400 bars from compressors.

Streamer:

The streamer was a digital 360 channel Sercel with active sections of a total active length of 4500m.

Power supply for the streamer and all data communication from the streamer took place through the umbilical cable.

17 birds located along the streamer give depth and heading of the streamer (Photo below).

Acquisition systems:

Data were recorded in SEG-D on a PC running the ECOS software from GENAVIR/IFREMER.

The controller was connected to ECOS via Ethernet and receiving the digitized signals from the streamer as well as auxiliary channels (1-14). On Aux. data from the source signature is recorded.

Portboard line of guns

Below: Streamer and bird during deployment



3.2. Data Acquisition

2D boxes:

The first 2D box is acquired along N-S and E-W profiles. The source is composed of 11 guns for a total volume of 2625 in³. The mean depth of the source is 12 m (between 10 and 14 m). The shot cadence is 20 s, corresponding to an inter-shot distance of 50 m at a velocity of 5 knts. The 360-channels streamer is 4500 m long with inter-receiver distance of 12.5 m. The streamer is immersed at 18 m depth. The data are recorded along 18 seconds with a sampling interval (SI) of 2 ms.

Pseudo 3D box (2.5D):

The same acquisition configuration is used in the pseudo 3D box. It consists in 18 N-S profiles with a constant spacing of ~100 m. It is 1700 m wide and ~ 24 km-long. It is localized on the main scarp of the spreading center, supposed to be an active detachment fault.

Shots on the OBS (wide-angle seismic):

The streamer was also deployed during the one wide-angle seismic experiment and thus some MCS processing can be performed. Nevertheless, we lacked time to process this data on board. The experiment is along 2 long profiles forming a cross: N-S and E-W. The source is more powerful with 14 guns for a total volume of 6790 in³. The mean depth of the source is 14 m (between 12 and 18 m). The shot cadence is at a constant distance for this experiment (see table 2): inter-shot distance of 150 m; or 300 m at the extremities of the profiles ((profile Smoo33)). The 360-channels streamer is 4500 m long with inter-receiver distance of 12.5 m. The streamer is immersed at 22.5 m depth. The data are recorded along 18 seconds with a sampling interval (SI) of 2 ms.

Table 2: Acquisition configuration and noticeable events during acquisition.

Line n°	Acquisition date	Mean fold	Guns	Streamer	SP	CMP	Direction	Comments		
1	29/09/2014	44 2D lines	Bd 1,2,3,4,5,6 Td 1,2,3,4,5	ok	1463	12329	N => S	Gun 5 Td (G gun) replaced by 6 Td (bolt) at SP 945		
2					1158	9913	S => N			
3					1079	9057	N => S			
4	30/09/2014		Bd 1,2,3,4,5,6 Td 1,2,3,4,6		1066	8765	S => N	Important feathering, Problems with gun 2Td at SP 870		
5					856	7284	N => S			
6	01/10/2014		Bd 1,2,3,4,5,6 Td 1,3,4,6		ok	461	3904	E => W	Rough seas 8-10 Hz noise => F, k filter	
7						653	5571	W => E		
8						956	8022	E => W	Gun 2Td is stopped during profile 6 at SP 350	
9						birds 1 to 6 shallow	236	2085	S => N	
10						1220	9793	W => E		
11	02/10/2014				ok	1041	8503	E => W		

Line n°	Acquisition date	Mean fold	Guns	Stream-mer	SP	CMP	Direction	Comments	
12					287	2549	SW => NE		
13					417	3519	N => S		
14					478	4205	S => N		
P0310					429	3238	E => W	Fold 48	
15	03/10/2014	44 2 D½	Bd 1,2,3,4,5,6 Td 1,2,3,4,5		459	4073	N => S	Initial source after reparation	
16	04/10/2014		Bd 1,2,3,4,5,6,7 Td 1,2,3,4		468	4203	S => N	Gun 5 Td (G gun) replaced by 7 Bd (bolt 9L) at SP 97	
17					497	4159	N => S		
18					467	4046	S => N	Gun 7 Bd stopped at SP 44	
19					453	3910	N => S		
20					487	4200	S => N		
21					447	3913	N => S		
22	05/10/2014		Bd 1,2,3,4,5,6 Td 1,2,3,4		497	4173	S => N		
23					481	4231	N => S		
24					494	4206	S => N		
25					484	4256	N => S		
26					485	4196	S => N		
27					493	4250	N => S		
28					496	4224	S => N		
29					06/10/2014	44 2D lines	Bd 1,2,3,4,5,6 Td 1,3,4,7	Bird 5 dead	487
30		Birds 5,8 dead	413	3645	S => N				
31			1583	12921	S => N				Bird 5 and 8 shallow.
32	07/10/2014				2761	22524	N => S	Continuation of line n° 3.	
33-1 33-2 33-3	16/10/2014	15 at 150m	Bd 1,3,4,5,6,7,8 Td 1,2,3,4,5,6,8		1-184 185- 518 519- 682	? 8316 ?	N => S	Change of inter-SP distance from 300 to 150m at SP 185, then 300m at SP 519. Gun 2 Bd (G gun) replaced by 6 Bd (bolt 9L) at SP 629. Dead trace 192 until the end.	
34	17/10/2014	7.5 at 300m	Bd 1,3,4,5,6,7 Td 1,2,3,4,5,6,7,8	ok	783	19072	SE => NW	Gun 8 Bd (bolt 16L) replaced by 7 Td (bolt 16L) at SP 218. Dead trace 192 until the end.	
35-1 35-2 35-3		OBS lines			1-215 216- 464 465- 600	? 5380 ?	W => E	Change of inter-SP distance from 300 to 150m at SP 216, then 300m at SP 465. Dead trace 192 until the end.	

Line n°	Acquisition date	Mean fold	Guns	Streamer	SP	CMP	Direction	Comments
36	19/10/2014		Bd 1,2,3,4,5,7,8 Td 1,2,3,4,5,7,8		270	6817	E => W	Inter-SP distance is 150 m. Gun 5 Td (bolt 9L) and 8 Bd (bolt 16L) replaced by 6 Bd (bolt 9L) and 7 Td (bolt 16L) at SP 200 and 212. Dead trace 192 until the end.
37			Bd 1,2,3,4,5,6,7Td 1,2,3,4,6,7,8		254	6062	150° then 120°	Inter-SP distance is 150m. Dead trace 192 until the end.
38			Bd 1,2,3,4,5,6,7,8 Td 1,2,3,4,6,7		416	10250	S => N	Inter-SP distance is 150m. Gun 8 Td (bolt 16L) replaced by 8 Bd (bolt 16L) at SP 6 Dead trace 192 until the end.
39	22/10/2014		Bd 1,2,3,4,5,7,8 Td 1,2,3,4,5,6,8		442	10868	N => S	Tail boy lost during previous turn (shark). All devices on board for reparation. Dead trace 192 until the end.
40					34	Turn	E => W	Inter-SP distance is 150m. Dead trace 192 until the end.
41					151	37072	S => N	
42					211	5352	SW => NE	
43					208	5378	E => W	

3.3. Seismic Processing

Comments on the seismic target:

The seismic target is the atypical oceanic “crust”, mainly composed of serpentized peridotites across and around the ultra-slow spreading ridge. There is none or very few sediments. Thus, we expect to image low frequency events at rather shallow depths below the seafloor. Moreover, we expect the serpentine seafloor to be highly reflective and thus to limit the penetration of the acoustic waves in the underground. We also observe patches of magmatic seafloor, which are known to prevent penetration in the underlying material. The seafloor is around 4500 m depth (5-6 sec TWTT) and thus the multiple should be deep enough to allow the oceanic “crust” imaging above it. The main structure is a large basement high (up to 3 sec TWTT) thought to result from a northward-dipping detachment fault. It should be possible to image it if the exhumed peridotites in the footwall and in the hanging-wall have different impedance (e.g. different densities due to different serpentization degrees) or if the fault contains fluids. It is also possible that magmatic rocks are intruded in the exhumed mantle: in this case, gabbroic intrusions could show higher densities, and thus a velocity contrast with the serpentized mantle, that we could possibly image.

Comments on the frequency content (Gabriel):

We choose to re-sample the traces at a sample interval of 4 ms to decrease consequently the computing time. We apply a low pass filter in order to remove aliased frequencies. The re-sampling implies a Nyquist frequency of 125 Hz ($F_{ny} = 1/(2*SI)$). Since we expect low frequency content of the data (no sediments), the re-sampling from 2 ms ($F_{ny} = 250$ Hz) to 4 ms ($F_{ny} = 125$ Hz) is appropriate. We thought to increase it at 8 ms ($F_{ny} = 62,5$ Hz) but it would have been a bit risky and was not necessary considering the computing time. Moreover the depth of the streamer (18m) creates a notch in the frequency spectrum at 42Hz, due to interferences with the ghost ($f_{ghost} = V_{water} / (2*depth_streamer)$). This explains the choice of re-sampling the data and the choice of the filter later.

3.3.1. Processing choices**Geometry and preparation of the data:**

The chosen acquisition geometry (for the 2D and 2.5D boxes) implies the following parameters:

- inter-shot = 20 sec ~50 m (if the boat speed is constant at 5 knts)
- inter-receiver = 12.5 m
- inter-CMP = 6.25 m (CMP: common mid points), this value is highly theoretical since the wave rays could reflect on slopes and thus are not always at equal distance from the source and the receiver. We choose a binning at 6.25m.

The fold can be calculate following the equation:

$$\text{Fold} = \text{Total receiver number} * \text{inter-CMP} / \text{inter-SP} = 360 * 6.25 / 50 = 45$$

The CMP numbers can be calculate following the equation:

$$\text{CMP } n^{\circ} = (\text{SP } n^{\circ} - 1) * \text{inter-SP} / \text{inter-CMP} + \text{Total receiver number} - \text{Receiver } n^{\circ} + 1$$

Sispeed® is a software developed by Yannick Thomas at Ifremer in order to prepare the seismic data for further processing. It allows to extract the X, Y navigation data from the auxiliary traces and to calculate the geometry of the common mid points (CMP), i.e. binning of the data every 6.25 m. We also check the shotpoints quality and the recorded delay between the shot order and the actual shot time (50 ms). We also performed a fast processing from Sispeed® such as stack with constant velocities (2000 to 3000 m/s) and migration (water velocity). This allows to obtain a first image for quality control helping the future velocity analysis.

The output data of Sispeed® for further on-board processing with GeoCluster® are raw data. Sispeed® allows to filter the output data but we choose to keep the data as raw as possible in GeoCluster®. Nevertheless, in order to decrease the data transfer duration and the computing time, data were windowed from 18 to 12 seconds. Indeed, we do not expect to image structures in the deep, more homogeneous mantle, far below the oceanic “crust” with the limited penetration of the waves (source and reflective seafloor).

Geometry corrections:

To improve the localization of the recorded events, several corrections are applied to the raw data before their recording in the processing format. We first apply the correction of the source delay (50 ms) so that the traces are correctly located in time. The X, Y navigation data are then stored in the auxiliary traces and the CMP numbers are corrected following the previous equation. If not corrected, the CMP number equals the shotpoint number. Finally, during the shotpoints quality control (QC), we sometimes observed crazy traces (receiver is too noisy and/or the signal is incoherent) or dead traces (the receiver did not record). In this case, we remove the bad traces and replace them by interpolating the neighboring traces. Moreover, we choose to perform a (F, k) filter on the data before their recording in the processing format. This choice is discussed in the filter part.

Amplitude enhancement:

To increase the amplitudes at depth, we first made tests on the dynamic equalization (DYNQU module). The amplitudes are equalized in a sliding processing window, whose length is defined by the user. The processing starts at the sea-bottom if the sea-bottom file is an input. We tested different values for the shallow processing window length: 200, 300, 500, 800, 1000, 1200, 1500, 2000 ms. Nevertheless, the high reflectivity of the seafloor generates very high amplitudes and the equalization was not very efficient and/or generated even higher amplitudes at the seafloor (patchy patterns). In consequence, the choices of the processing team were highly different from one person to another from 300 to 10000 ms in some cases. In parallel, we also tested different parameters for a time dependent amplitude recovery (REFOR): $(\text{Time}/250)^n$ where n is the chosen coefficient. We tested different values for n: 1, 1.4, 1.7, 1.8, 1.9.

Again, we observed very large discrepancies in the personal choices. Indeed, most of the data were not displaying significant improvement after the application of REFOR. A slight change could be observed in the frequency/amplitude spectrum but the seismic display was not improved for the human eyes.

In this frame, we preferred to apply a simple amplitude recovery (RECOV) with the values calculated following the software documentation: an operator length of 300 ms ($75 \cdot SI$) and an application window length of 800 ms ($200 \cdot SI$) in which the operator is applied.

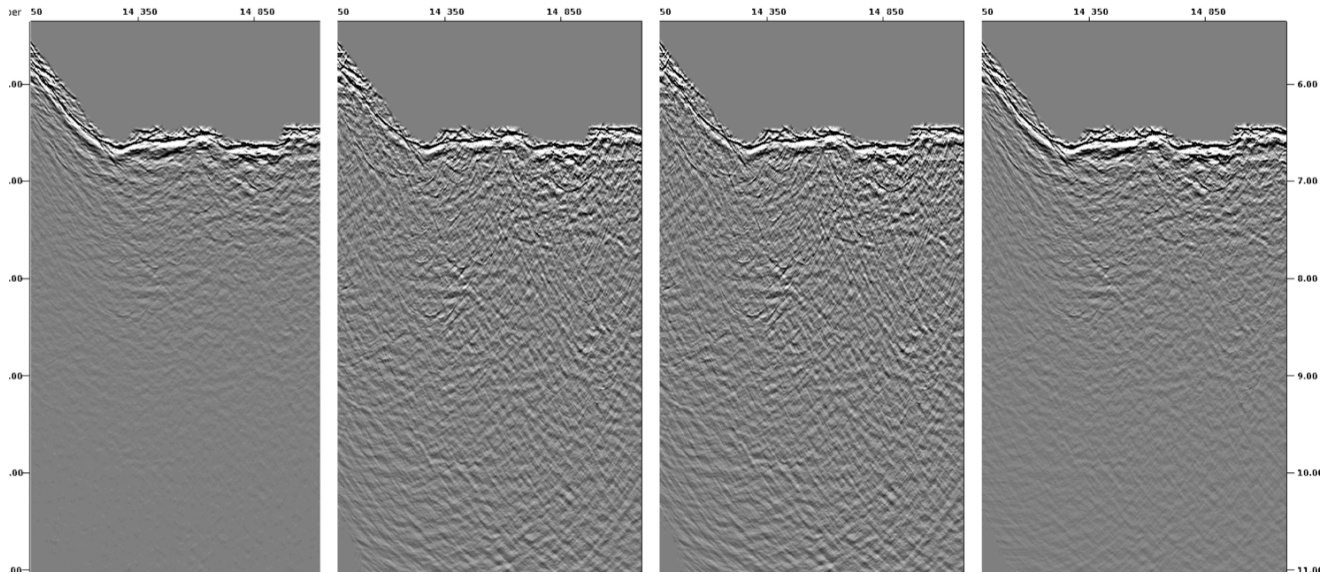


Fig. 3.1 - Comparison of the amplitude enhancement along stacked section SMOO32. From left to right: without enhancement of amplitude, with dynamic equalization (DYNQU, application window of 800 ms), with amplitude recovery (RECOV) and with time dependant amplitude recovery (REFOR).

Filters:

Marine seismic data need a Band Pass (BP) filter to remove all the frequencies that do not correspond to primary events but to noise. In the low frequency domain, waves create important noise generally below 5 Hz. In addition, we observed also swell noise at 8 to 10 Hz. However, primaries also show such frequencies and thus we could not cut them. Indeed, as explained previously, we expect the underground signal to be low frequency. In this frame, we choose the low BP at 1-5 Hz to keep as much as possible the low frequency primaries. In the high frequency domain, the notch at 42 Hz (interferences with the ghost) suggests that

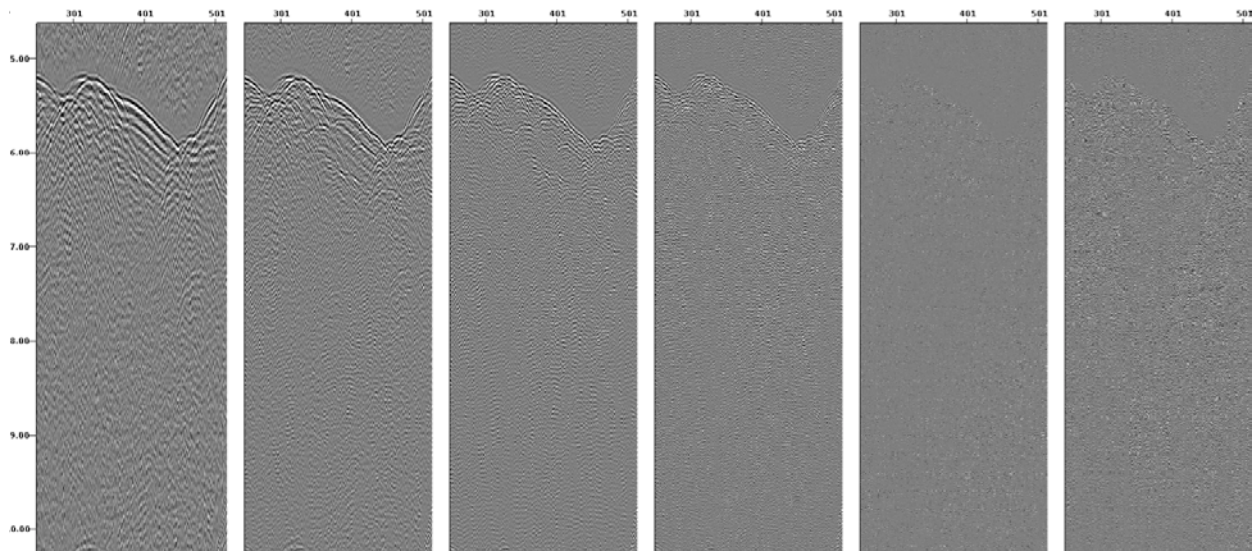


Fig. 3.2 - Comparison of different BP filters along the 150th monotrace of line SMOO32. The frequency range increases from left to right (frequencies in red). The frequency content above 45 Hz displays only noise. The low frequencies contain mainly primaries.

the data are poorly useful above it. Thus, we choose the high BP at 45-55 Hz. Additional tests were performed to check the data frequency content and show that the ejected frequencies display only noise.

To get rid of the 8-10 Hz swell noise, we perform a filter in the F, k domain. In the F-k spectrum we observe significant noise at low apparent velocities (i.e. at the base of the spectrum). In order to be sure that no primary event could be removed, we choose the cutting velocities at +/-1300 m/s (i.e. less than the water velocity). We also choose a taper of 200 m/s to avoid artifact creation.

We also tested F, k filters to remove negative dipping noise in the SP gathers. The velocity needed was up to 6000 m/s. The filter was very efficient. Nevertheless, we suspect that it also removed primary events and primary hyperbola branches, and thus reduced the data quality.

Mutes and sea-bottom picking:

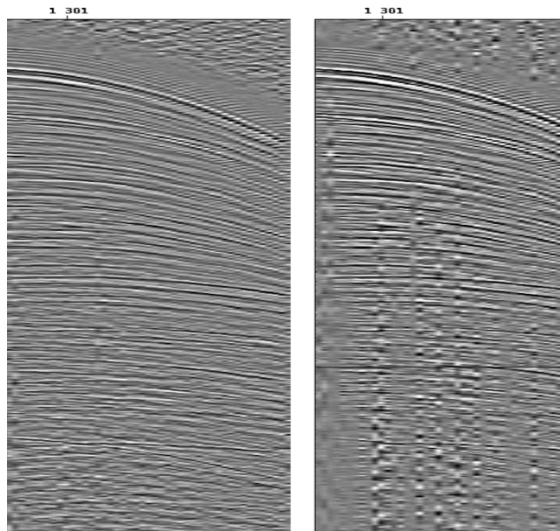


Fig. 3.3 : Effect of the F, k filter on shotpoint 1301s of line SMOO32. Left: with the F, k filter. Right: without F, k filter. Notice the removal of the low frequency noise.

Sea-bottom picks are useful to remove the noise in water but also to indicate the time depth of the computing windows used by classical seismic processing. Thus, we need such horizon early in the processing workflow and the first picking is realized at the very beginning of the processing by extracting the first single-channel image to pick on it. As the 1st single-channel trace contains the shorter time arrivals, the sea-bottom picks are valid for other single-channel traces. However, the seafloor is not always very clear as hyperbolas and noises hide it. The picker should pick a bit above what is observed to avoid any data removal (100-200 ms above). The final sea-bottom picking is realized on the constant velocity stack at 1500 m/s and migration at 1500 m/s. This time, the points can be picked directly above the observed seafloor but the picker should be aware of possible lateral echos.

Several mutes are picked on CMP gathers: 2 external mutes and 1 internal mute. The first “soft” external mute is picked on classical non-corrected CMP gathers. It consists in the removal of the refracted waves in order to keep only reflections. The second “hard” external mute is picked after the velocity analysis, on the normal move-out corrected super CMP gathers (360 traces, sea below for details). It consists in the removal of stretched far offset traces. Indeed, the normal move-out correction (NMO) induces a large stretching of the far-offset traces, which can drastically decrease the signal on noise ratio during the stack. It is common to remove half of the traces along 1 to 2 seconds. Since the hard mute is picked on the super CMP gathers, a large number of traces are kept (~180) and the stack is thus still very efficient. The internal mute is used to remove the multiple and all the signal below this level.

It is picked on the normal CMP gathers. The removal of the multiple allows also to remove all the over-migrated hyperbola branches, which can possibly overlay interesting deep events.

Deconvolution (Ekeabino and Lionel):

Both spiking deconvolution and source signature deconvolution were tested. They both attempt to convert the source wavelet to a spike. One uses a statistical approach to estimate the source wavelet (which is what we have done), while the other requires the exact source signature which is almost always impossible to know.

The spiking deconvolution is not deterministic because the source signature is not known precisely, hence it is approximated from the seismic trace itself by the auto-correlation of the trace. We defined a computation window that had only reflections. Within this window, the auto-correlation of the seismic trace is computed. The first energy at zero lag in the auto-correlogram usually approximates peak amplitude of the source wavelet, while the residual amplitudes correspond to the bubble pulse. After the deconvolution, this is compressed and the reverberating energy (due to the oscillating bubbles) are considerably reduced. The scheme is applied on a trace-by-trace basis, and boosts low and high frequency noise which necessitated the re-application of the bandpass filter. We tested different window lengths from 28 to 1000 ms (truncated version of an infinite operator length) in order to visualize the deconvolution effect on a shot gather. The direct wave is clearly compressed for values around 400 to 600 ms. Indeed the best result should be obtained for values similar to the length of the source wavelet.

The aim of performing pre-stack deconvolution is to visualize the continuity of reflections that could be more useful for velocity picking and reduce possible energy trailing primary reflections that could obscure other reflections. However, the 'spikiness' may be problematic as events which may be slightly displaced do not stack. This may be due to slight variations in streamer depth, for instance. Comparing the results of pre- and post-stack deconvolution, however, shows that deconvolution before stack is more effective in most of our cases. There is no harm in implementing two passes, before and after stack but I did not try this hitherto.

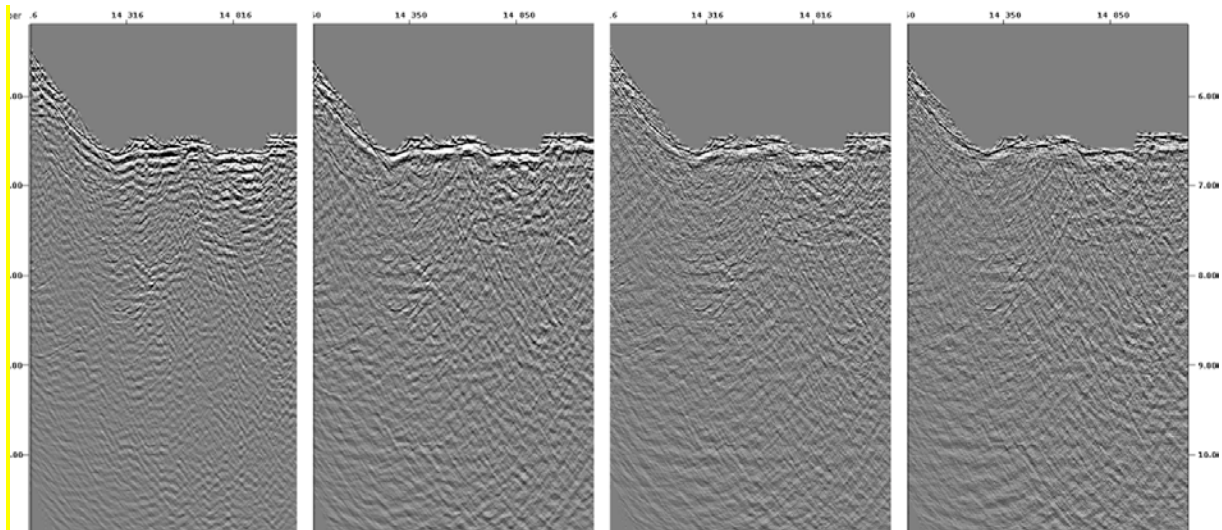


Fig. 3.4 - Effect of the deconvolution along stacked section SMOO32. From left to right: without deconvolution, only pre-stack deconvolution, only post-stack deconvolution, both the pre- and post-stack deconvolution. The pre-stack deconvolution gives nice results. However pre- and post-stack deconvolution should be tested with advanced processing again.

Super CMP gathers (SCMP):

We built SCMP by gathering 8 CMP every 100 CMP. This means that the SCMP gathers contain 360 traces ordered by offset value (8×45 traces). This is particularly useful for velocity analysis because the semblance spectrum is better defined and new amplitude concentration patches appears. It is also easier to control the flatness of the NMO-corrected SCMP display. The stretched traces are clearly identified and removes thanks to the hard external mute. For further advanced processing, it would be interesting to perform stack on the SCMP gathers. Indeed, we lack time on board to compute the specific geometry needed for SCMP gather stacking.

Velocity analysis:

Since we are 7 processing persons, it was very difficult to pick similar velocity laws. This fact was obvious as soon as we compared our velocity gradients. Moreover, the first velocity analysis were realized on normal CMP gathers and the semblance spectrum was very difficult to pick. Nevertheless, with experiences and time a global pattern was observed. Surprisingly, the RMS velocities are very slow (1500 to 1900 m/s) during 0,5 to 1 second below the seafloor. Converted in interval velocities, it means values around 2000 m/s. As we expected serpentinite, with P-wave values between 5000 and 7800 m/s, we suppose that the fracturing of the seafloor is intense and that the rock is full of water, which reduce the velocities. Then we observe a velocity jump to RMS velocity around 2500 to 3000 m/s, which could maybe coincide with less fractured serpentinites. We then decided to gradually increase the RMS velocity gradient until we reach a value of 8000 m/s in the interval value. In addition, we succeed in highlighting what could be the detachment fault at depth. This dipping event shows RMS velocities around 2500 m/s at 6500 ms and until 8500 ms. At the beginning of the cruise, the velocity analyzes followed a slower gradient, which was easier to recognize in the

semblance but was mostly corresponding to slow noises. The application of a common higher gradient clearly improved the imaging at depth.

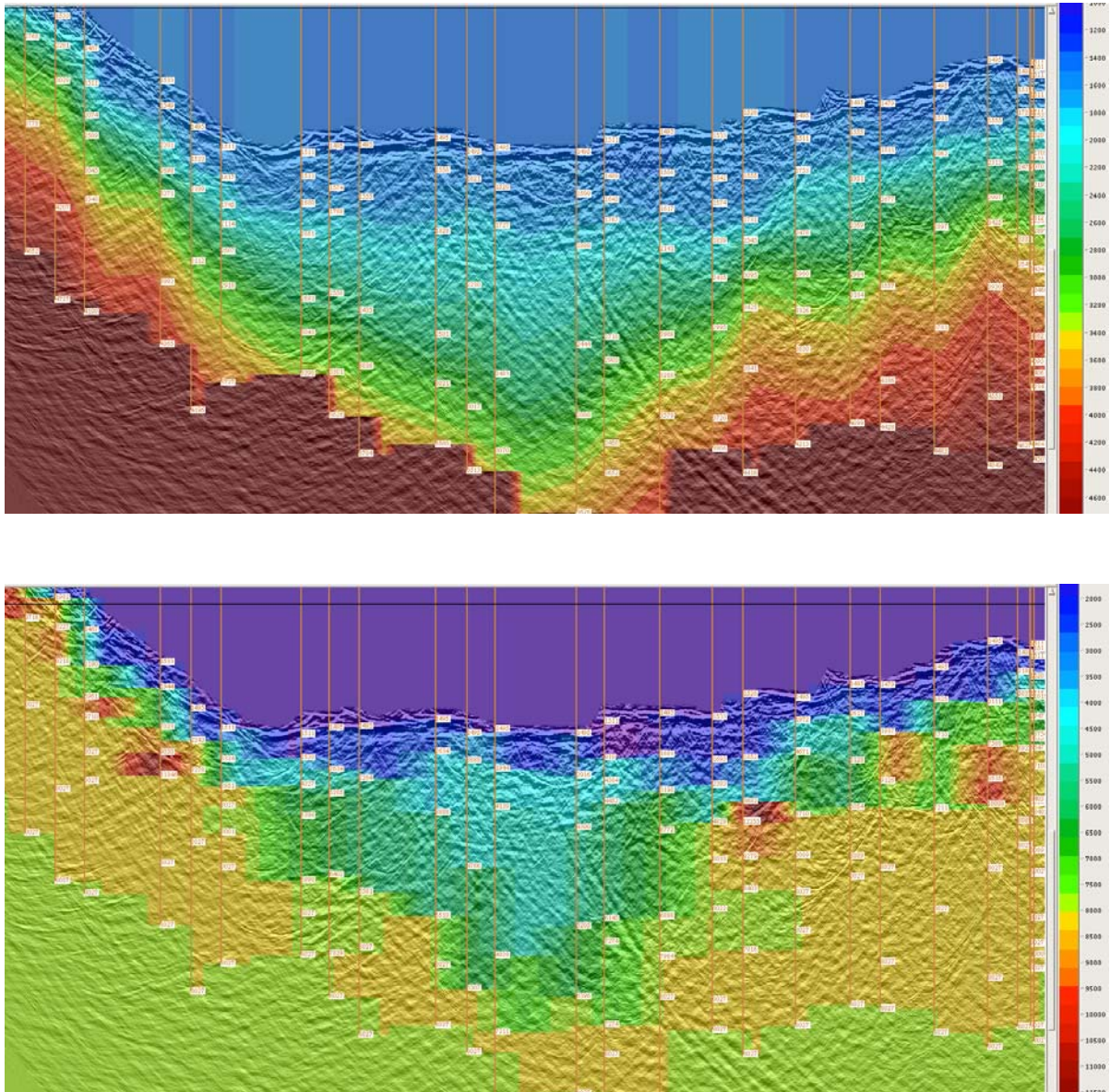


Fig. 3.5 - Example of a stacked section with interactive overlay of the picked velocities along the detachment fault (SMO032). Top: RMS velocities. Bottom: Interval velocities.

This pattern was recognized by using different tools:

- SCMP help to highlight high RMS velocity concentrations in the semblance spectrum.
- During the first 2 seconds, the flattening of the hyperbolas in the NMO-corrected SCMP display is clear enough, but at depth the low-velocity noise is too intense and the correction is difficult.
- The mini-stack at various percentages of the input velocity law help to discriminate between noise and primary events.
- To pick deep events, we first look at constant velocity stacks (1500, 1700, 2000, 2500, 3000, 4000, 5000). This allows recognizing possible primary events in stack section, to check if they are corrected for all the velocity range (which could be a indication of noise) and to estimate the right RMS velocity needed to correct the event.

- We also display a stack section with interactive overlay of the picked RMS velocities or interval velocities. It allows to accurately pick a chosen event and to follow it laterally in order to apply similar velocities laterally.
- We also use the display of the interval velocities gradient in order to avoid velocity inversions and to finish with an interval velocity of 8000 m/s.

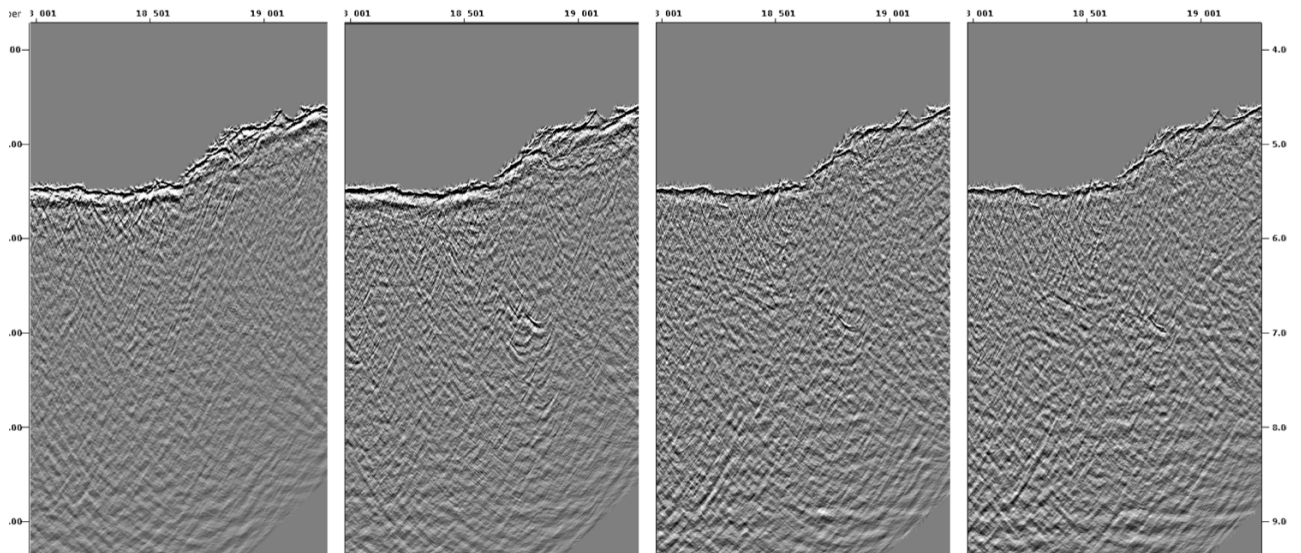


Fig. 3.6 - Constant velocity stacks along line SM0032. From left to right: Stack at 1500 m/s, at 1700 m/s, at 2500 m/s and at 4000 m/s. Notice the better resolution of the shallowest reflection at low stack velocities and the apparition of deep event at high velocities.

Dip move out correction (DMO):

As explain before, the location of the CMP gathers is theoretic since the wave rays could reflect on slopes and thus are not always at equal distance from the source and the receiver. As the seafloor presents high angle slopes ($\sim 20^\circ$), it is necessary to correct the effect of the slope on the CMP location. In this frame, we perform a dip move out correction on the CMP gathers (KIDMO). To perform DMO, the CMP gathers should be NMO-corrected. Then the traces are sorted by constant offset, which allow the dip correction by transforming the constant offset gather in zero offset gathers. Thus, the dispersion of the CMP is corrected and the RMS velocities are independent of the slope.

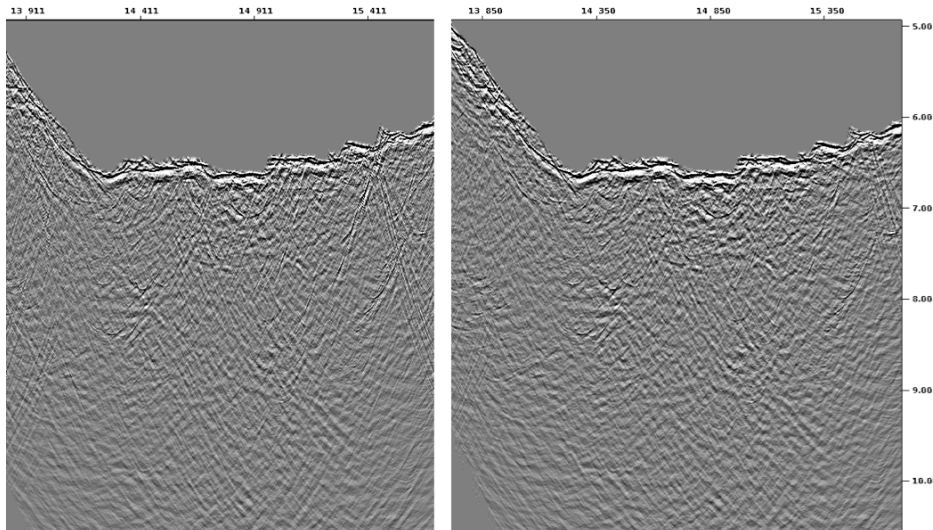


Fig. 3.7 - Effect of the dip move out (DMO) correction along stacked section SMOO32. Left: without DMO correction. Right: with DMO.

Migration:

We perform a post-stack migration in the F, k domain (FKMIG) at constant velocity (water velocity 1500 m/s). This fast processing is a good time/gain solution since it allows to remove

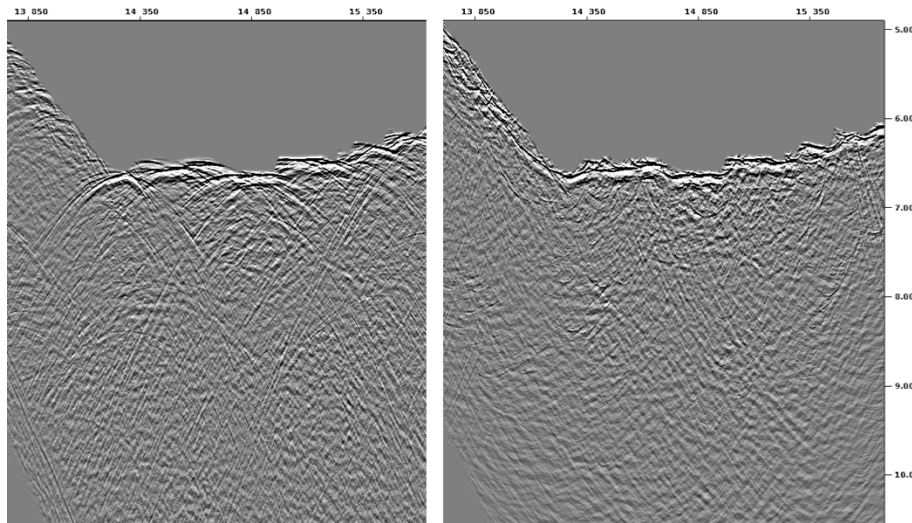


Fig. 3.8 - Effect of the F, k migration along stacked section SMOO32. Left: without migration. Right: migrated section.

most of the sea-bottom hyperbolas in the stacked section. It is fast considering computing time but also and mainly considering the facility to perform it. Of course, the advanced processing could use a more complex migration with variable velocities at depth.

Near- mid- and far-offset stacks (Gabriel):

The purpose of processing separately different offsets is to understand which information is contained in each. This can highlight structures more clearly which could be present, or at least better resolved, at only one offset. By comparing offsets, there are two main differences: the frequency content that will be lower at further offset, and the structures that could be different from one offset to another.

I choose to process the data at three different offsets following Violaine's work (Combiér, 2007): trace 1 to 120 (about 1500m), trace 121 to trace 240 (about 1500 to 3000m), trace 241 to 360 (about 3000 to 4500m). We can notice that in this case the stacking fold is only 15.

In the case of Violaine's data from Lucky Strike area on the Mid Atlantic ridge, sea depth was shallower, from 2 to 4s TWT, which gave some nice information at far offset. The sea depth in our case goes usually from 4s to 6s: to my observation there is poor, even sometimes no reliable information that I observed at far offsets. Therefore, further studies need to be done on the different lines to validate such observation. The middle offsets contain some information, which are worth to compare to near offset data. At near offset, the frequency content is the highest; we have a nice resolution of the sea floor in the 1st second TWT. It is also in this picture that I saw the most reliable information in the deepest parts.

I want to make an important note about the way the different offsets were processed. To produce the best images at each offsets, I used the same velocity model (obtained by velocity picking), but I used a different constant velocity at each offset for the f-k migration to optimized it: 1450m/s for near offset, 1350m/s for middle offset, 1000m/s for far offset (the usual velocity for full offset is 1500 m/s). This is explained easily by the fact that events are not flattened well the more you go to far offsets. The data will stack later than near offset, so a lower velocity is needed to avoid migration artifacts. This can probably be improved with a better deeper processing or improved velocity model. Please not that in Violaine's thesis, she only used the same 1500m/s velocity for each offset and she had good results. The consequence of a lack of accuracy for the velocity model is also that at full offset, far and middle offsets will not be properly migrated at 1500m/s velocity. Artifacts cover information of near offset. That is why I observe that the best image between the four different processing flows is the near offset one (higher resolution and better migrated).

Technical note about Geocluster: the way to process only a selected offset was tricky because it changes the total CMP number, which leads to problems in the workflow during the migration. A first run need to be done with the total CMP number for full offset, to obtain stack sections. Then you can read the new total CMP number at each offset in the stack section .cst file. You can then update this number in the migration module and run again the job.

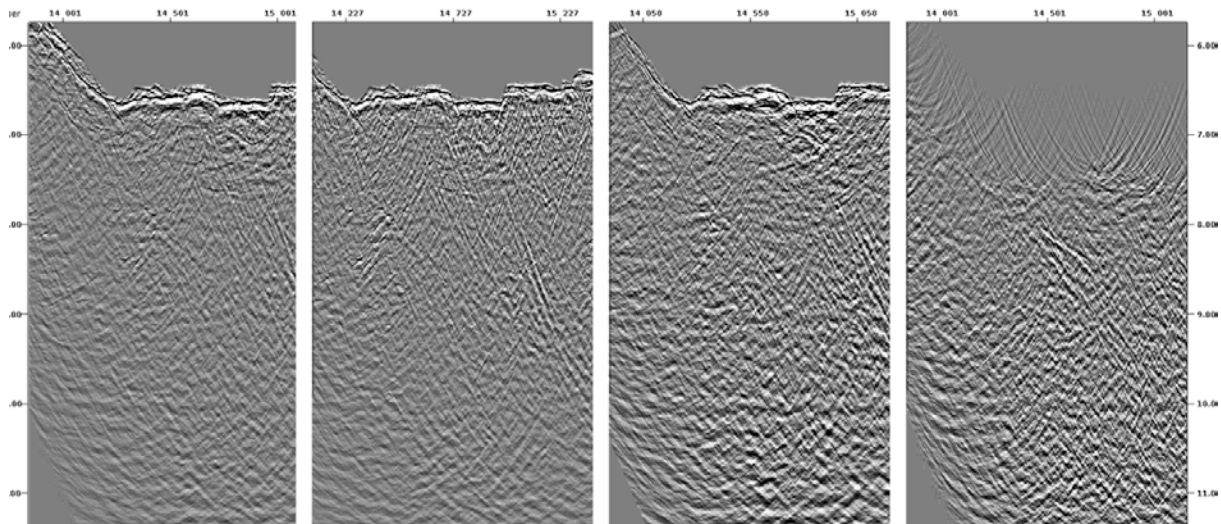


Fig. 3.9 - Display of the various offset stacked section. From left to right: all offset (AO), near offset (NO), mid offset (MO), far offset (FO). The far offset sea bottom is cut due to the external mute.

3.3.2. Final workflow

3.3.2.a. Data recovery and preliminary processing with Sispeed® (Ifremer, version 5.5)

- Copy of the shotpoints in SEG-D format in the specific Sispeed folder
- Extract navigation data from the SEG-D
- Quality control (QC) of navigation data (latitude, longitude, heading, birds, guns, magnetic field information)
- Automatic correction of the time, heading process, GPS positions of the ship.
- Calculation of X, Y positions of the source and receivers along the profile, then QC
- Data QC and test of BP filters on single channel profiles
- Auxiliary traces QC (check source synchronization and shot time delay = 50 ms)
- Common mid points are binned every 6,25m.
- Conversion of raw data, without filter, IEEE 32-bit floating point (big endian) segy format. Copy on server. The data are recorded during 18 sec but we keep only 12 sec for the following processing. The sample rate is 2 ms.
- Fast processing: Constant velocity stack (3000 m/s) and migration (water velocity)

3.3.2.b. Final GeoCluster® workflow (version 5000)

see also the report sheets for every profiles and the script files (.gsl) in annex

1. Extract single-channel n°1 for QC and sea-bottom picking
 - xx_SB_mono1.lfd
2. Conversion of the raw shotpoints gathers (SP) in GeoCluster format and QC: with re-sampling at 4 ms, re-calculation of X, Y positions and of the number of the common mid points (CMP). Amplitude recovery (RECOV) is used for data QC.
3. QC of near, mid and far offsets on 6 single channels (1, 5, 10, 150, 350, 360), removal of dead and crazy traces, then interpolation to replace them.
4. Creation of the CMP gathers. FKFIL (filter of the velocities in the F-k domain on the SP): removal of the ambient noise (-1100/-1300/1300/1100 m/s). Correction of the delay between shot order time and effective shot time (HISTA). CMP gathers QC. Picking of a soft external mute (removal of the refracted arrivals) and of the internal mute (removal of the multiple).
 - xx_soft_mutex.lmu
 - xx_mutin.lmu

Nomenclature of the data:

xx stands for the profile number

nnn stands for the file number

SMOOxx => Seismic profiles are named according to the Sismo-Smooth cruise name

P000nnnSMOOxx => raw data, shotpoint gathers in IEEE 32-bit floating point segy format

I011nnnSMOOxx => shotpoint gathers in GeoCluster format

I012nnnSMOOxx => common mid point gathers in GeoCluster format with initial processing (acquisition geometry and sea-bottom depth in auxiliary traces, source delay correction and light F, k filter to remove swell noise)

P123456SMOOxx => final processed profile in EEE 32-bit floating point segy format

5. Creation of the super CMP gathers (SCMP): 8 CMP every 100 CMP => 360 traces. SCMP are used for velocity analyzes. QC of the SCMP gathers.
6. Test band-pass filter parameters (FILTR): cruise default is 1 / 5 / 45 / 55 Hz.
7. Test deconvolution parameters (DECON): cruise default is a window of 50-2000 ms with an operator of 600 ms and prewhitening at 1010 with a sea-bottom picks file.
8. Stack of the CMP at different constant RMS velocities with migration at 1500 m/s: velocities are 1500, 1700, 2000, 2500, 3000, 4000 and 5000 m/s. The display in concertina in Teamview allows checking the best RMS velocity to correct a chosen event. New and more accurate sea-bottom picking on the 1500 m/s display.
 - xx_SB_mig.lfd
9. Creation of the semblance (velocity picking file, VESPA). If a good velocity law is already available, it is possible to apply the Dip Move Out correction (KIDMO) before the semblance in order to increase the picking quality.
 - xx_SemblanceZ.velcom => Z stands for velocity analysis iteration number

The default 1st input velocity law is:

- 1500 m/s RMS until the sea-bottom (sea-bottom picking used)
- 3000 or 4000 m/s as final velocity

In the case of the 3D box acquisition (100 m spaced profiles), the velocity law from another profile of the box can be used as 1st input.

The analysis tools are:

- spectrum/semblance panel of RMS velocities
- related interval velocities
- not corrected and NMO-corrected SCMP displays
- mini-stacks at various percentages of the input velocity law
- a stack section with interactive display of the picked velocities
- constant velocity stacks (see step 8)

2 to 3 velocity analyzes are realized depending on the profile. The specific RMS velocities required for the cruise seems to follow this general pattern:

- 1500 to 1800 m/s until 0,5 to 1 second below sea-bottom
- A velocity jump to ~2500 m/s
- A gradual increase of RMS velocities until it reaches an equivalent of 8000 m/s in interval velocity
- Output velocity law: VZ.lvi

Picking of the hard external mute on NMO corrected SCMP to remove stretched arrivals

- xx_hard_mutex.lmu

10. Final section:

- Amplitude recovery (RECOV)
- Application of the pre-stack spiking deconvolution (DECON)
- Application of the DMO correction (KIDMO) with final velocity law
- NMO correction and stack of the CMP with the velocity law picked on the SCMP
- Migration at constant velocity (1500 m/s, FKMIG)

11. Same workflow as step 10 is applied to near- mid- and far-offset stacks

12. Conversion in IEEE 32-bit floating point (big endian) segy format

13. Seismic Unix script to prepare the plot output in ps format:

Vertical exaggeration is the same for all profiles, clip included.

3.3.2.c. Examples of Seismic Profiles processed

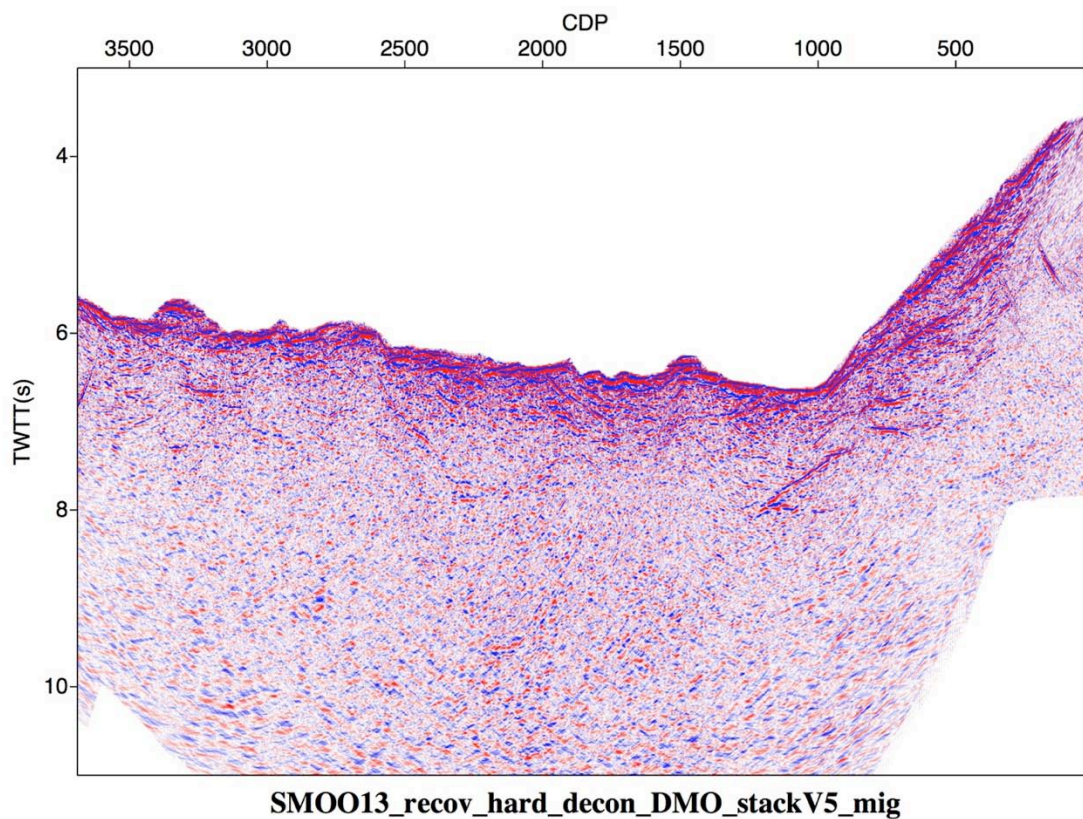


Fig. 3.10 – Profile SMOO13 oriented North-South and belonging to the 2.5D box. (see Map 4 – section 2 for location).

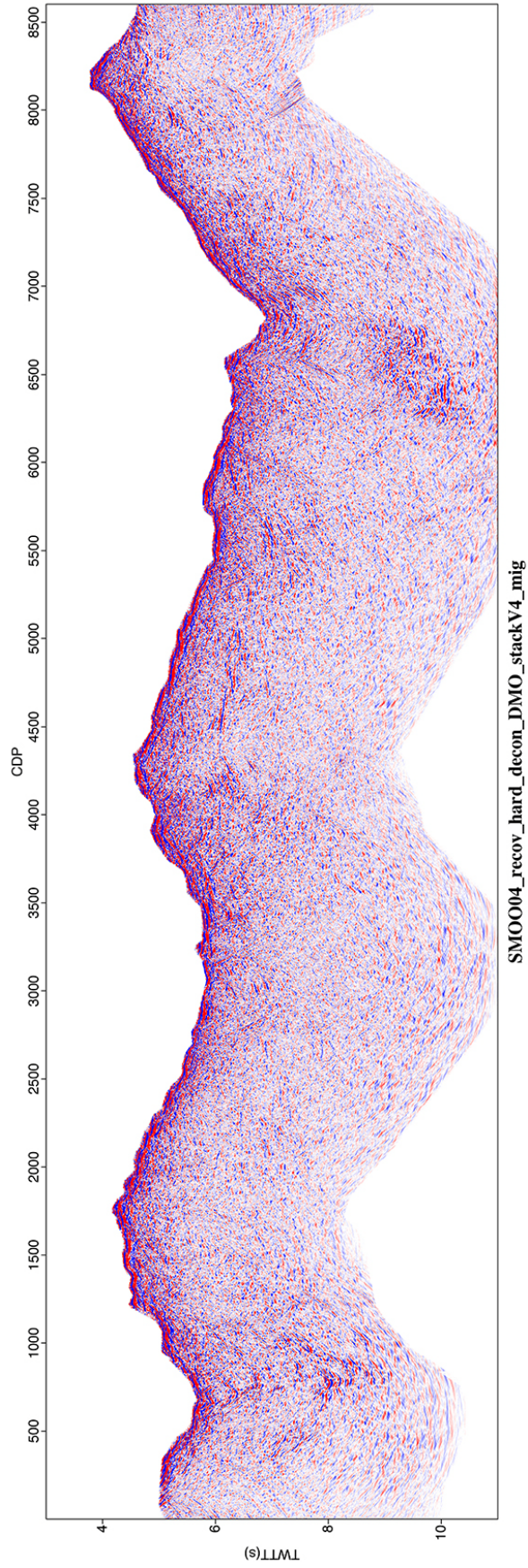


Fig. 3.11 – Profile SM0004 oriented North-South (see Map 3 – section 2 for location).

4.1.1. Canadian OBS

Twenty (20) Canadian ocean bottom seismometers (OBS) from Dalhousie University (DAL), from the Department of Fisheries and oceanography (DFO) and the Geological Survey of Canada (GSC) were deployed during the Sismo-Smooth program to record wide-angle seismic data from air gun shots and local earthquakes. A total of 38 deployments were made: 20 deployments in 2 groups within the 3D Box (MAP 2) and 18 deployments in 4 groups along the 2D cross lines (MAP 6). Three OBS were lost (two on the 3D Box, C03 and C04) and one for the 2D cross lines (C37). One instrument on the 2D cross lines (C33) was damaged and stopped recording after the 1st day, when one of its floatation balls imploded. All other instruments recorded useable data. Recording characteristics are presented in Table 3.

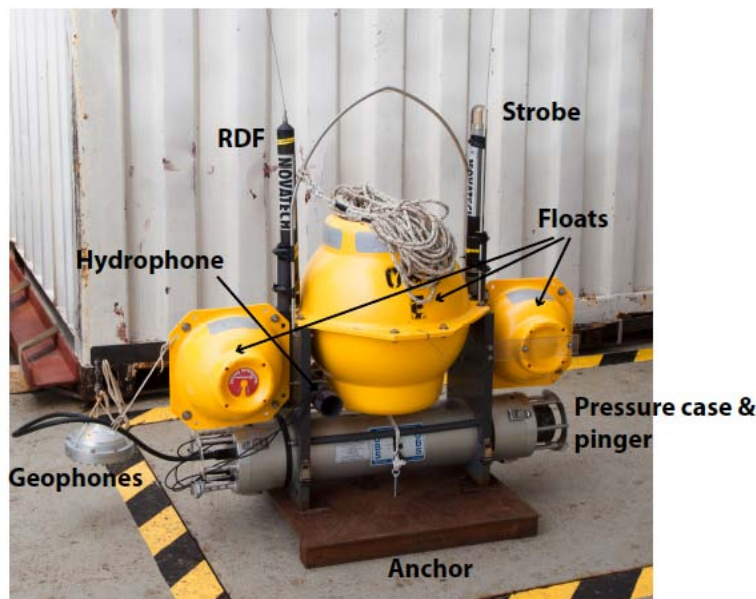


Figure 4.1 Photograph of OBS from Dalhousie University (DAL) and the Geological Survey of Canada (GSC).

Technical specifications for the Canadian OBS are given in table 4. The instruments (Figure x) record 4-C signals using a hydrophone and 3-C, 4.5 Hz geophones within a separate external geophone package. The geophone package drops onto the seafloor when a water-soluble release pin breaks approximately 5-6 hours after deployment. Specification of the sensors is given in the table 4 (Sercel L-28 geophone and HTI-90-U hydrophone). The instruments recorded at a 250 Hz sampling rate for each channel.

The OBS were deployed at positions and water depths (Table 3), determined by the vessel's GPS positioning and previous multibeam sounder data. The timing of the OBS data was controlled by internal Seascan clocks, with expected drift rates of up to several msec/day. The clocks were synchronized to UTC using a Zyfer GPStar® satellite receiver and timing unit that is accurate to < 1 µsec. Following recovery of the OBS, the linear drifts of their internal clocks were measured against UTC. Values of clock drift are given in the Table 3.

Table 4: Technical specifications for OBSs from Dalhousie University (DAL) and the Geological Survey of Canada (GSC).

Item	Specification
Housing/Platform	Uses existing design of BIO-OBS (6 km max water depth). Weight in air: instrument (82 kg); anchor (55 kg) Size: 1.1 m high, 1.2 m long, 0.6 m wide
Release	12.5 kHz Acoustic command + timed backup
Duration of recording	23 days @ 4ms sampling on 4 Gb flash card
Sampling rates / dynamic range	up to 5 kHz / 16 bit SAR ADC
Anti-alias filter	software selectable 8th order low-pass digital filter (LTC1164-7)
Gain	Variable settings software selectable: geophones (0-40 or 53-93 dB); hydrophone (0-40 or 34-74 dB)
Max electrical noise	< 125 nVrms on geophone input < 1uVrms on hydrophone input
Clock	Seascan precision clock, (4 MHz, drift<1 msec/day)
Data storage	Persistor CF2 data logger with variable length files stored on 4/8 Gb flash card; optional use of 2.5" HD up to 80 Gb
Sensors	3-component deployed geophone package (oil filled), deployed on bottom with corrosible link:
	4.5 Hz (Mark L-15B or L-28; 380 Ohm coil w/ 0.7 damping) hydrophone (OAS E-2SD)
External connectors	4-pin (RS-232 comm + time pulse) 3x1-pin (hydrophone+release)
Batteries	D-cell alkaline/lithium (analog+digital+data logger+clock) 9-volt alkaline (pinger+acoustic release) lifetime 18 days recording
Data transfer rates to PC	data transfer by USB2.0 flash card
Recovery Aids	Strobe + Radio beacon (Novatech ST400A, RF700A-1) 12.5 kHz pinger (ITC 3013 transducer)

4.1.2. French OBS

Eight (8) OBSs (seven short-period and one broadband; Figure x) from the INSU-IPGP facility were deployed during the Sismo-Smooth program to record wide-angle seismic data from air gun shots and local earthquakes. A total of 8 deployments were made, contributing to the OBS array for the 3D Box (MAP 2) and for the 2D cross lines (MAP 6). All the instruments were recovered and recorded useable data. Recording characteristics are presented in Table 3.

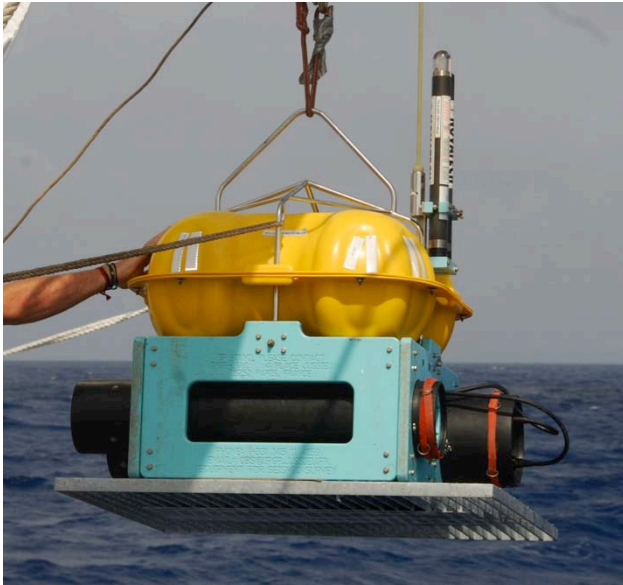


Fig. 4.2 Photographs of an INSU-IPGP OBS (above) and broadband OBS (right).

Short period OBSs. They can be operated at a maximum depth of 5000m. Their weight with the batteries but without the anchor is 125kg in air and -3.5kg in the water. With the anchor the weight in seawater is 29kg. The anchor is released upon reception of an acoustic signal (Edgetech, 2 coded channels with transducer and distancemeter) by electrolysis of an inox burn-wire. A VHF radio, a flash lamp and a red flag help locate the OBS at the sea surface.

The OBSs are equipped with 3 geophones (Sercel L28, leveled in oil, 4.5 - 300 Hz) and a High tech HTI-90u hydrophone (2 Hz to 20 KHz). Data acquisition is hosted in one cylinder (316L aluminum pressure case 80 cm-long x 18 cm in diameter), the release system (including the acoustics) in another cylinder (55 cm x 12 cm), and the geophones with their leveling system in a third and smaller cylinder (10 cm x 8 cm). The instrument is equipped with a Seascan clock (high precision SISMTB) with a typical drift of 4ms/day.

The signal is coded in 24 bits (analog to digital converter board Delta sigma Crystal CS5321 et CS5322). The effective bit number is 21 à 16 Hz or 20 à 125 Hz. The sampling rate options are: 16Hz, 125Hz, 31.25 Hz, 62.5 Hz, 125 Hz, 250 Hz, 500 Hz or 1KHz. The processor is a 1 CPU Motorola 68332 with 256K RAM, 256K EPROM (Real Time System; Fredericksburg, Texas, US). Data are first stored on a 8 Mbyte memory card, then dumped into a disk drive 80 Go IDE.

The OBSs works on lithium batteries and uses 340 mW @ 62.5 Sample/s to 400 mW @ 500 Sample/s. It has over 1 year autonomy @ 62.5Samples/s.

Broadband OBS. It can also be used at 5000 m max, and has the same release system, VHF, flash lamp and flag as the short period OBSs. With the batteries but without the anchor it weights 328 kg in air and -2kg in the water. With the anchor it weights 396 kg in air and 57 kg in the water. Compared to the shorter period instruments it has an additional cylinder for spare batteries (80 cm x 18 cm in diameter).

The seismometer is a Nanometrics Trillium 240 (240 seconds à 35 Hz) in a sphere that is deported from the instrument frame when the instrument reaches the seafloor. The instrument also hosts a differential pressure gauge. It has similar characteristics to the short period OBSs in terms of clock, digital to analog coder, sampling rates, and data storage. It also works on lithium batteries and uses less than 1W @ 62.5 Sample/s to 1.5W @ 500 Sample/s. With the additional batteries it has over 1 year autonomy @ 62,5Samples/s.

4.1.3. Taiwanese OBS

Ten (10) MicroOBS from the National Central University, Taiwan, were deployed during the Sismo-Smooth program to record wide-angle seismic data from air gun shots and local earthquakes. A total of 10 deployments were made, contributing to the OBS array for the 3D Box (MAP 2) and for the 2D cross lines (MAP 6). One OBS was lost (instrument 200- 022 on site T09). All other instruments recorded useable data. Recording characteristics are presented in Table 3.

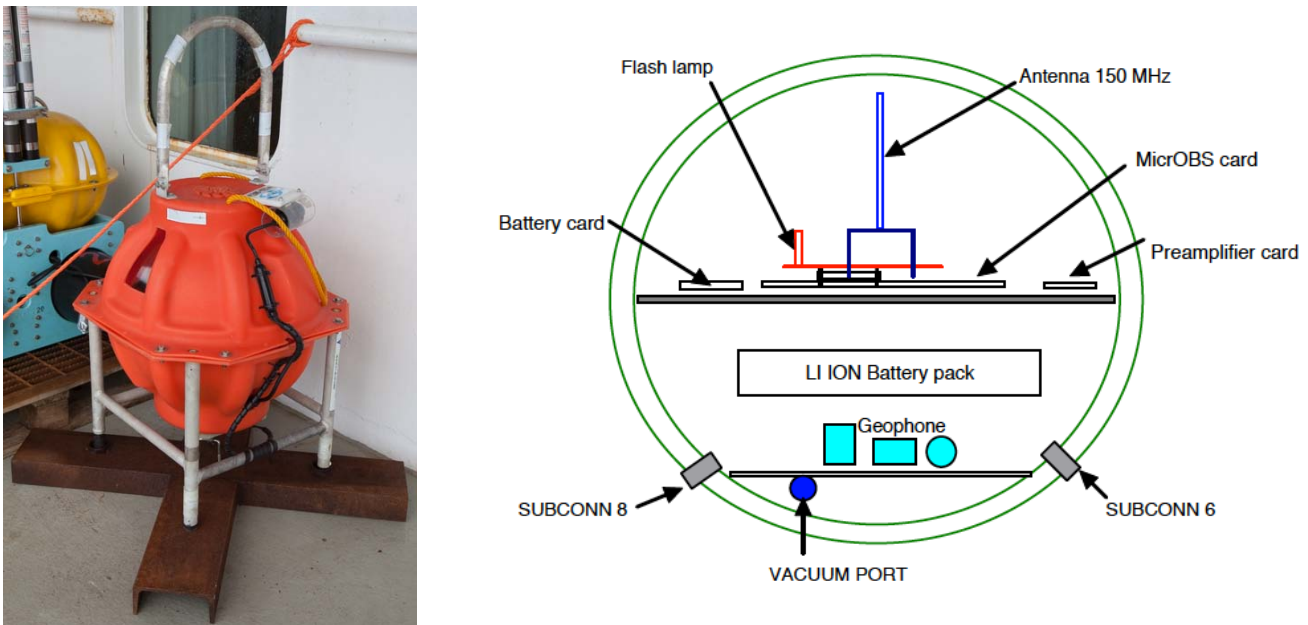


Figure 4.3 Photograph and sketch of one of the 10 MicroOBS from the National Central University, Taiwan.

The MicroOBS_Plus OBSs (Figure x3) are manufactured by SERCEL based on a design developed at Ifremer. The system is powered by rechargeable LI ION pack battery. A 32 days deployment can be achieved with the batteries. Continuous recording is possible over a period of 24 days at 4-ms sampling rate for 4 channels. It is limited by Compact flash capacity (8 GB) and battery power.

The instrument is housed in a 17 inches sphere glass including the sensors, datalogger and release system. It includes the following parts:

- the main electronic card performing the AD 24 bit digitization, the data recording, the acoustic release detection, and the external communication.
- the preamplifier card.
- the battery card
- the flash card for night recovery

- the VHF card for the localization on surface
- a LI ION battery
- and the geophone with a vertical and 2 horizontal channels.

A hydrophone is located outside the sphere and is connected to the electronic with a SUBCONN socket connector. The hydrophone records seismic activities and receives the acoustic release order. The sphere is covered by a protective shell and set in an aluminium frame. A 28Kg iron weight is attached to the MicrOBS_Plus to make it negatively buoyant. This anchor is released on receipt of a coded acoustic signal via the activation of a burn wire. Rise and sink velocities are about of 0.8 meters per second.

The acquisition system is based on a 4-channel 24 bits CS5372/76 analog to digital conversion with input signal amplification. The CS5372 are two-channel high dynamic range, fourth order modulators designed for geophysical applications. When used in combination with CS5376 digital filter, a unique high resolution A/D measurement system results, providing a higher dynamic range of 124 dB @411Hz bandwidth and lower total harmonic distortion than other industry modulators, while consuming significantly less power per channel. The modulators generate an oversampled serial bit stream at 512kbits per second when operated from a clock frequency of 2.048 MHz. MicrOBS_Plus digitizes data with 24-bit resolution and 4 channels can be sampled at the same time.

Each channel can be amplified before digitization. The gain (0dB to 36 dB by step of 6 dB for the hydrophone channel and 20 dB to 56 dB by step of 6 dB for the geophone channels) and the sampling rate (25 Hz, 50 Hz, 100 Hz, 125Hz, 250 Hz, 500 Hz or 1000 Hz) are selected (with a dedicated software) before deployment. A MC68332 Motorola microcontroller is used to collect data coming from the A/D converters before storage in Compact flash memory cards (8 GB).

4.1.4. Source for shooting

The sources used are named source OBS 90s, 150m or 300m depending on the operation done.

It consists for all the OBS experiment of two lines of 7 guns for a nominal volume of 6730in³. See annex for details on volume of each gun.

OBS 90s is used for the refraction 3D box (see map 2 of section 2)

4.2. Data recorded

4.2.1. Extraction of the data from the instruments and check of raw files

All the raw data and converted data file names are shown in the FileNames_OBS_data.xlsx Excel Spreadsheets (4 pages).

4.2.1.1. Canadian instruments

The data of the Canadian instruments are recorded on small binary files (6.145 kB) that are saved on a Compact Flash card on a regular basis. Amplitudes are coded as 2-byte integers. Datasets from these flash cards are backed-up on external hard-drives and on DVD.

A quick initial data check is made at this stage. We used a Matlab program (matlook) that reads the raw files and plot the data along the 4 channels in order to check that there were actual data in these files (check on 1 file out of 100, (Excel file DataCheckDal.xlsx done for the first deployment).

4.2.1.2. French instruments

The data is extracted from the instrument as a unique file containing all the data for every channel for each instrument. Raw data files were checked by Mathilde (CQ_OBS_INSUnew.xls), using lcpot.m.

4.2.1.3. Taiwanese instruments

The MicroOBS internal raw data are composed of (1) numbered data files, which contain alternatively the data of the 4 channels, and (2) one .XML file that contains the cruise parameters. The data files and XML parameter file are downloaded via the USB.

4.2.2. Clock drift

The clock of the instrument is synchronized with the GPS clock before deployment (calibration – start in OBS_Useful_Info.xls) and after recovery (calibration – end in OBS_Useful_Info.xls).

The “a/b” columns refer to the fact that the instrument clock can be either early or late compared to the GPS clock. An “a” means that the instrument clock was ahead (early) compared to the GPS clock at the moment of the calibration. A “b” means that the instrument clock was behind (late). This system is used to avoid confusions between the technicians and the scientists when we just use signed numbers.

4.2.2.1. Canadian instruments

The signed value of the clock drift of these instruments is equal to the OBS time minus the GPS time. All the information about the deployments and recoveries of the Canadian instruments are also available in the 3Dbox_OBS_Drop_Sheet_SismoSmooth_2014.xls and 2DCross_OBS_Drop_Sheet_SismoSmooth_2014.xls Excel files.

4.2.2.2. French instruments

The signed value of the clock drift of these instruments is equal to the GPS time minus the OBS time. All these instruments were ‘behind’.

All the information about the deployments and recoveries of the French instruments are also available in the OBS_INSU_TAIWAN_newformat.xls Excel file.

4.2.2.3. Taiwanese instruments

The raw data format is not usable for geophysical applications. So, the raw data files are split in separate files for each channel. Raw data are thus converted into Psegy (Pseudo-SEG-Y) format, which can be read by MicroOBS Control Center (MCC).

The clock drift of these instruments is taken into account during the conversion of the files using the Microbs Plus program. For now, we don't know if it means that the instrument clocks were early or late compared to the GPS clock during the synchronization. This value is also recorded in the .XML parameter file.

The clock drift is corrected at this stage. Four output Psegy files are created (Channel 1: hydrophone, channel 2: vertical geophone, channel 3 and 4: Horizontal geophones).

All the information about the deployments and recoveries of the Taiwanese instruments are also available in the OBS_INSU_TAIWAN_newformat.xls Excel file.

4.2.3. Shot tables and conversion into segy files

The format of data we need for active seismic SEG-Y. A SEG-Y file is organized as follow:

- A 3600-bytes main header, which contains information about the cruise and the instrument.
- The traces (one trace written after the other). In refraction data processing, traces are usually sorted into receiver gathers. Thus, one section (or file) contains the traces for every shots recorded by one instrument (and one channel here). One trace is coded as follow:
 - o A 240-bytes trace header that contains information about the instrument position, shot position, shot timing, sampling rate, number of samples...
 - o Followed by the actual trace data (amplitudes). The length of this section depends on the number of samples and on how many bytes the amplitudes are coded. The value for the number of samples along a trace is read from the trace header, so it is important to be sure that it is the right value. Also, always rewrite the sampling interval in the headers because the conversion programs sometimes converts floating numbers into integers without rounding (so 3999.999 microseconds becomes 3999 microseconds and can generate some problems in later processing). The time along the trace is computed from the sampling rate and the sample number. The endian of the computer used for the conversion, little for the Canadian and the Taiwanese data and big for the French data, is also important information to be able to read the data later on.

To create SEG-Y files, one first needs to build shot tables that are used by the conversion programs to extract the trace data and properly write its header information.

The three sets of instruments used during this cruise all use different programs for the conversion of the raw data into SEG-Y. And these 3 programs all require different formats and information in order to do the conversion.

4.2.3.1. Creation of the shot tables

Many lines have been shot during this cruise. So, in order to reduce the amount of work during the conversion stage, we chose to prepare only 5 shot tables that contain the shot

information of shots produced during the 5 following operations (reference to ‘operation’ section 2):

- MCS1 corresponds to operation 3 (MCS shots, first deployment of Canadian instruments, 1st phase)
- MCS2 corresponds to operation 5 (MCS shots, first deployment of Canadian instruments, 2nd phase)
- Refr3D corresponds to operation 7 (Refraction shots in the 3D refraction box, first deployment of Canadian instruments)
- Cross1 corresponds to operation 9 (Refraction shots, long profiles, second deployment of Canadian instruments, 1st phase)
- Cross2 corresponds to operation 12 (Refraction shots, long profiles, second deployment of Canadian instruments, 2nd phase)

Louise prepared 2 C-shell scripts to make the shot tables for this cruise:

The first script (`Extract_Shots_Nav_Dals_LCs_Mics_nocor.csh`) prepares shot tables that are not corrected from the shot position, the shot delay and the instrumental clock drift. These files are extracted from the ECOS files provided by Genavir and are named using the following suffix: ‘_uncor’. This script also prepared a navigation file (`Navigation.nav`) that is used for the correction of the Canadian shot tables.

The second script (`Make_cfg_files_run_shottab_allcor.csh`) is first used to create shot tables that are corrected from the shot position, the clock drift and the gun delay, and include the distance between the shot and the receiver for the Canadian instruments, using a python script (`PyShottab1.1.1`). Note that the distances are written as ‘signed offsets’, and these signs are probably unusable in 2D modeling because of the 3D configuration of the shots. One shot table is created per instrument and per shot phase. Then, the new positions computed for the Canadian shot tables are used to modify the shot tables for the French and Taiwanese instruments. This script uses the data from an Excel Spreadsheet (`OBS_Useful_Info.xls`, for Canadian instruments), which is exported into csv (ascii format rather than binary) with tabs as field separators (`OBS_infos.csv`).

These scripts and all the corresponding shot tables can be found in the ‘ShotTables’ directory (in the Canadian OBS data directory).

4.2.3.1.a. Canadian instruments

Shot table names:

C01_MCS1.sht to C20_MCS1.sht (excluding C03 and C04, which were lost),
 C01_MCS2.sht to C20_MCS2.sht (excluding C03 and C04, which were lost),
 C01_Refr3D.sht to C20_Refr3D.sht (excluding C03 and C04, which were lost),
 C21_Cross1.sht to C40_Cross1.sht (excluding C31 and C32, which were not deployed; C37, which was lost, *and we should be able to keep just the 181 first shots for C33 – did not succeed yet...*, which stopped recording after one of its glass sphere imploded),
 C21_Cross2.sht to C36_Cross2.sht (excluding C31 and C32, which were not deployed; C37 was lost; C33 was not recording anymore; and C38-C40 were already recovered).

Beginning of a shot table for a Canadian instrument (C01_Refr3D.sht):

Sismosmooth2014

-27.896690 64.504780 OBS Ref. latitude and longitude

268 5 50 0. Time of clock reset

.0000 Clock drift rate (ms/hr)

0 Delay in firing gun (interger msec)

0 Offset(interger msec):obs&ship clocks

SHOT DAY HR MM SEC LATITUDE LONGITUDE RANGE

1 282 9 12 0.2068 -27.808941 64.607180 14.005

2 282 9 13 30.2065 -27.811041 64.607189 13.845

3 282 9 15 0.2061 -27.813141 64.607194 13.687

4 282 9 16 30.2067 -27.815241 64.607191 13.530

5 282 9 18 0.2062 -27.817341 64.607194 13.376

6 282 9 19 30.2068 -27.819341 64.607196 13.232

7 282 9 21 0.2062 -27.821441 64.607195 13.082

8 282 9 22 30.2064 -27.823441 64.607194 12.942

9 282 9 24 0.2069 -27.825541 64.607092 12.790

10 282 9 25 30.2066 -27.827541 64.607091 12.654

4.2.3.1.b. French instruments

Note: the program that we use to convert the data from these instruments does not require the shot delay information. Thus, this information should be included in the shot file in order to extract the traces from the right bit, corresponding to the actual shot time.

The shot files in the Canadian OBS data directory should be corrected from the shot delay. This can be checked in the second script (a comment close to the end of the script, where this shot delay is added to the times of the shots).

Shot table names:

Shotfile.MCS1

Shotfile.MCS2

Shotfile.Refr3D

Shotfile.Cross1

Shotfile.Cross2

Beginning of a shot table for a French instrument (Shotfile.Cross1, shot delay included. Note that the program which does the conversion does not work if there is a header line in the shot table):

1 14 282 09 12 0.193614 -27 48.5365 64 36.4308

2 14 282 09 13 30.1933 -27 48.6625 64 36.4313

3 14 282 09 15 0.192908 -27 48.7885 64 36.4316

4 14 282 09 16 30.1934 -27 48.9145 64 36.4315

5 14 282 09 18 0.193016 -27 49.0405 64 36.4316

6 14 282 09 19 30.1936 -27 49.1605 64 36.4318

7 14 282 09 21 0.192959 -27 49.2865 64 36.4317

8 14 282 09 22 30.1932 -27 49.4065 64 36.4316

9 14 282 09 24 0.193708 -27 49.5325 64 36.4255

10 14 282 09 25 30.1934 -27 49.6525 64 36.4255

4.2.3.1.c. Taiwanese instruments

Shot table names:

MCS1_Mic.nav

MCS2_Mic.nav

Refr3D_Mic.nav

Cross1_Mic.nav

Cross2_Mic.nav

Beginning of a shot table for a Taiwanese instrument (MCS1_Mic.nav)

Shot	date	time	Latitude	Longitude
000001	29/09/14	08:34:00.1428170	-27.71936100	+064.62898000
000002	29/09/14	08:34:20.1424720	-27.71976100	+064.62898000
000003	29/09/14	08:34:40.1522640	-27.72026100	+064.62898100
000004	29/09/14	08:35:00.1419150	-27.72066100	+064.62898200
000005	29/09/14	08:35:20.1416970	-27.72116100	+064.62898300
000006	29/09/14	08:35:40.1522210	-27.72156100	+064.62898300
000007	29/09/14	08:36:00.1437030	-27.72206100	+064.62898400
000008	29/09/14	08:36:20.1425090	-27.72256100	+064.62908500
000009	29/09/14	08:36:40.1431460	-27.72296100	+064.62908600
000010	29/09/14	08:37:00.1428110	-27.72346100	+064.62908600

4.2.3.2. Conversion into SEG-Y

Trace lengths depend on the shot interval. We chose a 20 seconds trace length for the MCS1 and MCS2 SEG-Y files (MCS shots every 20 seconds) and a 60 seconds trace length for the Refr3D, Cross1 and Cross2 SEG-Y files (Refraction shots every 60 seconds minimum, 60 seconds is more than enough).

4.2.3.2.a. Canadian instruments

The raw data of the Canadian instruments are converted using a DOS program that runs under windows: Dobs2Sgy. This program requires the location of the raw data, the shot file, the trace length and a name for the output files in order to create one file per channel for one instrument and one shot table.

Channel 1 = Hydrophone, channel 2 = Vertical component of the geophone and channels 3 & 4 = Horizontal components of the geophone.

4.2.3.2.b. French instruments

I prepared a script (Make_all_folders_and_segys.csh) that creates the folders structure before running the Python script LCH2SEGY.PY, which prepares the input files and runs the program lch2segy, which finally creates the segy files. This script needs to find the shot tables in a Shotfiles directory (right next to the RawFiles directory) and information about the

instruments, deployments, recoveries and clock-drifts (OBS_INSU_Useful_Info.csv). This file is created by exporting Excel spreadsheet into csv (ascii format rather than binary) with commas as field separators. Add a comma in front of the lines with dates (problem of conversion of a complex xls file, with line breaks into cells, into csv).

The laptop we had during the cruise was very unstable with USB 3.0 hard drives, and did not have enough disk space to process the data on its local hard drive. We ended up producing a complete dataset before finding out that we did not include the shot delay in the shot tables and did not have the time to re-do the files. Thus (repeat), make sure your 'French' data is corrected from the shot delay before using it. It has been done in the Segynew/ directories.

For the broadband instrument: Channel 1 & 2 = Horizontal components of the geophone, channel 3 = Vertical component of the geophone and channel 4 = DPG.

For the short-period instruments: Channel 1 = Hydrophone, channels 2 & 3 = Horizontal components of the geophone and channel 4 = Vertical component of the geophone.

4.2.3.2.c. Taiwanese instruments

SEG-Y files are created from the Psegy files using shot files (*.nav) and split files (*.dec). The split file contains the number of the first and last shot of the profiles and refers to the shot files. The split file is used to cut the Psegy file in one or several Segy files using the shot numbers.

Example of split file (T03-Cross2_Mic.dec):

```
Cross2_Mic 14984 16262 50 14 4640.47 -27.94711777 64.62780803 60000
```

Channel 1 = Hydrophone, channel 2 = Vertical component of the geophone and channels 3 & 4 = Horizontal components of the geophone.

4.2.4. Examples of data in 2D and 3D

4.2.4.1. Examples in 2D

Figures 4.4; 4.5 and 4.6 show record sections from OBS C21 and C36 during shooting of the long, 2D cross profiles.

OBS C21 is an E-W profile along the rift axis. The relatively flat topography along the profile allows us to use the phase velocities shown by the refracted energy of 1st arrival times to estimate the crustal velocity with depth (Figure 4.4). Plotting the vertical time axis with a reduction velocity of 7 km/s means that phase velocities that dip down for ranges of 0 to +/- 10 km indicate a lower velocity in the uppermost crust, while phases that dip up for ranges >10 km indicate higher velocity at depth. Note early arrivals from off-axis topography for ranges 12-20 km and weak arrivals with higher phase velocity for ranges < -15 km that are probably produced by shallower topography.

The shallow structure of the crust is evidenced by arrivals closest to the OBS. In Fig. 4.5 we see evidence for a number of weak wide-angle reflections indicated by the arrows and letters. A is a prominent arrival at ~400 ms which corresponds to the refracted energy of the initial first-arrivals for ranges > 4 km offset. The velocity above this interface does not arrive as a

refracted phase and is not constrained by the OBS data. Deeper wide-angle reflections are indicated by the strong phase D and possible weaker phases B and C.

An example of a N-S profile crossing the rift axis with clear refracted arrivals is shown in Fig. 4.6 for OBS C36. In this case, the phase arrival times are highly distorted by the changes in topography along the profile that requires detailed 2D modeling to determine the velocity structure. However, it is clear that a major boundary in the velocity structure relates to the abrupt change in refracted phase velocity at ~ 17 km.

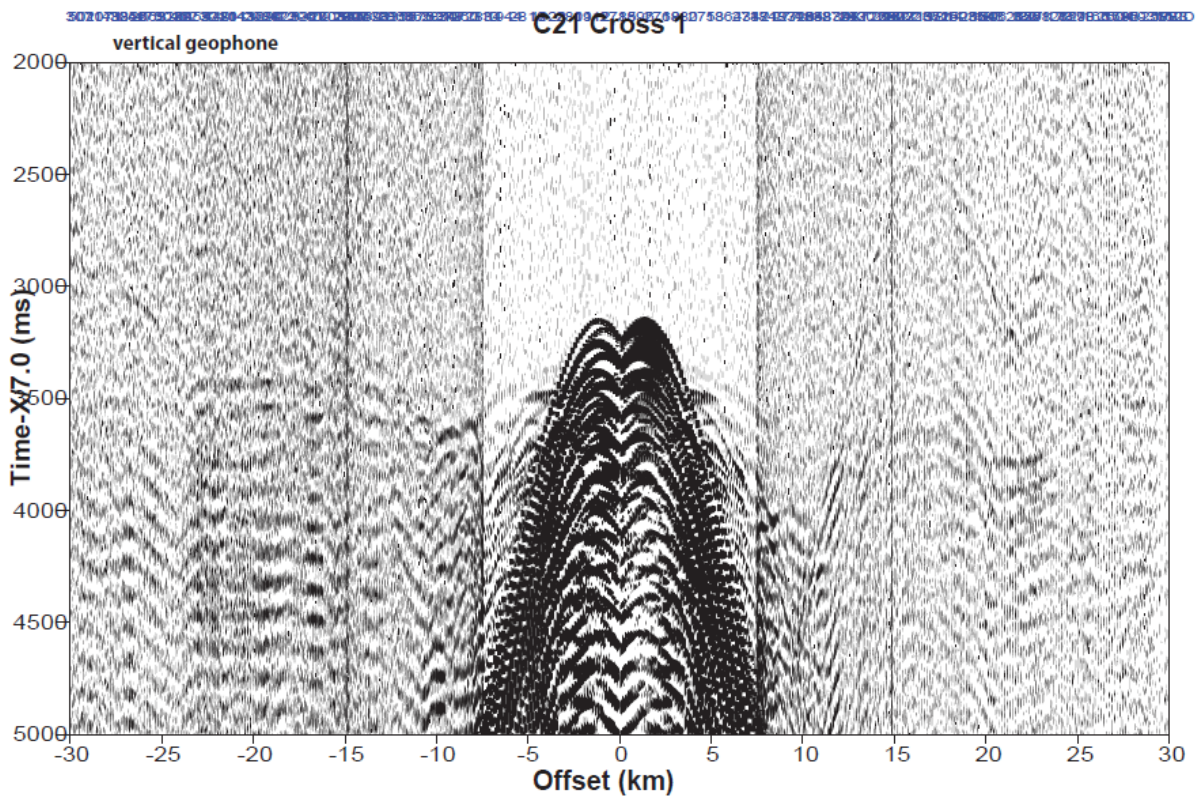


Fig. 4.4 : Example of 2D data, OBS C21 ch2 (during the Cross1 part of the experiment)

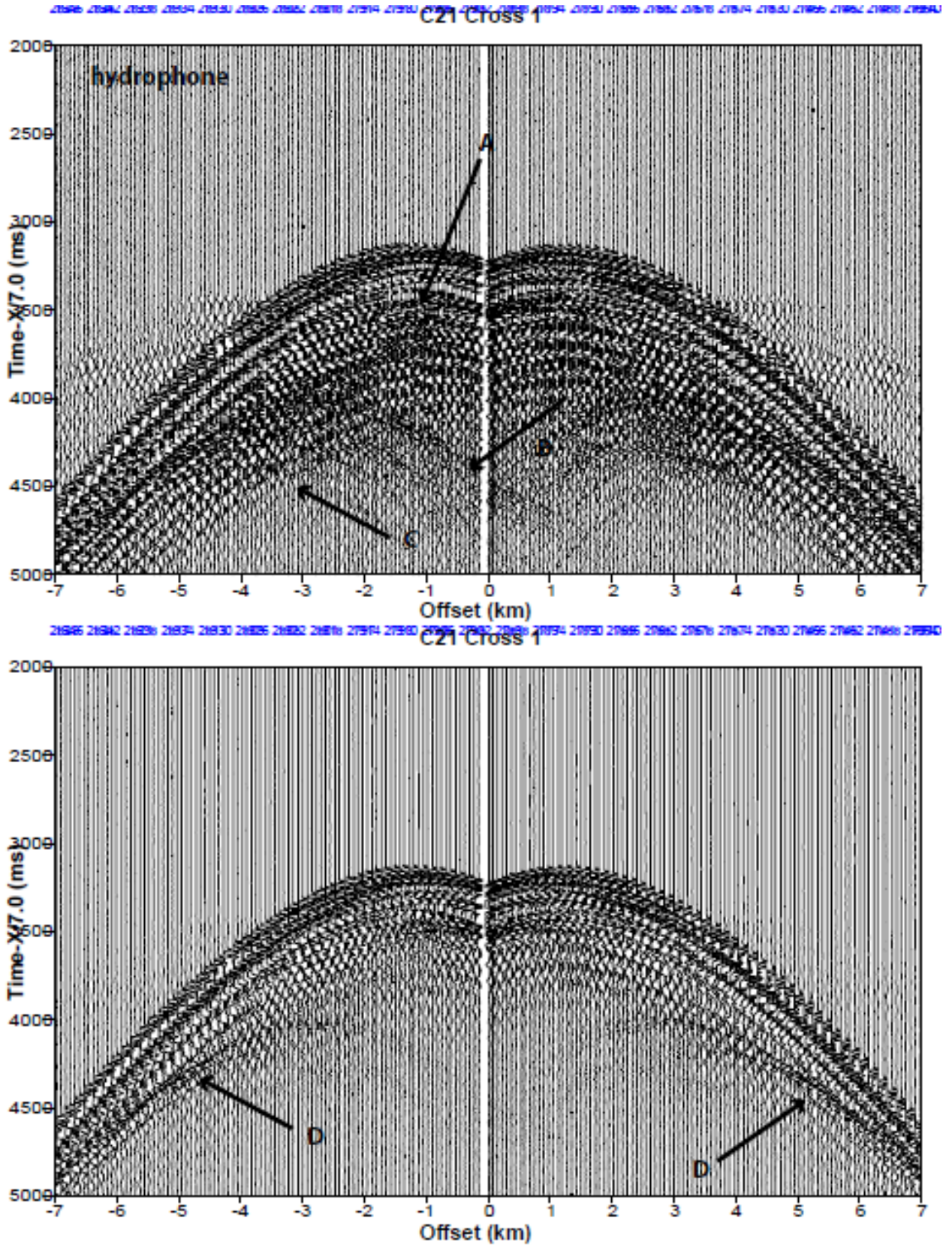


Figure 4.5: Close-ups of the data shown in figure X1, but for ch1, with different gains.

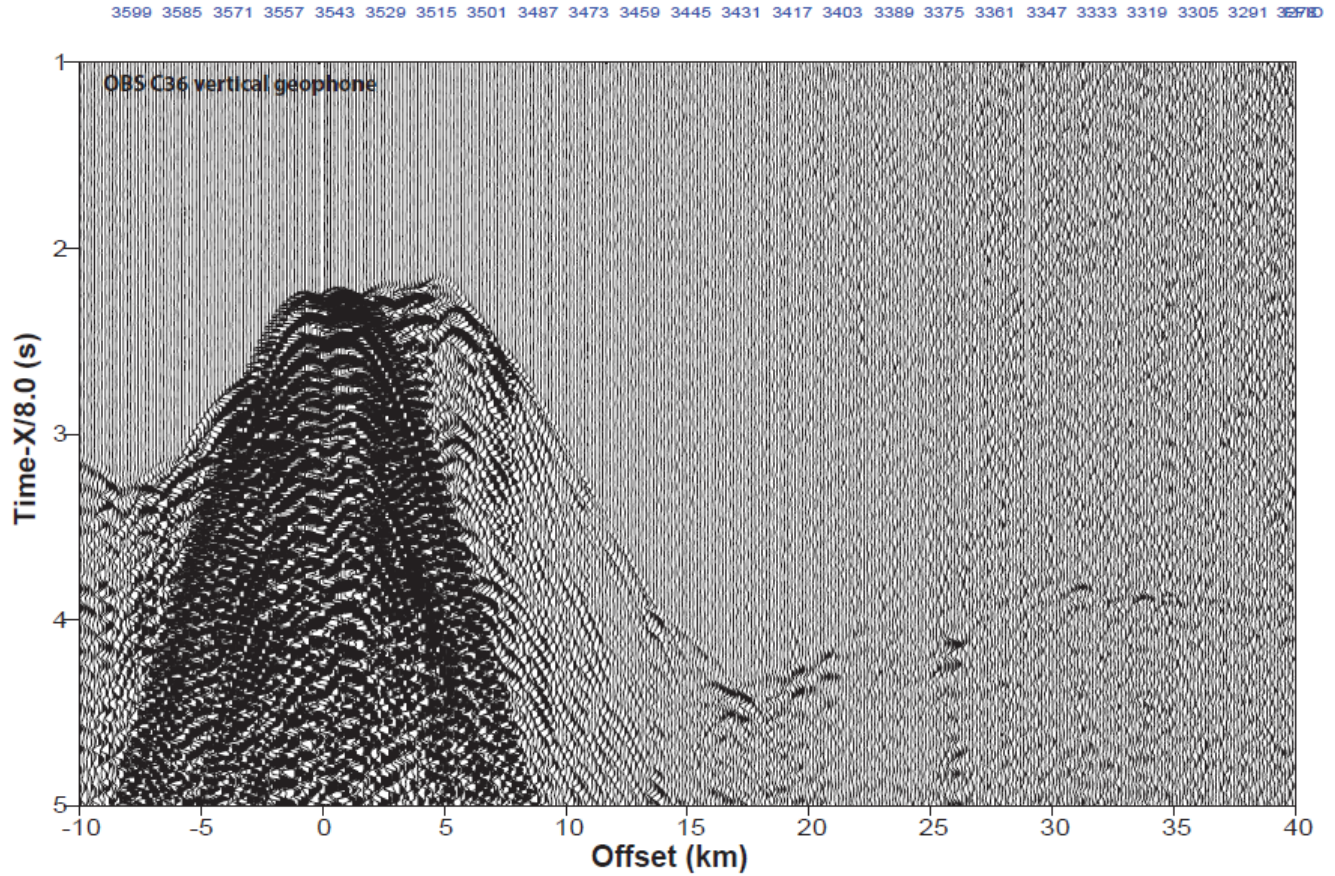


Figure 4.6: Example of 2D data, OBS C36 ch2 (during the Cross1 part of the experiment), showing the effect of the topography of the refracted arrival times.

4.2.4.2. Example in 3D

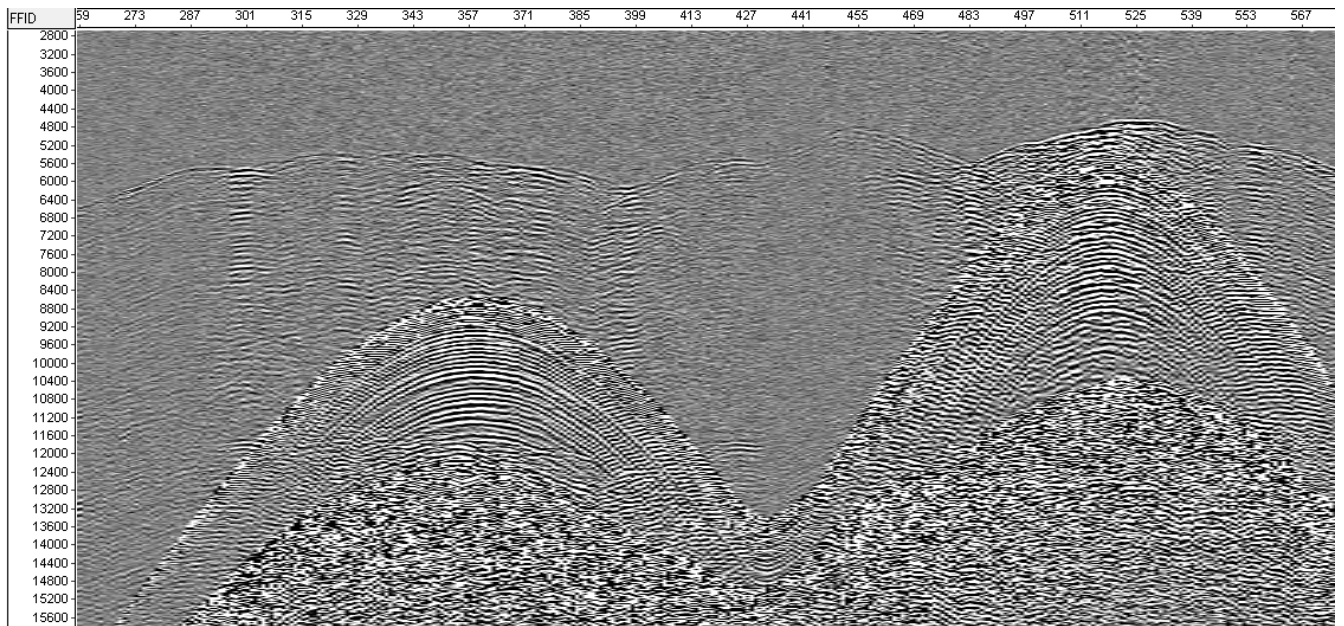


Figure 4.7: Example of 3D arrivals, OBS T09 ch2 (during the Refr3D part of the experiment)

4.3. Recording of local seismicity

Several seismic events have been recorded by the OBSs in their successive configurations (MAPs 2, 6 and 8). Events recorded during MCS or wide angle shooting periods will be difficult to pick, except for large amplitude events. The intervals between these operations are more favorable for a study of seismicity. These « no-shoot » periods are summarized in Table 5. They total 58 h for OBS configuration #1 (MAP 2), 12h21 for OBS configuration #2 (MAP 6), and 5h40 for the OBS array named « configuration #3 » (MAP 8) and resulting from partial recovery of the configuration #2 OBSs.

Table 5. No shot time intervals.

Operations	Start	End	OBS config.	Duration**
OBS deployment #1	28/09-01:37+2h	28/09-18:27+2h		
	No shot 1		(...) #1	(24h) 10h
MCS 1	29/09-06:21	02/10-19:50		
	No shot 2		#1	17h
MCS 1 (cont.)	03/10-12:54	08/10-00:00		
	No shot 3		#1	26h
Aborted ramp-up	09/10-02:24	09/10-02:50		
	No shot 4		#1	5h
Refraction OBS config. #1	09/10-08:07	13/10-03:16		
OBS recov.+deployment #2	13/10-05:05	16/10-00:26+2h		
	No shot 5		(#1...) #2	(74h) 5h
MCS-OBS config.#2	16/10-07:47	19/10-21:23		
OBS partial recovery	20/10-04:44	21/10-20:46		
	No shot 6		#2 (...#3*)	7h21 (53h)
MCS-OBS config.#3	22/10-02:30	23/10-00:52		
OBS final recovery	23/10-06:22	27/10/14-11 :00-3h		
	No shot 6		#3 (#3....)	5h40 (108h18)

* OBS configuration #3 follows partial recovery of the instruments of conf. #2

** Between brackets: maximum no-shot time interval (one or more OBSs of given configuration is-are operational)

Longer « no-shot » periods (between brackets in Table 5) correspond to operations of OBS deployment and recovery. It is possible to figure out which instruments were on the seafloor during these periods, using Table 6 that lists all recovered OBSs with their deployment and retrieval dates.

Preliminary check onboard has focused on seismic events recorded by 5 INSU instruments (I1- I5) during « no-shoot » period #3 (8/10/14-00:00 to 9/10/14-02:24). This preliminary check reveals > 50 events in the record of each OBS for this 26h period, with at least 9 earthquakes that are recorded by the 5 instruments. An example is shown in Figure 4.8. We also detected several periods of sustained but low amplitude ground motion, that do not appear to be recorded by more than one OBS and have most of their amplitude in the horizontal geophone channels. An example is shown in Figure 4.9. The nature of these events is enigmatic. Similar events (earthquakes and strange periods of ground motion) have also been detected at several times in the Canadian OBS records. Data from the Taiwanese instruments have not been examined onboard.

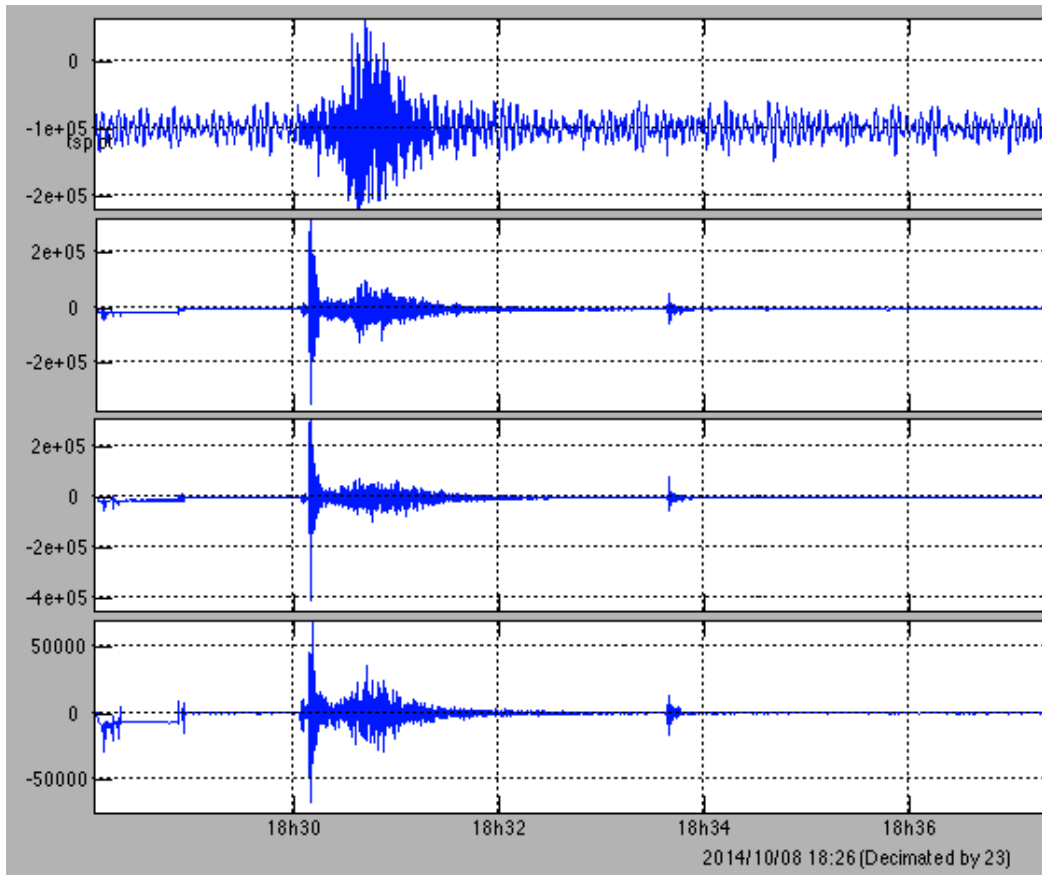


Figure 4.8. Example of earthquake recorded by OBS I2 at 18h30 on October 8, 2014. The upper panel is the hydrophone, the second and third are the horizontal geophone channels, and the lower panel is the vertical geophone channel.

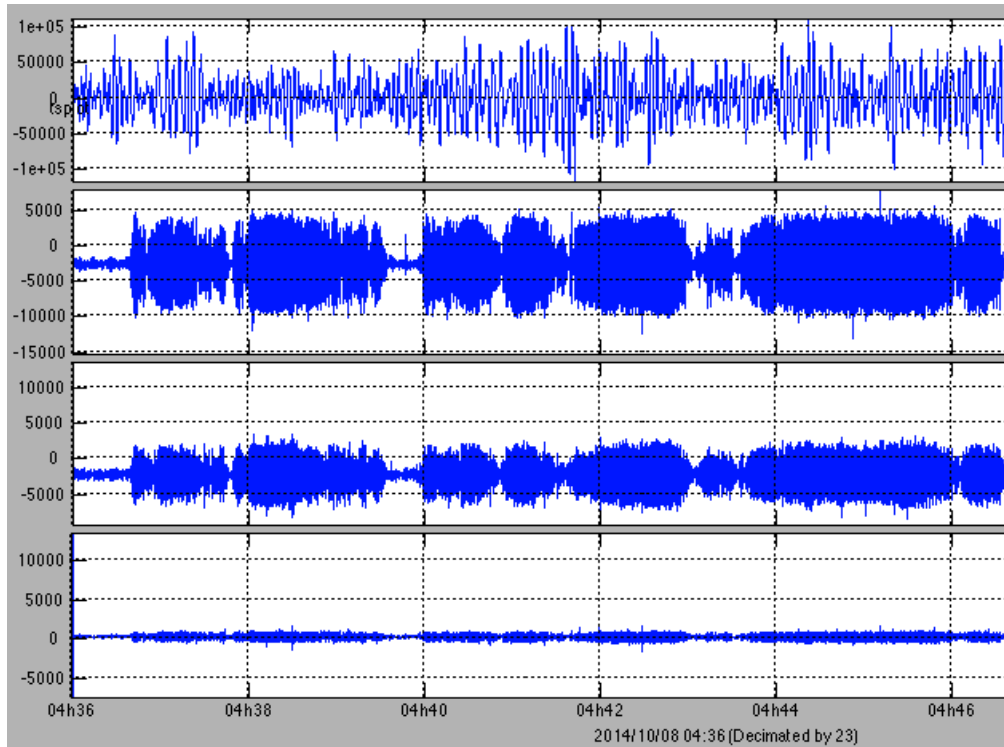


Figure 4.9. Example of strange ground motion sequence recorded by OBS I2 at 04h36 on October 8, 2014. The upper panel is the hydrophone, the second and third are the horizontal geophone channels, and the lower panel is the vertical geophone channel.

4.4. Summary and Quality Control OBS DATA

The output SEG-Y files have been visualized using Seismic-Unix in order to achieve a quick quality control. Observations are shown in an Excel file (QC_OBS_data.xlsx). In this table, JD stands for Julian Day (number of days since the beginning of the year) and the codes from 0 to 3 mean:

- 0 = no usable data
- 1 = very noisy data, might be hard to use
- 2 = a little bit noisy, usually a low frequency noise that is really easy to get rid of using a bandpass filter
- 3 = data looks nice

Note that on all geophone data from the French instruments, there is a high amplitude noise that lasts during 1 or 2 minutes every couple of hours. This noise is very hard to get rid of but does not affect the rest of the data. It can be a problem for further OBS processing (using the waveform for example) but is fine for velocity modeling (plots may look a little bit 'stripy').

NB: To read the SEG-Y data using Seismic-Unix:

```
segypread tape=French_data.segy endian=0 conv=0 | segyclean > output.su
```

```
segypread tape=Canadian_or_Taiwanese_data.segy endian=1 | segyclean > output.su
```

(the segyclean is not always mandatory but it avoids problems with headers in Seismic Unix)

Table 6. Summary of deployment and retrieval date of OBSs

ID	Instrument	Deployment			Retrieval			Position		
		Jday	Date	Time	Jday	Date	Time / deck	Latitude	Longitude	Depth (m)
C33	GSC-H	288	15/10/14	22:10	298	25/10/14	07:36	-27.86783	64.60467	4293
T1	200-073	270	27/09/14	02:09	298	25/10/14	01:35	-27.94700	64.50500	4600
C01	DAL-K	271	28/09/14	01:37	286	13/10/14	10:08	-27.89669	64.50478	4782
C13	DAL-D	271	28/09/14	02:40	286	13/10/14	12:24	-27.99422	64.50501	4564
C14	DAL-I	271	28/09/14	03:09	286	13/10/14	20:07	-28.04350	64.50497	3792
C15	GSC-A	271	28/09/14	03:38	286	13/10/14	21:55	-28.09219	64.50510	3235
C16	GSC-P	271	28/09/14	04:06	287	14/10/14	03:12	-28.13791	64.50592	3403
C17	GSC-C	271	28/09/14	04:40	287	14/10/14	05:38	-28.18456	64.55549	3565
C18	GSC-J	271	28/09/14	05:07	287	14/10/14	01:15	-28.13735	64.55507	3584
C19	GSC-K	271	28/09/14	05:30	286	13/10/14	23:55	-28.09147	64.55532	3602
C20	DFO-M	271	28/09/14	06:18	286	13/10/14	18:06	-28.04303	64.55611	4255
C12	DAL-E	271	28/09/14	06:45	286	13/10/14	15:34	-27.99322	64.55536	4450
I6	OBS07	271	28/09/14	07:10	293	20/10/14	08:26	-27.94600	64.55600	4586
VB1	BB01	271	28/09/14	07:36	297	24/10/14	06:42	-27.89700	64.55500	4897
I1	OBS11	271	28/09/14	08:06	297	24/10/14	03:19	-27.89700	64.60600	4981
T5	200-021	271	28/09/14	08:28	297	24/10/14	07:56	-27.92400	64.60500	5013
I2	OBS15	271	28/09/14	09:23	293	20/10/14	13:31	-27.94800	64.60400	4799
T2	200-023	271	28/09/14	09:45	293	20/10/14	10:28	-27.94700	64.58200	4787
T6	200-059	271	28/09/14	09:45	293	20/10/14	16:01	-27.97100	64.60600	4510
I3	OBS17	271	28/09/14	10:28	293	20/10/14	18:15	-27.99500	64.60500	4425
T7	200-025	271	28/09/14	10:44	294	21/10/14	20:49	-28.01900	64.60500	4240
I4	OBS16	271	28/09/14	11:05	293	20/10/14	20:08	-28.04400	64.60500	3893
T8	200-024	271	28/09/14	11:22	294	21/10/14	19:06	-28.07000	64.60500	4033
I5	OBS18	271	28/09/14	11:39	293	20/10/14	22:05	-28.09300	64.60500	4125
T10	200-043	271	28/09/14	12:08	293	20/10/14	23:45	-28.13900	64.60600	4034
C07	DFO-Z	271	28/09/14	13:02	288	15/10/14	15:15	-28.18290	64.65339	3173
C08	GSC-H	271	28/09/14	13:31	288	15/10/14	13:24	-28.13772	64.65272	4009
C09	GSC-E	271	28/09/14	13:58	288	15/10/14	10:18	-28.09164	64.65274	4206
T3	200-074	271	28/09/14	14:26	297	24/10/14	09:15	-27.94700	64.62700	4730
C10	DAL-F	271	28/09/14	14:28	288	15/10/14	06:31	-28.04297	64.65257	3711
C11	DAL-A	271	28/09/14	14:58	288	15/10/14	02:20	-27.99266	64.65202	4178
I7	OBS20	271	28/09/14	15:46	297	24/10/14	11:04	-27.94700	64.65200	4541
C02	DFO-S	271	28/09/14	16:14	287	14/10/14	16:56	-27.89650	64.65205	4999
T4	200-077	271	28/09/14	17:09	297	24/10/14	13:00	-27.94800	64.70400	4591
C05	DAL-J	271	28/09/14	18:01	288	15/10/14	04:23	-28.04418	64.70491	3752
C06	DAL-G	271	28/09/14	18:29	288	15/10/14	08:04	-28.09256	64.70493	4261
C38	DAL-K	287	14/10/14	06:21	294	21/10/14	06:53	-28.23597	64.60535	4262
C39	DAL-D	287	14/10/14	06:53	294	21/10/14	11:50	-28.28662	64.60580	3298
C40	DAL-E	287	14/10/14	07:24	294	21/10/14	13:40	-28.34275	64.60593	4626
C26	DFO-M	287	14/10/14	10:34	296	23/10/14	09:31	-27.94617	64.29700	4361
C25	DAL-I	287	14/10/14	11:07	296	23/10/14	12:25	-27.94650	64.34350	4207
C24	GSC-A	287	14/10/14	11:46	296	23/10/14	16:36	-27.94650	64.39767	4561
C23	GSC-K	287	14/10/14	12:15	296	23/10/14	18:19	-27.94633	64.43867	4448
C22	GSC-J	287	14/10/14	12:43	296	23/10/14	20:54	-27.94650	64.47950	4435
C21	GSC-P	287	14/10/14	13:20	298	25/10/14	04:39	-27.94667	64.52983	4858
C30	DAL-G	288	15/10/14	19:50	300	27/10/14	09:37	-27.94700	64.80133	4496
C29	DAL-F	288	15/10/14	20:19	297	24/10/14	18:21	-27.94683	64.76533	4620
C28	GSC-J	288	15/10/14	20:46	299	26/10/14	23:32	-27.94683	64.72767	4733
C27	GSC-C	288	15/10/14	21:23	299	26/10/14	19:37	-27.94700	64.67817	4476
C34	GSC-E	288	15/10/14	22:36	298	25/10/14	10:33	-27.84283	64.60467	3057
C35	DFO-Z	288	15/10/14	23:05	298	25/10/14	12:13	-27.81267	64.60483	2525
C36	DAL-A	288	15/10/14	23:35	298	25/10/14	14:55	-27.77850	64.60483	3456

4.4.a. CAN

Table 7. QC for OBS Can data

Station ID	Channel #	MCS1	MCS2	Refr3D	Comments	
C01	1	3	3/0	0	Acquisition problem. Data starts fading out from MCS2-SP23462 to MCS2-SP23906 (from JD278 - 15:14 to 17:42)	
	2	3	3/0	0		
	3	3	3/0	0		
	4	3	3/0	0		
C02	1	3	3	3		
	2	3	3	3		
	3	3	3	3		
	4	3	3	3		
C05	1	3	3	3/2	Data starts fading out from Refr3D-SP3255 (JD 285 - 18:33). Still ~ OK until the end of the acquisition but probably not for earthquakes	
	2	3	3	3/2		
	3	3	3	3/2		
	4	3	3	3/2		
C06	1	3	3	3/1	Good data until Refr3D-SP3302	
	2	3/1	3/1	(3)/1	Same as channel 1 + very bad in many other places	
	3	3/1	3/1	(3)/1		
	4	3	3	3		
C07	1	3	3	3/2	Data starts fading out from Refr3D-SP3407 (JD 285 - 22:21). Still ~ OK until the end of the acquisition but probably not for earthquakes	
	2	3	3	3/2		
	3	3	3	3/2		
	4	3	3	3/2		
C08	1	3	3/2	3/2	Just needs a gentle BP filter in some places	
	2	3	3	3		
	3	3	3	3		
	4	3	3	3		
C09	1	1/2/3	3/2	3/2	Very variable quality	
	2	3	3	3		
	3	3	3	3		
	4	3	3	3		
C10	1	1/2/3	1	1	Generally very noisy	
	2	1/2/3	3/2/1	3/1	Very variable quality	
	3	1/2/3	3/2/1	3/1		
	4	3/2/(1)	3/(2)	3/1	Variable, more good than bad though	
C11	1	3	3	3/2	Data starts fading out from Refr3D-SP3256 (JD 285 - 18:34). Still ~ OK until the end of the acquisition but probably not for earthquakes	
	2	3	3	3/2		
	3	3	3	3/2		
	4	3	3	3/2		
C12	1	3	3	3		
	2	3	3	3		
	3	3	3	3		
	4	3	3	3		
C13	1	3	3	3		
	2	2/3	2/3	2		
	3	1/2/3	3/2/1	3/(1)		Variable quality of data
	4	0	0	0		Just noise

Station ID	Channel #	MCS1	MCS2	Refr3D	Comments
C14	1	3	3	3/2	Data starts fading out from Refr3D-SP3181 (JD 285 - 16:42). Still ~ OK until the end of the acquisition but probably not for earthquakes
	2	3	3	3/2	
	3	3	3	3/2	
	4	3	3	3/2	
C15	1	2	2	2	Needs low frequency bandpass filter
	2	3	3	3	
	3	3	3	3	
	4	3	3	3	
C16	1	3	3/2	3/(2)	Low frequency noise in some places + spikes
	2	3	3	3	
	3	3	3	3	
	4	3	3	3	
C17	1	3	3	3	
	2	3	3	3	
	3	3	3	3	
	4	3	3	3	
C18	1	2	2	2	
	2	3	3	3	
	3	3	3	3	
	4	3	3	3	
C19	1	3	3	3/0	Just noise from Refr3D-SP2640 (JD 285 - 03:10) Geophone data starts fading out (brutal for channel 3) from Refr3D-SP3212 (JD 285 - 17:28). Not sure for later earthquake data
	2	3	3	3/2	
	3	3/2	2	2/0	
	4	3/2	3/2	3/2	
C20	1	3	3	3	Generally good data, variable noise (low frequency for channel 3)
	2	3/1	3/1	3/2	
	3	3/2	3/2	3/2	
	4	3	3	3	
C21	1	1/2	2/1		Variable quality
	2	3/(1)	3		Stripes of noisy data
	3	3	3		
	4	3	3		Noise stripe at SP 700-770
C22	1	2	2		Low frequency noise
	2	3/(1)	3		Stripes of noisy data
	3	1	1		Bad quality / recording problem?
	4	3/(1)	3		Stripes of noisy data
C23	1	2	3/2		high amplitude low frequency noise???
	2	3	3/2		Stripes of noisy data
	3	3/1	3/1		Not much refracted arrivals
	4	2/(1)	2		Low frequency noise
C24	1	2	2		Low frequency noise, some bursts
	2	3	3		
	3	1	1/(2)		Bursts, recording problem
	4	2	2		Stripes of noisy data

Station ID	Channel #	Cross1	Cross2	Comments
C25	1	2	3	Stripes of noisy data, low frequency noise
	2	3/1	3/(1)	Large stripes of low frequency noise
	3	1/3	1/3	
	4	1/3	1/3	
C26	1	3/(1)	3	Stripes of low frequency noise
	2	2/1	2	Low amplitudes but things to see
	3	1	1	Low amplitudes
	4	1	1	Low amplitudes
C27	1	1/(2)	2/1	Bursts, low frequency noise, things to see
	2	1/(2)	3/2	Stripes of noisy data
	3	1/(3)	3	Very noisy but nice data in between
	4	1/3	3	Very noisy but nice data in between
C28	1	1/3	3	Very noisy but nice data in between, bursts
	2	2/3	3/2	Stripes of noisy data
	3	3/1	3	Stripes of noisy data
	4	3/1	3/1	6 Hz noise
C29	1	0/1	0	Very low amplitude, almost all white
	2	1	1	Vey noisy all along the data, 6 Hz noise
	3	0/1	0/1	Stripes of low amplitudes
	4	1/2	3/1	Vey noisy all along the data, 6 Hz noise
C30	1	3/2	3	Noise, stripes of low frequency noise
	2	1/(2)	1	Low frequency noise all along the data
	3	1/(2)	1	Low frequency noise all along the data
	4	1/(2)	1	Low frequency noise all along the data
C33	1	not yet		
	2	not yet		
	3	not yet		
	4	not yet		
C34	1	3/2	3/2	Presence of spikes + low frequency noise
	2	3	3	
	3	3/2	3/2	
	4	3	3	But little refracted arrivals
C35	1	3/2	3/2	Low frequency noise
	2	3/1	3/1	Stripes of noise
	3	3/1	3/1	
	4	(3)/1	(3)/1	
C36	1	3/2	3/2	~ Low frequency noise
	2	3	3	
	3	3	3	
	4	3	3	
C38	1	3/2		Low frequency noise
	2	3/1		Stipes of 6 Hz noise. S-waves?
	3	3/2		Noisy but not as bad as channel 2
	4	3/2		Not much refracted arrivals and noisy like ch3
C39	1	2/1		? Very noisy but things to see / picks
	2	3/1		
	3	3		
	4	0		

Station ID	Channel #	Cross1	Cross2	Comments
C40	1	3/2		Low frequency noise
	2	3		
	3	3/1		(?) Noisy / weak signal ?
	4	3/1		

4.4.b. INSU

Table 8. QC for OBS Insu-lpgp data

Site	OBS#	Recording Starts	Ends	Overall quality	Near shots
I1	11	28/09-23:00	24/10-03:11	No record of vertical channel and one horizontal channel is intermittent	9/10-10:05-10:20 & 11/10-11:40-11:55
I2	15	29/09-15:00	20/10-13:23	OK	9/10-10:42-10:55 & 11/10-07:44-07:58
I3	17	29/09-15:00	20/10-18:01	No record of one horizontal channel	9/10-11:16-11:28 & 11/10-04:11-04:23
I4	16	29/09-02:00	20/10-20:13	No record of vertical channel	9/10-11:51-12:02 & 11/10-00:09-00:21
I5	18	29/09-02:00	20/10-22:12	OK	9/10-12:27-12:38 & 10/10-20:39-20:51
I6	7	28/09-19:00	20/10-08:36	No record of vertical channel	9/10-21:58-22:11 & 11/10-07:13-07:26
I7	20	29/10-02:00	24/10-10:49	OK	10/10-05:41-05:54 & 11/10-08:1608:27
VB1	BB01	28/09-19:00	24/10-06:28	4 channels, one horizontal is noisy	9/10-21:20-21:40 & 11/10-12:15-12:30

Station ID	Channel #	MCS1	MCS2	Refr3D	Cross1	Cross2	Comments
I01	1	2/3	3/2	3/2	3/2	3/2	Low frequency noise
	2	0	0	0	0	0	All white / no data
	3	3	3	3/0?	3/2?	3	White vertical lines (see report) + missing traces in Refr3D for ch3
	4	3	3	3	3/2	3	
I02	1	3/2	3/(2)	3/2	3/2		Low frequency noise
	2	3	3	3	3		White vertical lines + low amplitude noise (white stripes) for ch2 & 3
	3	3	3	3	3		
	4	3	3	3	3		
I03	1	3/2	3/2	3/2	3/2		Low frequency noise
	2	0	0	0/3	3		Woke up at some point (did not check the SP and time)
	3	3/2	3/2	3	3/2		White vertical lines + stripes of noisy data (6 Hz?)
	4	3/2	3/2	3	3/2		

Station ID	Channel #	MCS1	MCS2	Refr3D	Cross1	Cross2	Comments
I04	1	3/2	3/2	3/2	3/2		Low frequency noise
	2	0	0	0	0		
	3	3/2	3/2	3	3/2		White vertical lines + noisy
	4	3	3	3	3/(2)		White vertical lines + low amplitude noise (sometimes)
I05	1	3/2	3/2	3/2	3/2		Low frequency noise
	2	3	3/(2)	3/(2)	3		White vertical lines + noisy
	3	3/2	3/(2)	3/(2)	3		As ch2 + 6 Hz noise (?)
	4	3/2	3	3	3		
I06	1	3/2	3/2	3/2	3/2		Low frequency noise
	2	2/1	2	3	3		Not much refracted arrivals
	3	1/2	2/1	2	2/1		Stripes of noisy data + not much refracted arrivals
	4	0	0	0	0		No data
I07	1	3/2	3/2	3/2	3/2	3/2	Low frequency noise
	2	3/(1)	3/(1)	3	3	3	Stripes of noisy data + 6 Hz noise
	3	3/2	3/2	3	3/(2)	3	Stripes of noisy data
	4	3	3/(1)	3/(1)	3/(1)	3	6 Hz noise
VBB1	1	2	2	0(?)	0(?)	0(?)	Definitely needs a low frequency filter and data is uncertain for Refr3D and Cross1 and 2...
	2	2	2	0(?)	0(?)	0(?)	
	3	2	3	2(?)	2(?)	2(?)	
	4	2	2	2(?)	0(?)	0(?)	

4.4.c. Taiwan

Table 9. QC for OBS Taiwanese data

Station ID	Channel #	MCS1	MCS2	Refr3D	Cross1	Cross2	Comments	No data
T01	1	2/3	2/3	2/3	2/3	2/0	Low frequency noise	Stopped recording at Cross2 SP4114 (JD 295 - 11:54)
	2	3	3	3	3	3/0	Noisy traces	
	3	3	3	3	3	3/0	Little refractions	
	4	3	3	3	3	3/0	(?) + noisy traces	
T02	1	0/2	2	2	2		Low frequency noise	Started recording at MCS1 SP160 (JD 272 - 09:27)
	2	0/3	3	3	3			
	3	0/3	3	3	3		Little refractions	
	4	0/3	3	3	3			
T03	1	2/3	2/3	2/3	2/3	2/0	Low frequency noise	Stopped recording at Cross2 SP4537 (JD 295 - 18:55)
	2	3	3	3	3	3/0		
	3	3	3	3	3	3/0	Little refractions	
	4	3	3	3	3	3/0		

Station ID	Channel #	MCS1	MCS2	Refr3D	Cross1	Cross2	Comments	No data
T04	1	3	3	3	3	3/0		Stopped recording at Cross2 SP4536 (JD 295 - 18:54)
	2	3	3	3	3	3/0	Noisy traces here and there	
	3	3	3	3	3	3/0	Little refractions	
	4	3	3	3	3	3/0		
T05	1	0/3	3	3	3	3	Low frequency noise	Started recording at MCS1 SP1156 (JD 272 - 14:59)
	2	0/3	3	3	3	3		
	3	0/3	3	3	3	3		
	4	0/3	3	3	3	3		
T06	1	0/2	2	2	2		Low frequency noise	Started recording at MCS1 SP1156 (JD 272 - 14:59)
	2	0/3	3	3	3			
	3	0/3	3	3	3		Little refractions	
	4	0/3	3	3	3			
T07	1	2/3	2/3	2/3	2/3		Low frequency noise	
	2	1/2	1/2	1/2	1/2		Noisy or weak? + little refractions	
	3	1/2	1/2	1/2	1/2		Little refractions	
	4	2/1	2/1	2/1	2/1			
T08	1	3	3	3	3			
	2	3	3	3	3			
	3	3	3	3	3		Little refractions	
	4	3	3	3	3			
T10	1	2/3	2/3	2/3	2/3		Low frequency noise	
	2	3	3	3	3			
	3	3	3	3	3			
	4	3	3	3	3			

5. Magnetism

5.1. Magnetic field data acquisition

IPEV's SeaSPY marine magnetometer was used during the transit to measure the value of the earth's magnetic field. Once in the survey area this magnetometer was removed. During the MCS survey magnetic data were collected using the GENAVIR SeaSPY magnetometer located at the very end of the streamer. We use these data to map the magnetic anomalies in the survey area. By magnetic anomaly we mean deviations from the usual intensity of the earth's magnetic field. The unit of measurement used to express the intensity of the earth's magnetic field is the nanotesla.

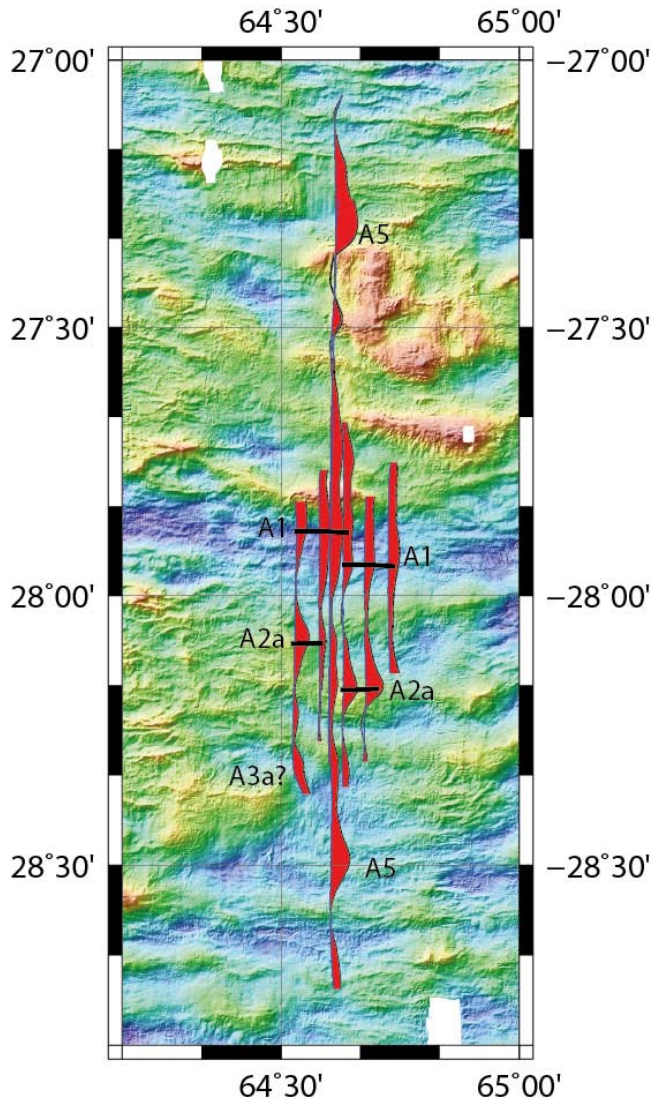
SeaSPY is an Overhauser magnetometer. Although still relying on proton spin resonance, Overhauser magnetometers are different from the magnetometers known as "proton magnetometers". Since Overhauser magnetometers measure the same proton-resonance spectral line as standard proton magnetometers, they exhibit the same excellent accuracy and long-term stability characteristics. Added to this are larger bandwidth, lower power consumption, and sensitivity that is one to two orders of magnitude better.

The tow cable on the R/V Marion Dufresne is 360 m long. Genavir's SeaSPY magnetometer is located 50m behind the tail buoy of the streamer. Magnetic data of the SeaSPY magnetometers were archived in raw data files and made available in the board sensors database. See the READ_ME files in each sub directory (e.g. "Mag/Mag_data_1st_MCS_survey") explaining how the files are obtained. The scripts containing the awk line commands are in the "./Mag/Cmd_awks" directory.

5.2. Data Processing

Here we focus on the magnetic data from the GENAVIR magnetometer (Fig. 5.1) that are archived in daily "date.ECO" data files. Date, time, GPS location of the tail buoy and the value of the magnetic field are extracted using an awk command from messages beginning by "\$NAECO,<date>,NATIR, ...". These messages are recorded at each shot, that is every 20s for the first MCS survey and 120-50s for the following ones. Date, time and location are then used to calculate the reference field (IGRF) at every shot points.

The magnetic anomaly is obtained by subtracting the International Geomagnetic Reference Field (IGRF2010) from the observed field data. As the distance between the tail buoy and the magnetometer is small (50m) relatively to the distance to the sources at or below the seafloor we have not recalculated the position of the magnetometer and have disregarded this distance between the tail buoy and the magnetometer. This calculation is probably not accurate as we use the predicted magnetic field. As the magnetic field is changing rather "quickly" this calculation should be redone with the new IGRF which will come out in a few months.



The overall quality of the data is very good: there are no spikes and the noise level is very low. We calculated the difference of the values of the magnetic anomaly at the crossing points for the two MCS surveys. The mean of the absolute values of these differences is low (9.0 nT with a standard deviation of 8.7 nT) indicating consistent measurements along the MCS surveys.

Figure 5.1 shows the magnetic anomalies plotted along the ship track for a projection azimuth of 90 degrees. This plot best reveals East-West trending anomalies that may be related to sea floor spreading.

5.3. Interpretation

Magnetic anomalies can be used to identify the position of specific magnetic reversals on the sea floor and determine the age of the ocean floor as shown on figures 5.1 and 5.2. However, the ultra slow spreading of the SWIR produces small magnetized bodies with opposite polarity whose signatures are merging leading often to weak ill defined magnetic anomalies especially in the exhumed mantle domains. The contamination between blocs of contrasted magnetization can be modeled (see figure 5.3) showing that small anomalies can almost disappear or at least could be very subdued. Therefore, the identification of small anomalies like C2 or C2a is difficult and other isochrons than the well marked C5n should be taken with caution.

We have used all the magnetic anomaly data (including the turns) to make a new grid in the survey area. We subtract 52.8nT to the data as this value is the mean difference between the Sismo-Smooth data and older data from previous cruises. This is probably because the calculation of the magnetic anomaly is not accurate as we use the predictive magnetic field. We then could calculate the grid by merging the Sismo-Smooth data with earlier data. The new grid shows better defined anomalies as the survey area is better sampled as before (Figure 5.4). The arrow in figure 4 shows an interruption of a magnetic anomaly that was not seen before with sea surface data but only with deep towed data. This

anomaly may correspond to anomaly C2a (see Figures 5.1 and 5.2). The new grid shows now a clear NS offset with the eastern part 9 km more to the south relative to the western part. This may have been produced by detachment faulting occurring to the east while volcanism is dominating to the west.

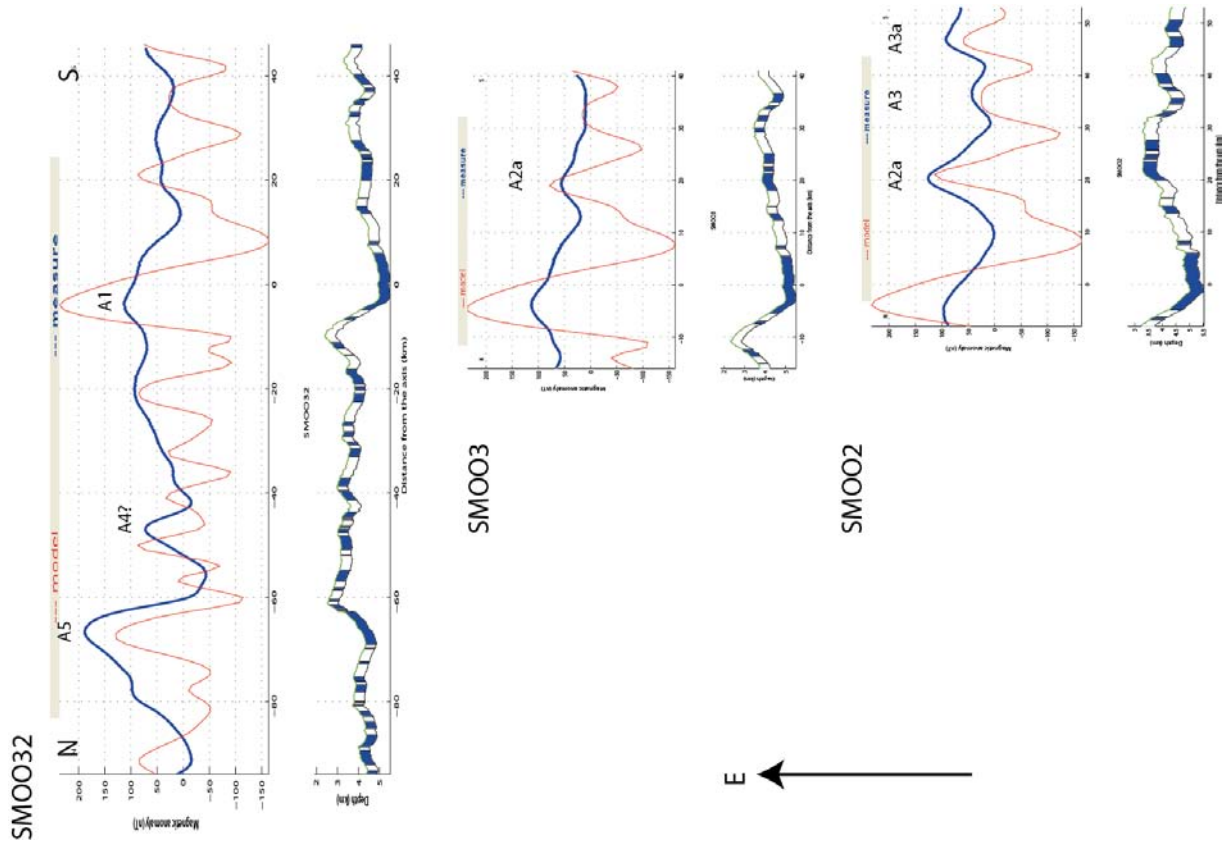


Figure 5.2: Observed magnetic anomaly (in blue) along profiles 2 to 5 and synthetic magnetic anomaly profiles (in red). These models are calculated from a two-dimensional block model (bottom) incorporating calibrated magnetic inversion time scale of Cande and Kent (1995), with a 14 km/Myr spreading rate. We assume a constant 500m thick magnetic layer draped on bathymetry with a ± 10 A/m magnetization for the central anomaly and an uniform ± 5 A/m magnetization elsewhere, as usual.

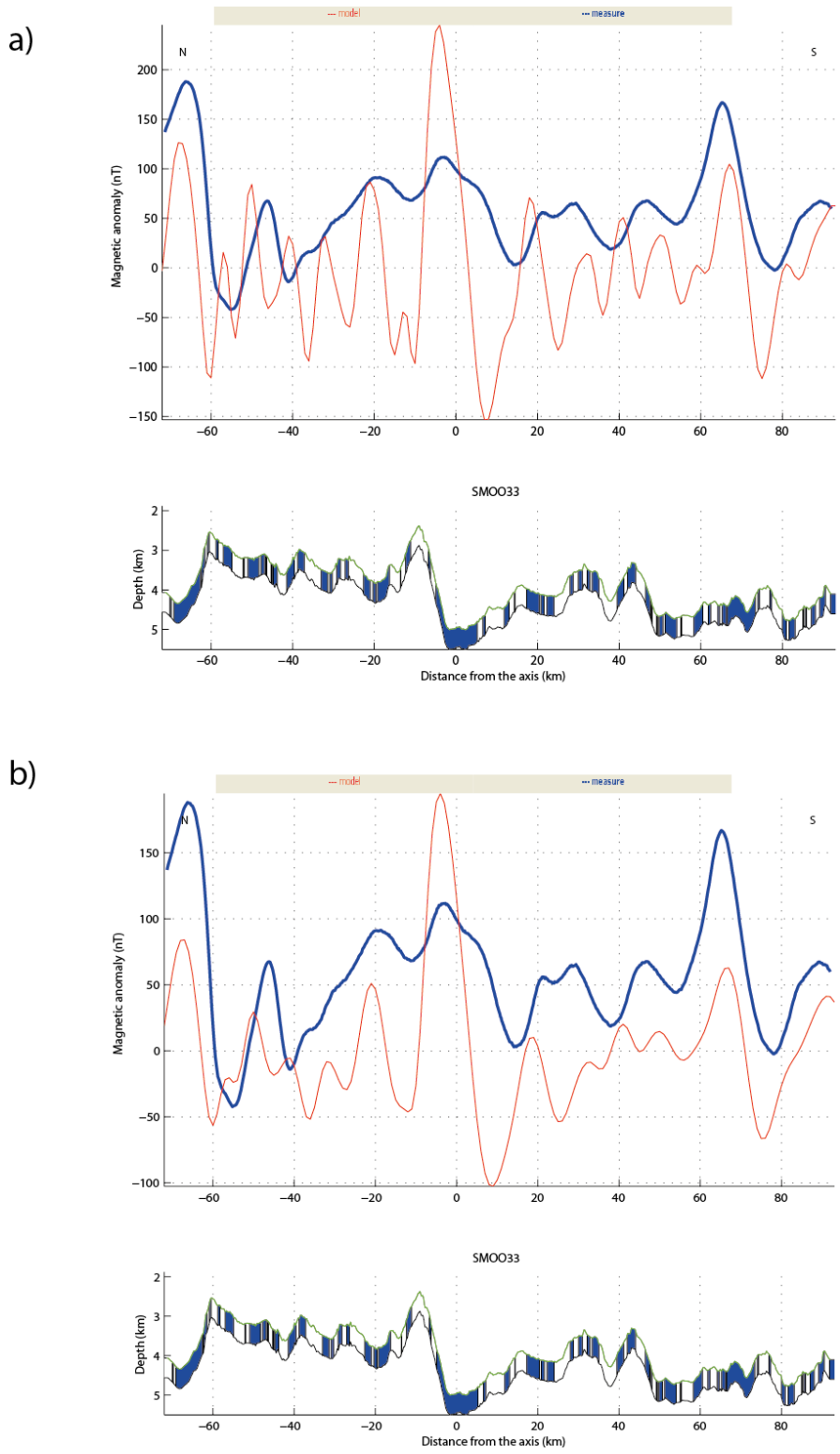


Figure 5.3. Observed magnetic anomaly (in blue) along profile 33 and synthetic magnetic anomaly profiles (in red). Top: as in figure 5.2 (no contamination). Below: contamination between bodies of reversed polarity is used to better render the ill defined anomalies.

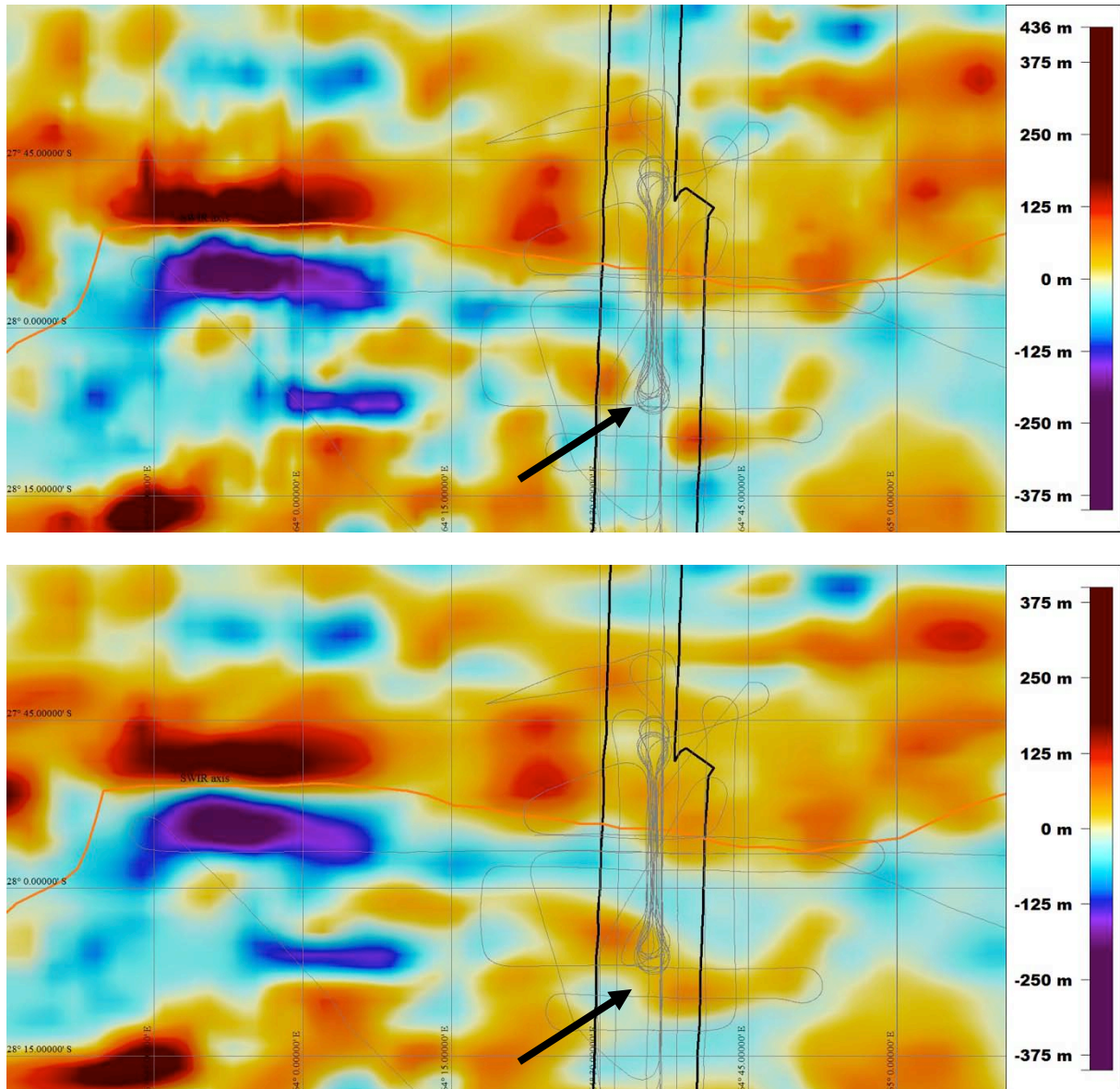


Figure 5.4: Magnetic anomaly map of the SWIR ridge axis using the Sismo-Smooth data (top) compared with the map made with previous data (bottom).

6. Sub-bottom profiles (SBP)

6.1. The 3.5 kHz sub-bottom profiler of the Marion Dufresne

(from the technical prospectus written by Xavier Morin, IPEV)

The Seafalcon 11 echosounder also includes a sub-bottom profiler. Beam forming from many signals received on each sensor provides a very narrow antenna diagram (high directivity), during transmission (7.4°) and reception (5.6°). This beam formation also achieves a high acoustic signal level. Indeed, one of the main features of this profiler is the use of a large dedicated transmission array, and the use of the large bandwidth and long size multibeam reception array in order to create a high acoustic level signal and a very narrow beamwidth. While classical profilers beamwidths are usually wide (20° to 30°), the Seafalcon 11 echosounder produces a 7.4° width beam. This feature prevents interferences between different objects located in the illuminated scene, and achieves a very good along-track resolution. The central frequency used for this system is equal to 3.75 KHz. As for the “bathymetry and imaging” mode, the transmitted wave is linearly frequency modulated. The corresponding correlation gain is equal to 23 dB. The large transmitted bandwidth (1.6 KHz) achieves a small vertical resolution (0.45 metres).

Five beams are created on reception (the central beam is vertical), separated from each other by 5°. This diversity provides an opportunity to record good quality profiles when the across-track slope is steep. Typically, 100 metres penetrations are achieved for a 4000 metres depth. The maximal observed penetrations are around 200 metres.

The ship’s attitudes are used in order to determine the exact location of each sounding. Two high performance Heading and Vertical Reference Unit (HVRU) are installed on the Marion-Dufresne to measure the ship’s attitudes.

6.2. 3.5 KHz data acquisition and shipboard processing

Sub-bottom profiler data were acquired: - on September 28 and 29 during the transit to the study area, at ship’s speeds > 10 knots; and on October 8 and 9 at 2 knots. Data from the first survey are noisy and frequently interrupted. Data for the low speed survey are better, but the area surveyed (the axial valley floor in the area of the first OBS deployment; see MAP 5 in the Operations section 2) lacks a significant sediment cover. The data does, however, show the offsets of several minor normal faults.

Data files from the Thomson sub-bottom profiler are acoustic profiles in time, written in an “owner” format (*.SBP; stored in the SCIENCE/SBP/SBP_SBP folder) that can only be read by SBP-Visu, an IPEV software available on board. SBP-Visu allows to play the data set in order to obtain reflection profiles in “pseudo-depth”. In order to convert the values from time to depth, the software uses a constant celerity value of 1500 m/s in the seawater and in the sediments.

SBP-Visu is used in a real time mode during acquisition and automatically saves images. We also made screen copies that are stored in the SCIENCE/SBP/VISU_SBP folder.

We used the sbp2segy.exe script (IPEV) to convert the *.SBP files to SEG Y files (stored in the SCIENCE/SBP/SBP_SEGY folder) that may be processed later, using more realistic celerity profiles for the sediment layers and using the data from the 4 side beams.

7. Multibeam Bathymetry

The multibeam echo sounder Thomson Seafalcon has been switched on for filling small gaps in the bathymetric grid obtained with previously collected data (figure 7.1). The survey began the 25th of October at 23:00 up to the 26th at 02:00 while waiting for the automatic release of OBS T09.

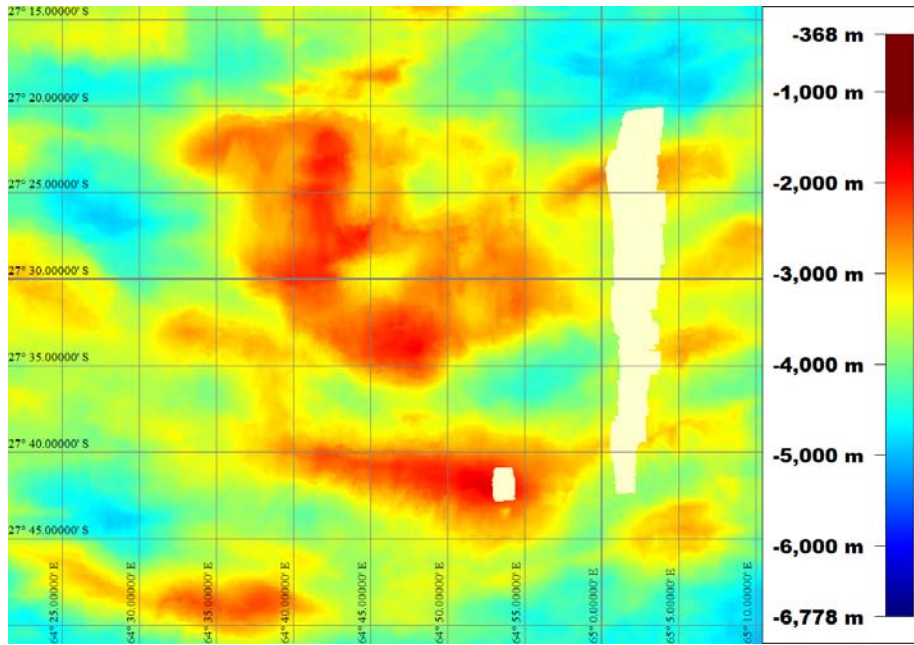


Figure 7.1: Multibeam bathymetric grid before the survey.

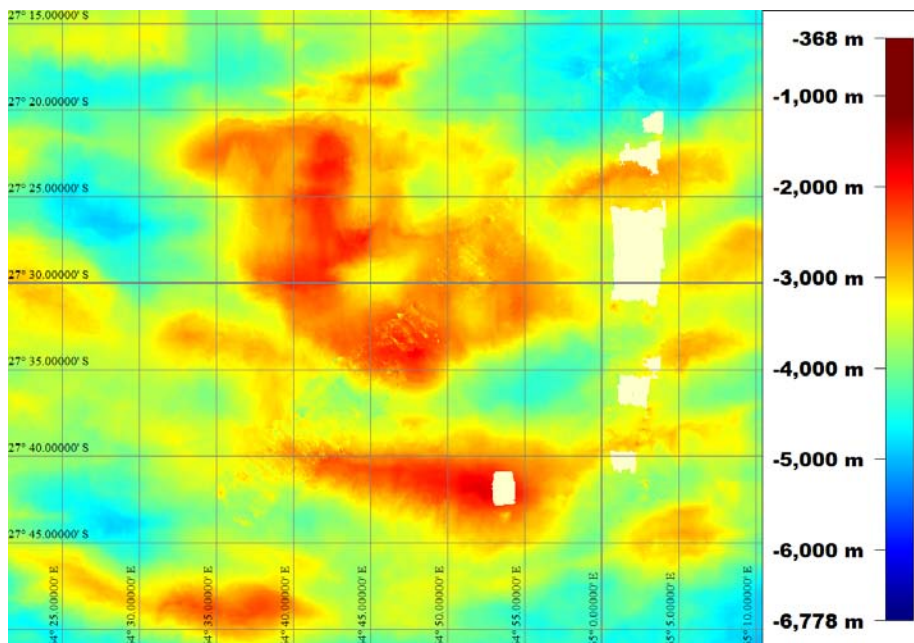


Figure 7.2: Multibeam bathymetric grid with superimposed new bathymetric data filtered using CARAIBES software to remove noise.

8. Conclusions

Upon arrival in the area, 28th September, the team deployed the OBSs (Ocean Bottom Seismometers) and began the acquisition of 2D and 2.5D seismic reflection profiles, then seismic wide-angle in 2D and 3D configurations. After recovery and redeployment of some of the OBSs in another configuration, the acquisition continued.

We were able to collect more than 2700 km of seismic reflection profiles and refraction and retrieve good data on 33 of the 38 OBSs deployed. Preliminary onboard processing shows promising indications and in particular:

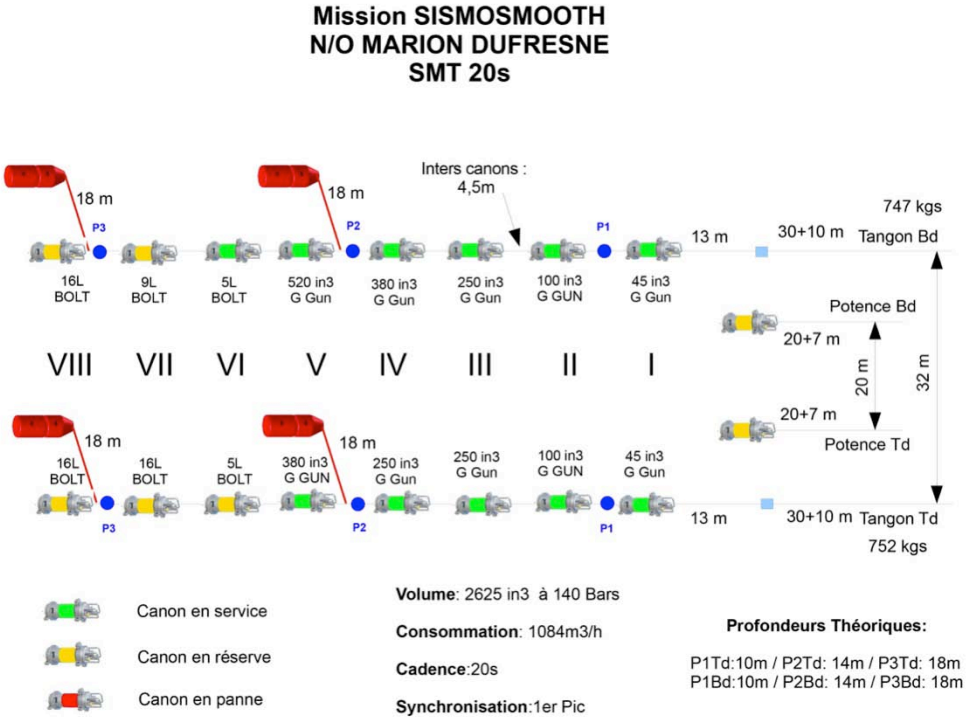
- The seismic crust is very thin and consists of a first layer of a few hundred meters with very low seismic velocities, topping a domain of high velocities passing more or less gradually to typical velocities of fresh mantle.
- The lower crust and mantle seismic underlying show many reflectors, whose origin, faults, magma injections or contrasts of degrees of serpentinization, remains to be studied. Some of these reflectors may be located at significant depths (greater than 6 km).

These data will be obviously processed more in details which will clarify these first results. Anyway, the cruise is a success and the collected data should allow us to test the hypotheses proposed in the proposal.

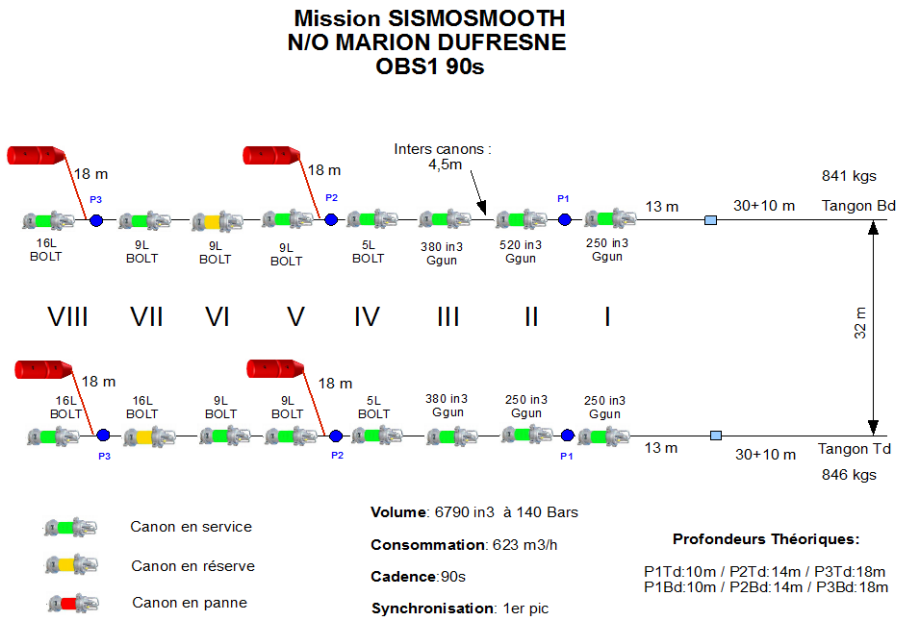
9. Annex

9.1. Source designs

9.1.1. SMT 20s

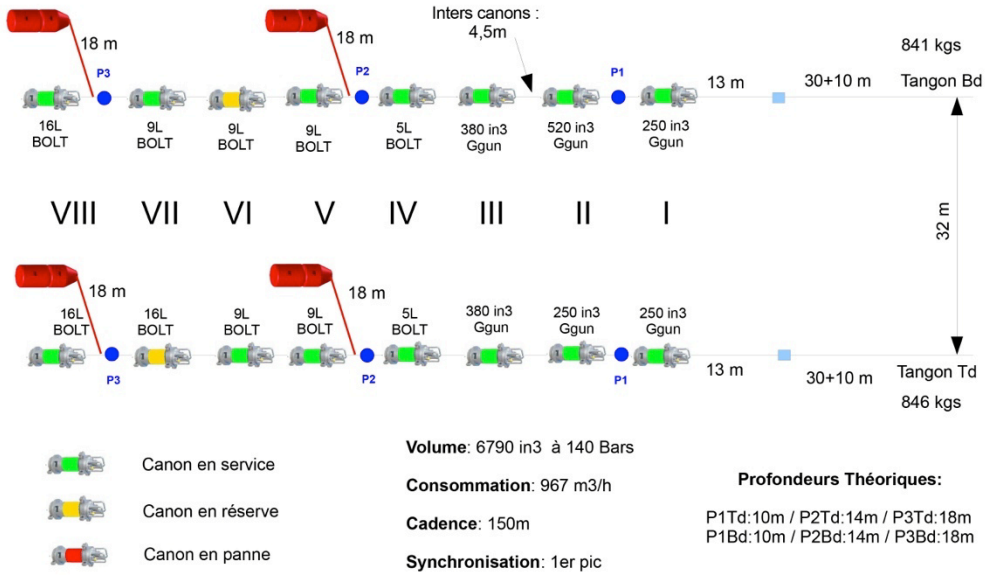


9.1.2. OBS 90s



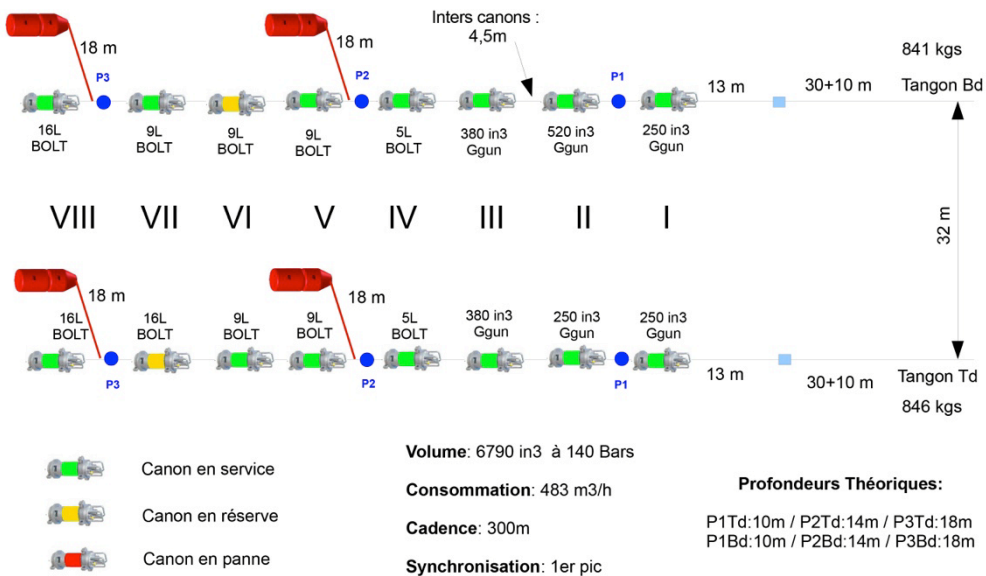
9.1.3. OBS 150 m

Mission SISMOSMOOTH N/O MARION DUFRESNE OBS2 150m



9.1.4. OBS 300 m

Mission SISMOSMOOTH N/O MARION DUFRESNE OBS2 300m



9.2. Summary of sources used for each profiles

Source Information

	Heure TU	N tir	Observations :	
				N°profil
			Source MCS cadence 20s	
29/09/14	13:49	945	Activation of gun 6Td (5Td not working)	1
30/09/14	16:14	870	Gun 2T don't respond anymore . Manometer freeze	4
30/09/14	19:47	26	Gun 7B leaking (out of order)	5
01/10/14	2:47	350	Stop shot 2 Td	6
01/10/14	6:31		Gun 8Bd (not used) out of order	7
02/10/14	15:22	150	Gun 1Td stop, leaking.	GIR
04/10/14	20:44	15	Gun 5T lost, leaking.	16
04/10/14	21:10	97	Activation of gun 7Bd	16
04/10/14	6:35	44	Stop gun 7B	18
06/10/14	11:32	99	Stop gun 2Tb (leaking)	GIR
06/10/14	13:15	407	Activation gun 7Tb	GIR
06/10/14	13:17	413	7 Tb work with a 30 ms delay	GIR
16/10/14	11:51		Beginning profile (2D1) 300m shots interval	33A
16/10/14	17:49	184	End of (2D2) 300m shots interval	33A
16/10/14	17:50	185	Beginning (2D2), 150m shots interval (shot number problem)	33A
16/10/14	23:17	519	End of (2D3), shot every 150m	33A
16/10/14	23:20	520	Beginning (2D3) shot every 300m	33A
16/10/14	23:25	522	Ecos number freeze, ON/OFF of shots	33A
17/10/14	2:59	629	Activation gun 6Bd (9L Bolt) replacing the gun 2Bd (520 in3) (out of order)	33A
17/10/14	11:07	218	Gun 8Bd out of order, replaced by gun 7Td	34
17/10/14	23:02	1	Beginning of the profile, 2 nM before 2D5, 300m shot interval	35
18/10/14	6:06	215	2D6 150m shot interval	35
18/10/14	9:41	425	2D7 (shot number Ecos freeze), 300m shot spacing	35
18/10/14	9:43	427	Re set shot number Ecos, 300m shot interval	35
18/10/14	15:38	1	Beginning of the profile, 120s shot interval	GIR2D8
18/10/14	16:32	28	Fin de remise à bord. Montée en allure à 5nds	GIR2D8
18/10/14	17:36	58	Beginning of the experimental profile. 60s 3,5nds	GIR2D8
18/10/14	18:30	110	Change to 120s shot interval, 5nds.	GIR2D8
18/10/14	19:32	142	Start putting Guns line Bd in the sea	GIR2D8
18/10/14	20:50	180	End and test guns Bd (all are OK)	GIR2D8
19/10/14	2:37	349	Start profile, 150m shot interval	36
19/10/14	5:51	543	Gun 5T leaking. stop.	36
19/10/14	5:56	548	Activation of gun 6B	36
19/10/14	6:07	560	Activation of gun 7T, 8B in standby.	36
19/10/14	13:08	1	Beginning of the profile, gun 8Tb out of order	38
19/10/14	13:14	6	Activation of the gun 8 Bd (8Td leaking)	38
22/10/14			Nominal OBS1 150 m configuration	39-42

9.3. Streamer designs and geometry

From 29th September

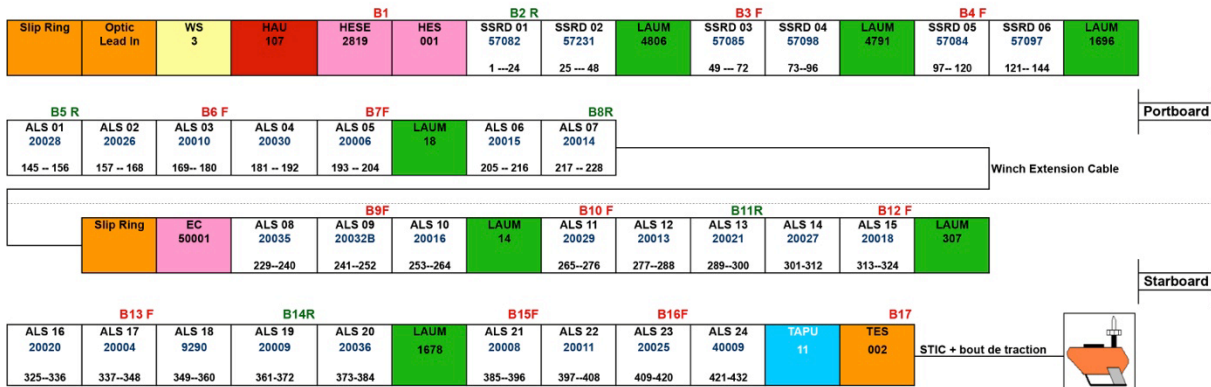


STREAMER 4500m - 6 SSRD + 24 ALS
 432 traces: 1-144: 6,25m
 145-432: 12,50m

CLIENT : IPG
 Navire : MARION DUFRESNE

Configuration SISMO SMOOTH
 Après mise à bord : 29/09/14

Lest ALS : 6 bronzes + 5 plastiques.
 Tête: BBBPBBPBBP Queue
 Lest SSRD: 3 bronzes + x plastiques
 Tête: Queue
 Acquisition Module (DC1) Deck Cable LAUXM 104
 T° : 18,8 °C
 Sal: 35,6 PSU
 Ballast: 4,7 Kg
 Nb lests Bronze/ALS 6



Légende
 Chaque ALS comprend 12 traces de 12,5 mètres, Chaque trace comprend 16 hydrophones.
 Chaque SSRD comprend 24 traces de 6,25 mètres, Chaque trace comprend 4 hydrophones.
 WS = Weight section Section (10m)
 HESE=Head Elastic Section Extension (50m)
 HES = Head Elastic Section (50m)
 TES = Tail Elastic Section (50m)
 SHES = Short HES (6m)
 SSRD, ALS = Acquisition Line Section (150m)
 LAUM = Line Acquisition Unit Marine (50 cm)
 HAU = Head Auxiliary Unit (40 cm)
 TAPU = Tail Auxiliary & Power Unit (50 cm)
 bout de traction = 36 m
 STIC = Streamer to Tail Interface Cable (25m)
 BX = Bird Unit
 R = Retriever
 F = Float
 1 --- 12 = Group number

From 16th October

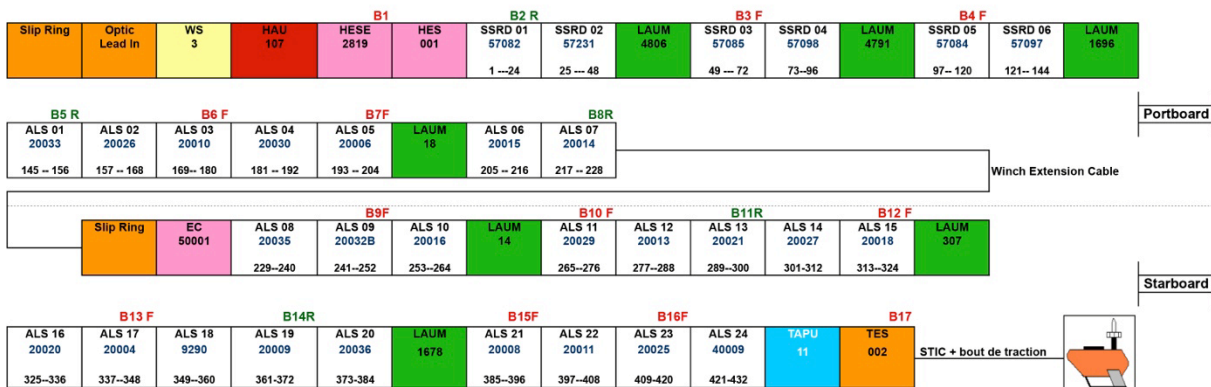


STREAMER 4500m - 6 SSRD + 24 ALS
 432 traces: 1-144: 6,25m
 145-432: 12,50m

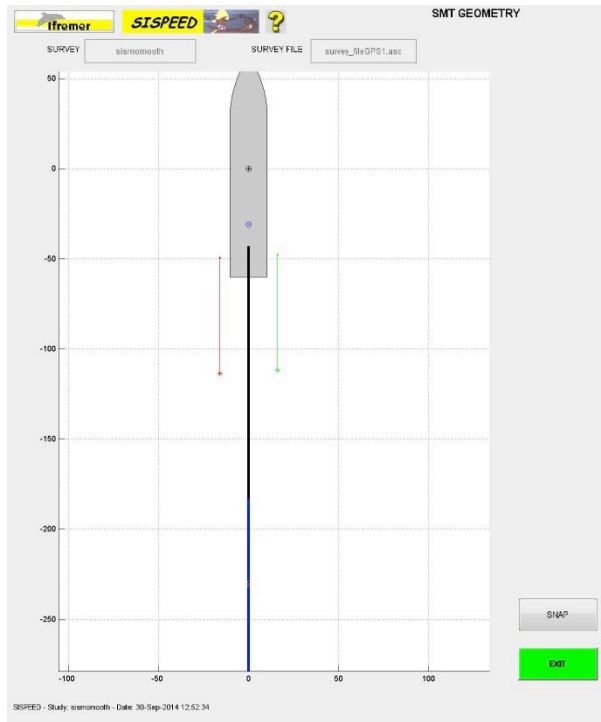
CLIENT : IPG
 Navire : MARION DUFRESNE

Configuration SISMO SMOOTH
 Après mise à bord : 16/10/14

Lest ALS : 6 bronzes + 5 plastiques.
 Tête: BBBPBBPBBP Queue
 Lest SSRD: 3 bronzes + x plastiques
 Tête: Queue
 Acquisition Module (DC1) Deck Cable LAUXM 104
 T° : 18,8 °C
 Sal: 35,6 PSU
 Ballast: 4,7 Kg
 Nb lests Bronze/ALS 6



Légende
 Chaque ALS comprend 12 traces de 12,5 mètres, Chaque trace comprend 16 hydrophones.
 Chaque SSRD comprend 24 traces de 6,25 mètres, Chaque trace comprend 4 hydrophones.
 WS = Weight section Section (10m)
 HESE=Head Elastic Section Extension (50m)
 HES = Head Elastic Section (50m)
 TES = Tail Elastic Section (50m)
 SHES = Short HES (6m)
 SSRD, ALS = Acquisition Line Section (150m)
 LAUM = Line Acquisition Unit Marine (50 cm)
 HAU = Head Auxiliary Unit (40 cm)
 TAPU = Tail Auxiliary & Power Unit (50 cm)
 bout de traction = 36 m
 STIC = Streamer to Tail Interface Cable (25m)
 BX = Bird Unit
 R = Retriever
 F = Float
 1 --- 12 = Group number



SISPEED Ifremer **SISPEED** ?

SURVEY DESIGN - SMT GEOMETRY RESET DEFAULT MARION

STREAMER

Towing Point dx: 0 m, dy: -43 m

Lead-in section payed out length: 130 m

Number WS (10m): 1

Number HES (50m): 2

Number ALS (150m): 30

Number TES (50m): 1

Tail rope length: 61 m

Number of traces: 360

Trace distance: 12.5

Dist. centre first trace: 246.25 m

Total payed out length: 4851 m

SOURCE

Starboard Source

Towing Point dx: 16 m, dy: -47.7 m

Source cable payed out length: 64 m

Port Side Source

Towing Point dx: -16 m, dy: -49.5 m

Source cable payed out length: 64 m

DEPTH CONTROLLERS

BIRDS: 17

BIRD 1: Tail HES 1	BIRD 12: Tail ALS 21
BIRD 2: Tail ALS 1	BIRD 13: Tail ALS 23
BIRD 3: Tail ALS 3	BIRD 14: Tail ALS 25
BIRD 4: Tail ALS 5	BIRD 15: Tail ALS 27
BIRD 5: Tail ALS 7	BIRD 16: Tail ALS 29
BIRD 6: Tail ALS 9	BIRD 17: Tail TES 1
BIRD 7: Tail ALS 11	BIRD 18:
BIRD 8: Tail ALS 13	BIRD 19:
BIRD 9: Tail ALS 15	BIRD 20:
BIRD 10: Tail ALS 17	BIRD 21:
BIRD 11: Tail ALS 19	BIRD 22:

VESSEL GPS

Raw GPS ECOS: integrated

dx: 0 m, dy: -31 m

dx: 0 m, dy: 0 m

Source - Traces offset

min: 177 m, max: 4864 m